File: Solar Cell Reports

NG.

N#

[redacted]

BOEING

SEATTLE, WASHINGTON

BOEING AIRPLANE COMPANY

SEATTLE 24, WASHINGTON

[redacted]

DOCUMENT NO. D2-90041-A

UNCLASSIFIED TITLE Concentrator Structure For A Solar Energy Photovoltaic Conversion System - Final Report

MODEL NO. Research CONTRACT NO. JPL 950122

ISSUE NO. 3 ISSUED TO Dan Meredith

CLASSIFIED TITLE _____
(STATE CLASSIFICATION)

WORK ORDER NO. UNIT NO. ITEM NO.

SPECIAL LIMITATIONS ON ASTIA DISTRIBUTION

ASTIA may distribute this report to requesting agencies subject to their security agreement, approved fields of interest, and the following:

☐ UNLIMITED — To all agencies of the Department of Defense and their contractors.

☒ LIMITED — To U. S. Military organizations only.

This report may be distributed to non military agencies not approved subject to BAC approval of each request.

NOTE: the LIMITED category may be checked only because of actual or potential patent, proprietary, ethical, or similar implications.

E. J. Zapel 11-16-61
E. J. Zapel (Date)

Roger B. Gillette 11/17/61
R. B. Gillette (Date)

PREPARED BY R. J. Tallent A. Klammer, Jr. 11-16-61
R. J. Tallent and A. Klammer, Jr. (Date)

SUPERVISED BY H. Owen & A. Olken 11/17
H. Owen & A. M. Scroggs (Date)

APPROVED BY J. C. Evensen 11/17
J. C. Evensen (DATE)

Class. & Distr.
Approved By. A. L. Odmark 11/17/61
A. L. Odmark (Date)

NO OF PAGES 111 (EXCLUDING TITLE AND REVISION AND ADDITION PAGES.)

BAC 324 BR-7

DOCUMENT TITLE PAGE

JPL Subcontract 950122
R1

TABLE OF CONTENTS

1. SUMMARY

Jet Propulsion Laboratory (JPL) Contract 950122 to The Boeing Company calls for the design, fabrication and evaluation of V-ridge concentrating structures for use in a solar energy photovoltaic conversion system. In this type of concentrator the direct sunlight arriving at a solar cell is supplemented by sunlight reflected from the concentrator sides (Fig. 1). Specific requirements of the contract include the delivery of two 9-inch by 9-inch concentrators, EOM-1 and EOM-2 along with an Interim Report within six weeks after contract execution; and the delivery of a type-approval 10-inch by 18-inch CS-1 concentrator along with this Final Report at the completion of the contract, 12 weeks after execution. The contract required that the CS-1 structure be capable of withstanding an environmental vibration test, weigh less than 0.4 pound exclusive of the wiring, solar cells and jig attachment clips, and develop a specific power equal to at least 90 percent of the power output of a non-concentrating panel having 85 percent of its area covered with cells.

Development of the concentrator design has involved investigation of the performance of solar cells at high light intensities, the effect of non-normal incident light on solar-cell and cover-glass combinations, and the effectiveness of reflecting surfaces.

Investigations were conducted to determine the optimum angle between the plane of the solar cells and the reflecting surface . Optical analyses and tests indicated that a 60-degree angle was best. Weight computations also indicated that a 60-degree angle resulted in nearly minimum weight. An angle of 60 degrees was adopted, and appropriate forming tools and welding jigs were built.

A total of thirteen 9-inch by 9-inch concentrating structures were fabricated. The first nine of these structures were constructed from 6061-T4 aluminum alloy. The last four structures were made from ALCOA unprocessed lighting sheet in the H25 condition. In all of the structures the aluminum sheet was joined to supporting "hat" sections with multiple spot welds. The reflecting surfaces on all structures were coated with a film-forming lacquer and then aluminized with vapor-deposited high-purity aluminum.

Several 9-inch by 9-inch concentrators were tested at the vibration levels specified in the JPL Contract. No structural damage occurred during the tests and no resonance was observed during any of the complex-wave tests. A search for resonant frequencies was conducted, and the resonant frequencies of the panels were found to vary from 240 to 340 cps.

Ten of the 9-inch by 9-inch concentrators were tested in sunlight. The first concentrators had concentration ratios of 1.65 to 1.73 (compared with 2.0 theoretical). Better aluminized-lacquer reflecting surfaces were developed for later concentrators.

Four EOM concentrators were built. As shown in the Performance Summary below, the three EOM concentrators tested at Boeing exceeded the 90-percent specific power ratio required by the contract. The fourth EOM concentrator was shipped to JPL without being tested at Boeing. EOM-1A and EOM-2A concentrators were coated prior to shipment with a strippable lacquer for protection of reflecting surfaces. Strippable lacquer had been used to protect reflecting surfaces, but had not been previously sprayed over solar cells. Unfortunately, the lacquer reacted with the bonding agent between the solar cells and their cover glasses, resulting in cracking of cover glasses. Subsequently the solar cells have been protected during the spraying of this strippable lacquer. EOM-1B and 2B concentrators were shipped to JPL.

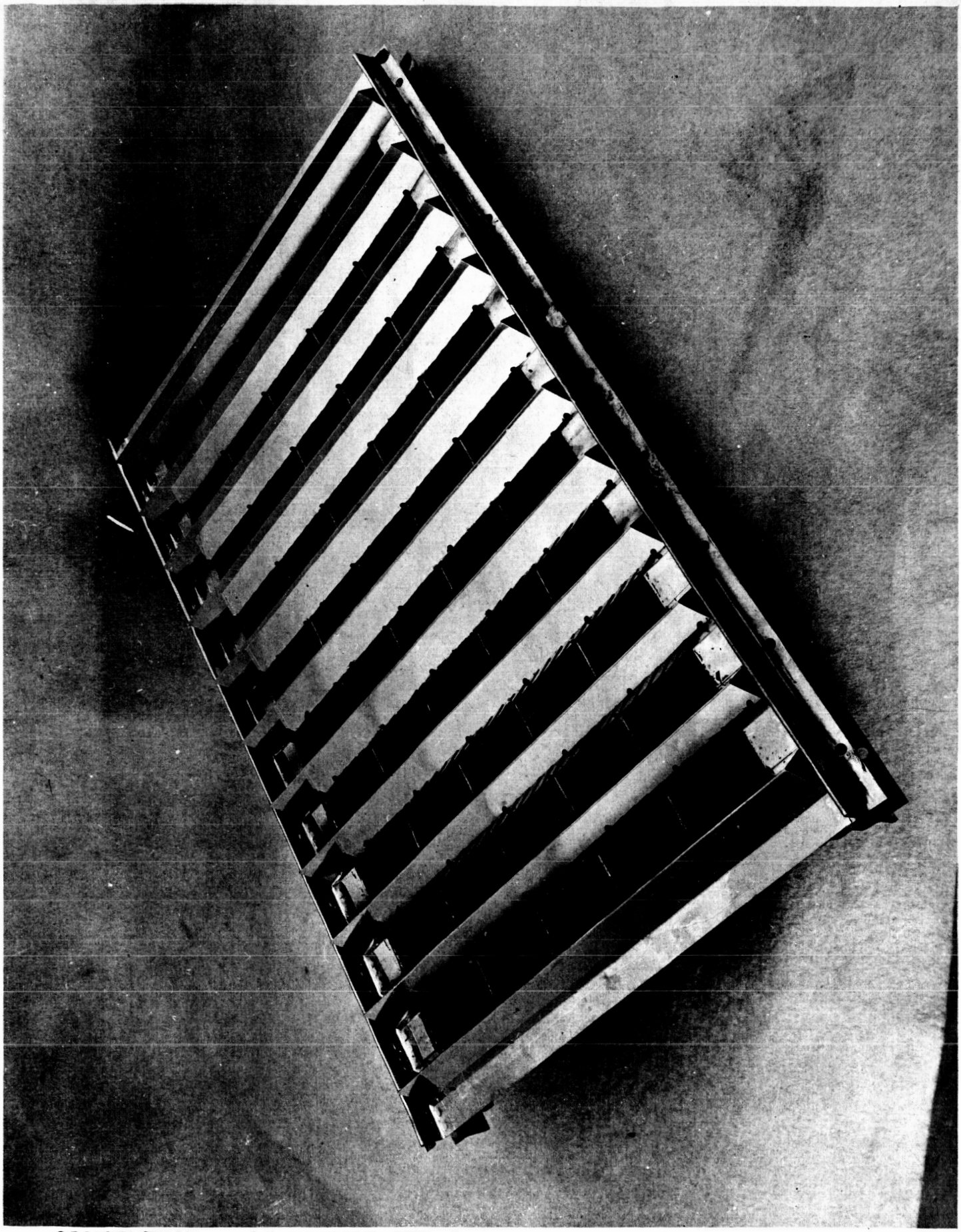

CONCENTRATOR STRUCTURE FOR A SOLAR ENERGY PHOTOVOLTAIC CONVERSION SYSTEM

FIG. 1

The CS-1 concentrator design was based on EOM concentrator experience. The 60-degree nominal angle between the plane of solar cells and reflecting surface was retained. Aluminized lacquer was used for the reflecting surfaces. Three of these concentrators were fabricated from ALCOA unprocessed lighting sheet — one was vibration tested, another solar tested and delivered to JPL, and the third was a spare. The CS-1 concentrator actually is 10.67 by 18 inches in size, and its weight without cells, adhesive, wiring, and vibration-test clips, but with aluminized lacquer, is 0.451 pounds. The weight of the complete concentrator with cells, wiring, adhesive, and reflecting surface, but without vibration-test mounting clips, is 0.768 pounds. This corresponds to 0.575 pounds per sq. ft.

The structural-test CS-1 concentrator was vibrated in accordance with the contract. The only damage was the loosening of a soldered connection between a lead from a cell and the paralleling bus. The first natural frequency of the concentrator was calculated to be 214 cps. From a bending test it was determined that the EI value is 4,010 inches-squared pounds per corrugation.

The electrical-optical performance of the CS-1 concentrator, as measured in solar tests, is shown in the Performance Summary Table. It will be noted that the contract specific power ratio requirement of 90 percent was exceeded.

CONCENTRATOR PERFORMANCE SUMMARY

Concentrator Designation	Structural Material	Specific Power Ratio, Percent With 85 Percent Area Ratio*	With 92 Percent Area Ratio	Disposition
EOM-1A	6061-T4	97.4	90.0	Damaged
EOM-1B	UPLS	Not tested at Boeing		Delivered to JPL
EOM-2A	6061-T4	102.8	94.8	Damaged
EOM-2B	UPLS	105.5	97.4	Delivered to JPL
CS-1	UPLS	106.2	98.1	Delivered to JPL

* Designated in contract

UPLS - ALCOA unprocessed lighting sheet

NOTE: All concentrators had 5-cell shingles except EOM-2A and EOM-2B which had 15-cell shingles.

II. INTRODUCTION

Silicon solar cells have been a good source of power for satellites and space probes. Their applicability for future vehicles with larger electric loads seems to be limited by cost and weight. Concentrating sunlight on solar cells would seem to be a way of partially overcoming these limitations. If the power output per cell could be doubled, the cost per kilowatt would be halved. If lightweight reflecting surfaces could be substituted for silicon photovoltaic material, the weight per kilowatt would be reduced. The weight might be reduced even more significantly if the reflecting material could also serve as a supporting structure.

The Boeing Company has been investigating concentrating structures for solar-cell power supplies for a year and a half. This investigation was accelerated on August 29, 1961 when the Jet Propulsion Laboratory (JPL) awarded Boeing the Contract 950122, "Concentrator Structure for a Solar Energy Photovoltaic Conversion System."

The contract covers the design, fabrication, and evaluation of small models of a concentrating structure in which solar cells are illuminated by both direct sunlight and sunlight reflected from aluminum concentrator surfaces. Two electrical-optical model concentrators (EOM 1 and 2) and a type-approval concentrator (CS-1) are to be delivered.

A contract requirement is that a design of a 10-inch by 18-inch CS-1 type approval concentrator be submitted to JPL six weeks after execution of the contract. To accomplish this design it was necessary to undertake these three categories of work simultaneously:

1. Analysis of design factors
2. Basic investigations
3. Manufacture and test of concentrators

The analysis of design factors involved the derivation of geometric relations in a V-ridge concentrator, the development of structural design criteria, a heat balance determination, and development of application techniques. This work is discussed in Section III.

The basic investigations involved laboratory-type research into the performance of solar cells in high light intensities, the performance of solar cells with non-normal incident light, analysis of curved reflectors, and the testing of reflecting surfaces. These investigations are described in Section IV.

The design of electrical-optical model (EOM) concentrators, the type-approval (CS-1) concentrator, and larger concentrators is discussed in Section V. The manufacturing procedure is described in Section VI, and Section VII contains the results of solar and structural testing.

III. ANALYSIS OF DESIGN FACTORS

The analysis of design factors is covered in this section. First the geometry of V-ridge concentrators is analyzed, and an equation is derived for the geometry that gives the maximum concentration per unit of weight. The structure of V-ridge type concentrators is next analyzed, and structural design criteria are developed. A method for obtaining solar-cell temperature in a concentrator structure in space is developed. Finally the application of these analyses to EOM and CS-1 design is illustrated.

A. Optimum Reflector Angle

A requirement of the contract is that the angle between the plane of the solar cells and reflecting surface be optimized. The relation between this angle and system weight has been analyzed, and the angle at which the power output-to-weight ratio is maximum has been derived. The symbols used in the derivation are shown below. This derivation is based on ideal flat reflecting surfaces.

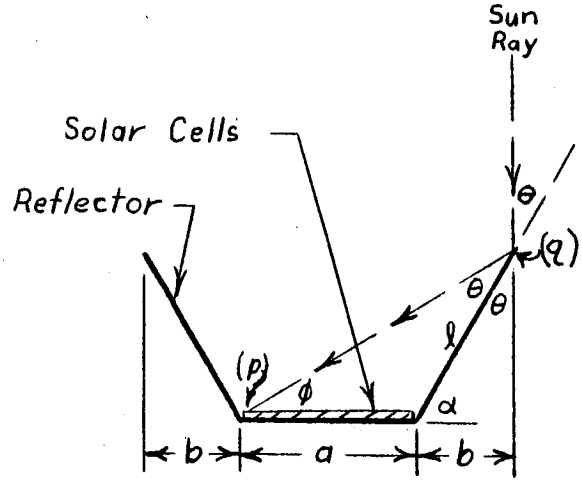

An assumed requirement of the reflector geometry is that the entire cell area is illuminated. Thus, the light striking the highest point on the reflector (q) must be reflected to the far side of the solar cell (p) as shown. This means that for a given reflector angle α, there can be only one reflector length (ℓ) and concentration ratio (C). From the geometry of the reflector, the relation between α and ϕ is,

$$\phi = \alpha - \theta$$
$$= 90 - 2\theta$$

The theoretical concentration ratio in sunlight (C) is

$$C = \frac{a + 2bR}{a}$$

$$= \frac{a + 2\ell R \sin\theta}{a} \qquad (1)$$

Where R = concentrator reflectance

When there are no concentrating surfaces b = 0 and C = 1; thus, the cells are illuminated only by the normal-incidence solar radiation. As the reflector becomes more nearly vertical (α gets larger), the concentration ratio increases and reaches a maximum only with an infinitely long reflector ($\ell \to \infty$). As α approaches 45 degrees from larger angles, ϕ approaches zero (Eq. 1), and no light is reflected to the solar-cell surface; thus, the region of practical interest is,

$$45° < \alpha < 90°$$

The length of the reflecting surface (ℓ) can be written,

$$\ell = \frac{a \sin (\alpha - \theta)}{\sin \theta} \qquad \theta = 90° - \alpha$$

$$= \frac{a \sin (2\alpha - 90°)}{\sin (90° - \alpha)} \qquad (2)$$

and substituting ℓ into equation (1),

$$C = 1 - 2R \cos 2\alpha \qquad (3)$$

The weight of the trough (solar cells, cover glasses, wiring, and aluminum) plus the weight of the reflecting surfaces is,

$$W = m_1 + 2n_1 \ell$$

m_1 = weight of trough and solar cells, lbs/inch of length

n_1 = weight of reflector, lbs/inch of length and width.

Substituting Eq. (2) for ℓ ,

$$W = m_1 + \frac{2n_1 a \sin (2\alpha - 90°)}{\sin (90° - \alpha)} \qquad (4)$$

$$W = m_1 - \frac{2n_1 a \cos 2\alpha}{\cos \alpha}$$

To find the optimum angle (α) which gives the maximum concentration-to-weight ratio, Eqs. (3) and (4) are combined.

$$\frac{C}{W} = \frac{1 - 2R \cos 2\alpha}{m_1 - \frac{2n_1 a \cos 2\alpha}{\cos \alpha}}$$

$$\frac{C}{W} = \frac{\cos \alpha (1 - 2R \cos 2\alpha)}{m_1 \cos \alpha - 2 n_1 a \cos 2\alpha} \qquad (5)$$

Equation (5) will give an optimum angle for each combination of reflector unit weight (n_1) and trough-and-cell weight (m_1). The optimum angle, for reflectances (R) of 100 and 80 percent, was computed for the following (m_1) and (n_1) values which were used in the EOM concentrator:

Item	Weight, Pounds per Sq. Ft.	Value of Constant
Trough - 0.010 inch aluminum	0.14	
Trough - solar cells, cover glasses, wiring, bonding	0.60	
m_1 - Trough, total	0.74	4.12×10^{-3} lbs/inch
n_1 - Reflector, 0.010 inch aluminum	0.14	1×10^{-3} lbs/sq.in.

The C/W values for these conditions and varying angle α are plotted in Fig. 2. It can be seen that the maximum C/W ratio occurs at an angle (α) of about 62 degrees for an ideal case with 100 percent reflectance. If a reflectance of 80 percent is assumed, the optimum angle shifts to 60 degrees.

The reflector angle of 60° chosen for the EOM concentrators was based on the above study and the data in Section IV-B, showing the energy loss as a function of angle of incidence on the cell cover glass.

B. Structural Analysis

The factors which enter into concentrator design are solar cell size, reflector angle, reflecting surface type, metal thickness, required structural stiffness and allowable weight. Since the solar cell size is fixed, much of the geometry is likewise fixed.

The contract requires that the total weight of the CS-1 concentrator (exclusive of cells, wiring, adhesive, jig attachments, and simulation load) shall be 0.4 pounds or less (equivalent to 0.32 pounds per sq. ft.). For this reason an aluminum alloy structure was chosen. The structure is composed of an aluminum sheet bent into V-ridges and troughs, with hat-section stiffeners at right angles to the V-ridges.

In the initial design considered, the hat-section stiffeners would have been dip brazed to the concentrator structure. However, the moist environments to which the structure would be exposed under actual launch conditions would create a severe stress corrosion problem due to trapped brazing flux. Bonded joints were discarded as prime structure attachments because of difficult quality control problems inherent in the production of bonded joints.

The final design employs spot welds. Since an intrinsic problem in a spot weld design is the poor fatigue life of single lap joints with only one row of welds, and because the concentrator structure is subject to random structural vibration, the spot welds were placed much closer together than they would be in a conventional joint. This tends to transfer the bending deformations from one sheet to the next along a line contact instead of at several isolated points, thus reducing the high local strains at the leading edges of the spot welds and increasing the fatigue life without increasing the weight.

$$\frac{C}{W} = \frac{\cos\alpha\,(1-2R\cos 2\alpha)}{m_1\cos\alpha - 2n_1 a\cos 2\alpha}$$

ASSUMPTIONS

$m_1 = 4.12 \times 10^{-3}$ lbs/inch

$n_1 = 1 \times 10^{-5}$ lbs/inch^2

MATERIAL ~ ALUMINUM

REFLECTOR THICK. = .010 in.

R = REFLECTANCE

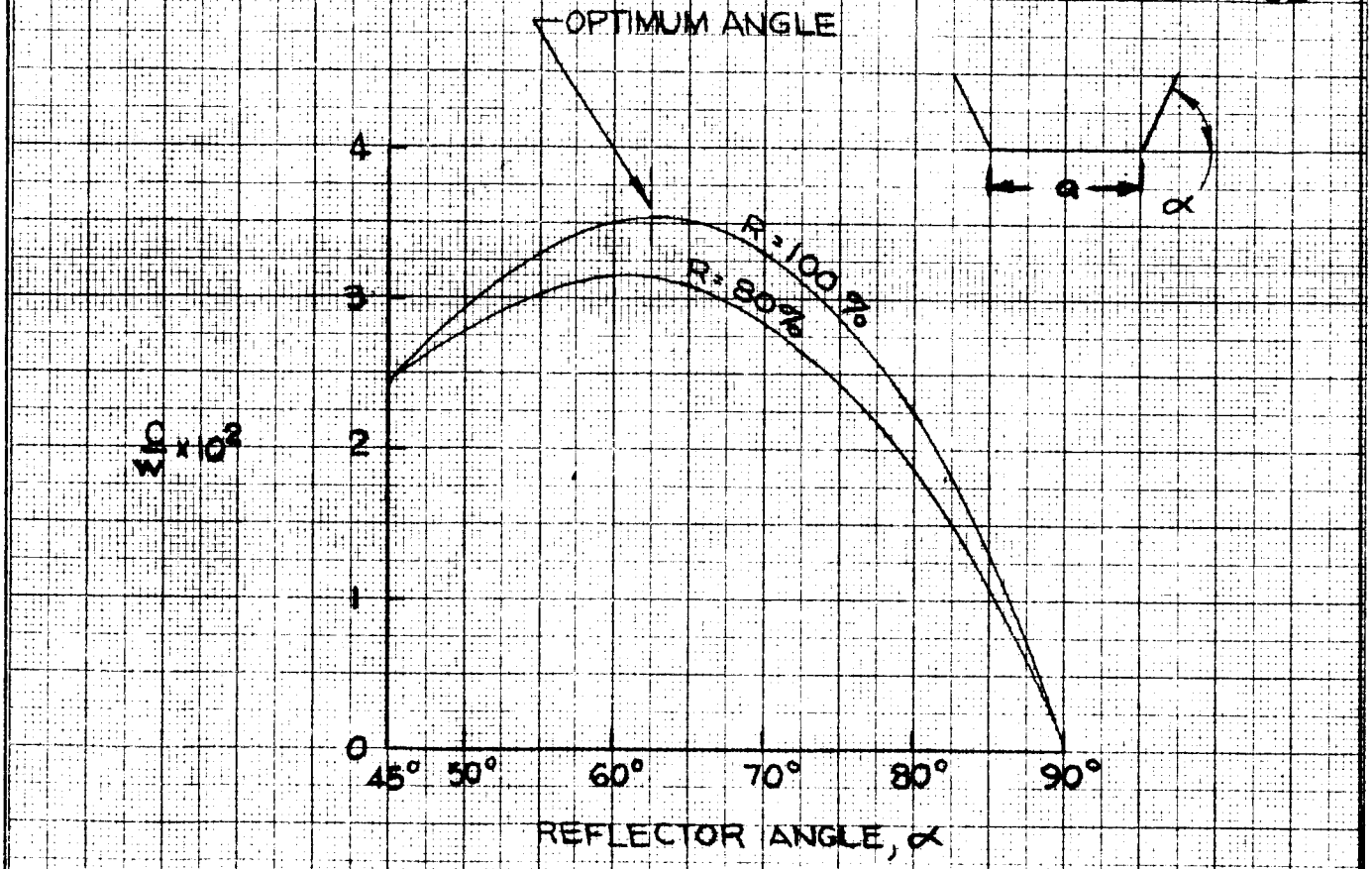

CALC			REVISED	DATE	PLOT OF CONCENTRATION RATIO (C)-TO-WEIGHT RATIO FOR DETERMINING OPTIMUM REFLECTOR ANGLE	FIG 2
CHECK						D2-90041-A
APR					THE BOEING COMPANY	PAGE 8
APR						

Holes were required in the structure at the ends of the solar cell shingles for electric wires going to connections on the back side. The initial design had a 0.250-inch diameter hole in the bottom of the trough near each of the stiffeners. This size hole is equivalent to a 30 percent reduction of trough cross sectional area; therefore, doublers were installed on the first fabricated panels. The calculated and measured weights for these panels with doublers were more than the contract limitation of 0.32 lbs/sq. ft. Therefore, the wiring technique was modified to reduce the hole diameter to 0.12 inch and move the hole location to a less sensitive area in the base of the reflecting facet adjacent to the trough. This change allowed elimination of the doublers and resulted in a design weight of 0.293 lbs/sq. ft.

The initial design of the V-ridge concentrator structure utilized flat reflecting surfaces with a 60° angle between the reflector and the plane of the solar cells. All weight, stiffness, resonance, and concentration ratio calculations were based upon this design. However, in the course of the investigations it was found that a slightly concave reflector surface would be advantageous from the standpoint of reducing the light dispersion and allowing moderate forming tolerances; consequently, the reflecting surfaces were made 0.85 inches wide instead of 0.80 inches wide. The 0.80 inches would be obtained if all angles were 60 degrees. For some of the EOM panels the included apex angle of the reflectors was made 53 degrees while the base angle of 60 degrees remained unchanged. The resulting reflecting surface was approximately a segment from a right circular cylinder having a 12.2 inch radius. The curved reflector design used on these particular EOM panels was not optimized to achieve uniform illumination but was only intended to reduce light dispersion. The curved reflector design was therefore relegated to the status of a research project for further investigation. The resulting panel weight for this configuration was increased approximately 8 percent to 0.304 lbs/sq. ft.

The CS-1 concentrator design was changed to a flat sided reflector design with included apex angles of 56 degrees and base angles of 62 degrees with reflector sides 0.85 inches wide. This revision of the design was selected because of "bright spots" found on the solar cells in the curved reflector EOM panels. With the smaller apex angle, the reflected light from each reflector did not fully illuminate the cell. As a consequence, a bright line was formed on the cells where the reflected illumination overlapped.

Of the materials investigated, 6061-T4 aluminum alloy offered the best fatigue resistance while ALCOA unprocessed lighting sheet (1100 H25 aluminum) appeared to have the best reflectance. Therefore, concentrator structures with and without doublers were made from both materials and tested in vibration.

Structural Stiffness Calculation

The panel stiffness I_s in the stiffener direction is nearly independent of the reflector angle. It was calculated by assuming that one inch of the trough was effective in bending with the stiffener in the region of the trough, and computing the effective (I_s) over a single trough-reflector combination by the equations:

$$I_s = \left[\frac{I_t}{L_{st}} + \frac{I_{sr}}{L_{sr}} \right] \left[\frac{L_{st} + L_{sr}}{4} \right] \qquad (6)$$

where: I_t = moment of inertia of the trough area

I_{sr} = moment of inertia of the stiffener

L_{st} = length of stiffener across the trough

L_{sr} = length of stiffener across the reflectors

For 0.01 inch thick material the values are:

$I_t = 0.000106$ in.^{4}

$I_{sr} = 0.000042$ in.^{4}

$L_{sr} = 0.90$ in.

$L_{st} = 0.80$ in.

$I_s = 0.000074$ in.^{4}

This low value of I_s indicated that a V-ridge concentrator panel cannot be supported only from the hat-section ends in a vibration environment. This becomes apparent when I_s is compared with panel stiffness in the V-ridge direction (I_v).

The panel stiffness in the V-ridge direction was calculated from the following equation and plotted in Fig. 3. This equation was derived from the concentrator geometry previously described.

$$I_v = \frac{ta^3 \sin^2\alpha}{3\cos^3\alpha}(1-2\cos^2\alpha)^3\left[\frac{1+2\cos\alpha-2\cos^2\alpha}{2+\cos\alpha-4\cos^2\alpha}\right] \qquad (7)$$

where t = material thickness

For the EOM concentrators,

$t = 0.010$ in.

$a = 0.80$ in.

$\alpha = 60°$

Then, $I_v = 0.0013$ in.^{4}

Resonant Frequency

The resonant frequency of the panel vibrating as a cantilever beam was calculated from the classical solution for a vibrating uniform beam and is plotted in Fig. 4. The resonant frequency of the panel vibrating as a pin ended beam is plotted in Fig. 5. The resonant beam frequency is

$$\omega = \beta^2\sqrt{\frac{EI}{m}} \qquad (8)$$

where, β is the solution from the transcendental equation resulting from the substitution of boundary conditions.

The β values, where L is in inches, are:

1. Cantilever beam $\beta_1 = 1.875/L$, $\beta_2 = 4.695/L$, $\beta_n = (2n-1)\pi/2L$, $n > 2$
2. Fixed ended beam $\beta_1 = 4.77/L$, $\beta_2 = 5\ \pi/2L$, $\beta_n = (2n+1)\ \pi/2L$, $n > 2$
3. Pin ended beam $\beta_1 = \pi/L$, $\beta_2 = 2\ \pi/L$, $\beta_n = n\pi/L$

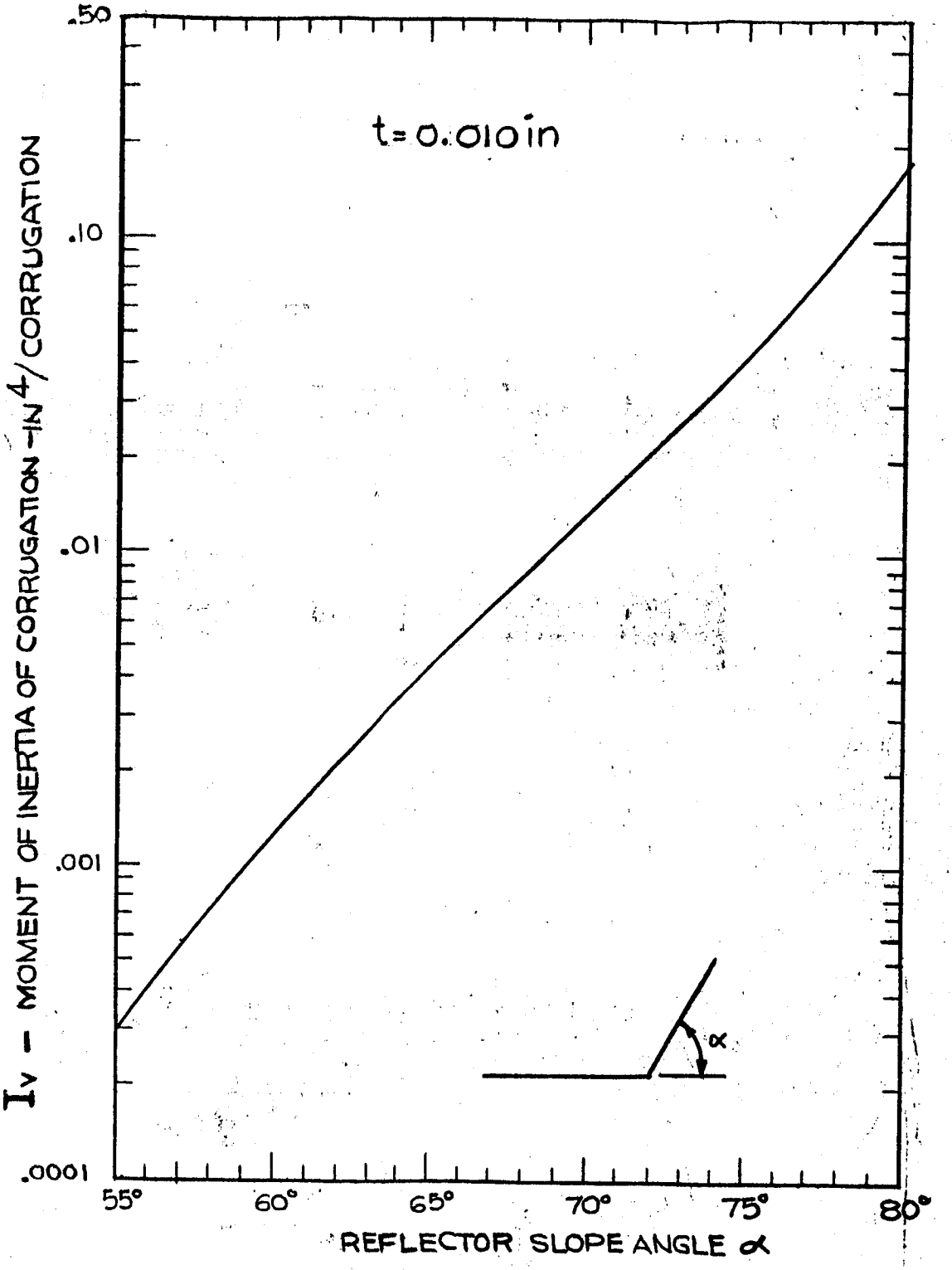

CALC			REVISED	DATE	PANEL STIFFNESS IN REFLECTOR DIRECTION
CHECK					
APPD					
APPD					BOEING AIRPLANE COMPANY

FIG 3

D2-90041-1

PAGE 11

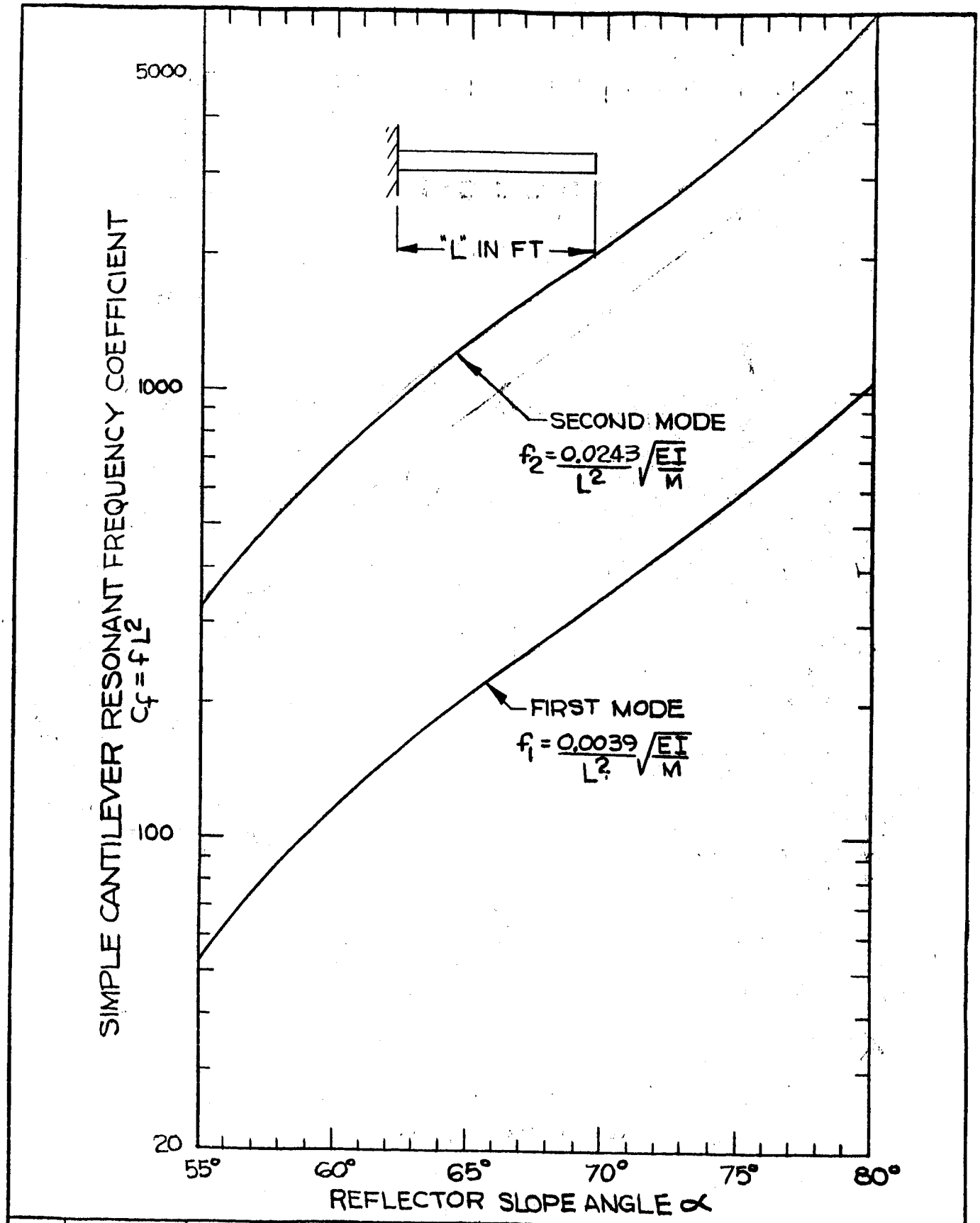

CALC			REVISED	DATE	RESONANT FREQUENCY FOR CONCENTRATOR PANELS (CANTILEVER BEAM)
CHECK					
APPD					
APPD					
					BOEING AIRPLANE COMPANY

FIG 4

D2-90041-A

PAGE 12

U3 4036 3000 (WAS BAC 973D-R3) REQ 10388

8-7000

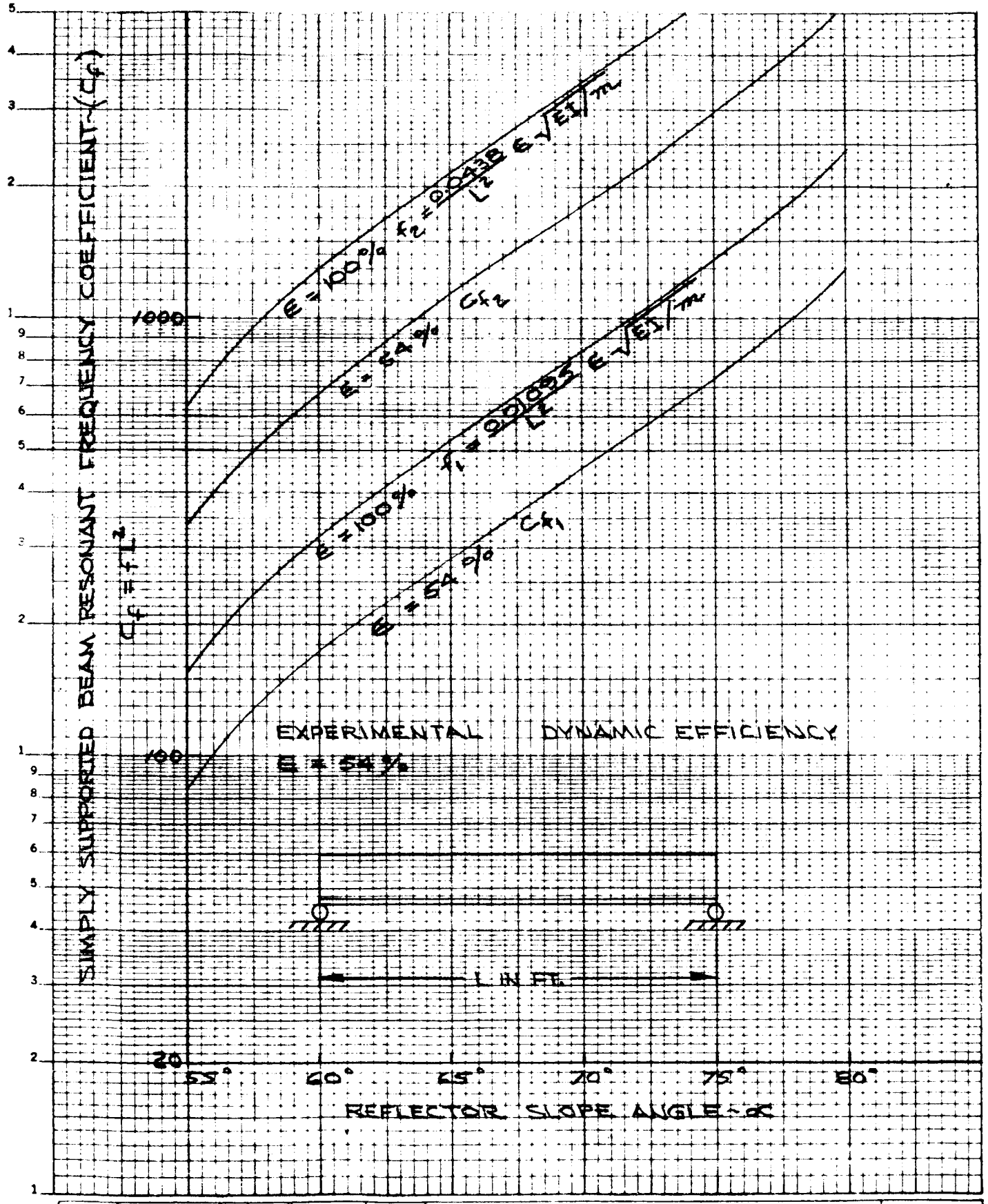

CALC		REVISED	DATE	RESONANT FREQUENCY FOR CONCENTRATOR PANELS (PIN ENDED BEAM)	FIG. 5
CHECK					
APR				BOEING AIRPLANE COMPANY	D2-90041-A
APR					PAGE OF 13
CONTRACT NO.					

Then the resonant frequency is,

$$f = \frac{\omega}{2\pi} \text{ cps} \tag{9}$$

For a 60 degree reflector angle (α) and structure of 0.010 inch aluminum,

$$\sqrt{\frac{EI}{m}} = 28.8 \times 10^{3} \tag{10}$$

Then for a cantilever beam the resonant frequency is,

$$f = \frac{111}{L^2} \text{ cps} \tag{11}$$

and for a simply supported beam,

$$f = \frac{314}{L^2} \text{ cps} \tag{12}$$

where L is in ft.

Weight Analysis

The panel weights were calculated from the following equation which was derived from concentrator geometry and plotted in Fig. 6:

$$W = \frac{ta\rho}{\cos\alpha}\left[2 - 4\cos^2\alpha + \cos\alpha\right] + \frac{1.11t\rho}{1.85}\left[a_n + 2a\left(1 - 2\cos^2\alpha\right)\right] \tag{13}$$

Where ρ = material density

The first expression is the weight of the reflector panel and the second is the weight of the associated stiffener divided by the stiffener spacing.

For a 60 degree reflector angle of 0.010 inch aluminum,

$$W = (0.01)(0.80)(0.097)\left[\frac{2-1+0.5}{0.5} + \frac{1.11(1+2-1)}{1.85}\right]$$

$$= 0.00326 \text{ pounds/running inch.}$$

Then the weight per sq. ft. is:

$$W = \left(\frac{0.00326}{1.60}\right)144 = 0.293 \text{ lbs/sq ft}$$

Normalized Area Calculation

The power output (P) from the concentrator structure is,

$$P = (A_c + R\,A_r)\,S\,\eta \tag{14}$$

NOTE: SLIGHTLY CONCAVE REFLECTORS WERE USED IN EOM-1B & 2B CONCENTRATORS ONLY.

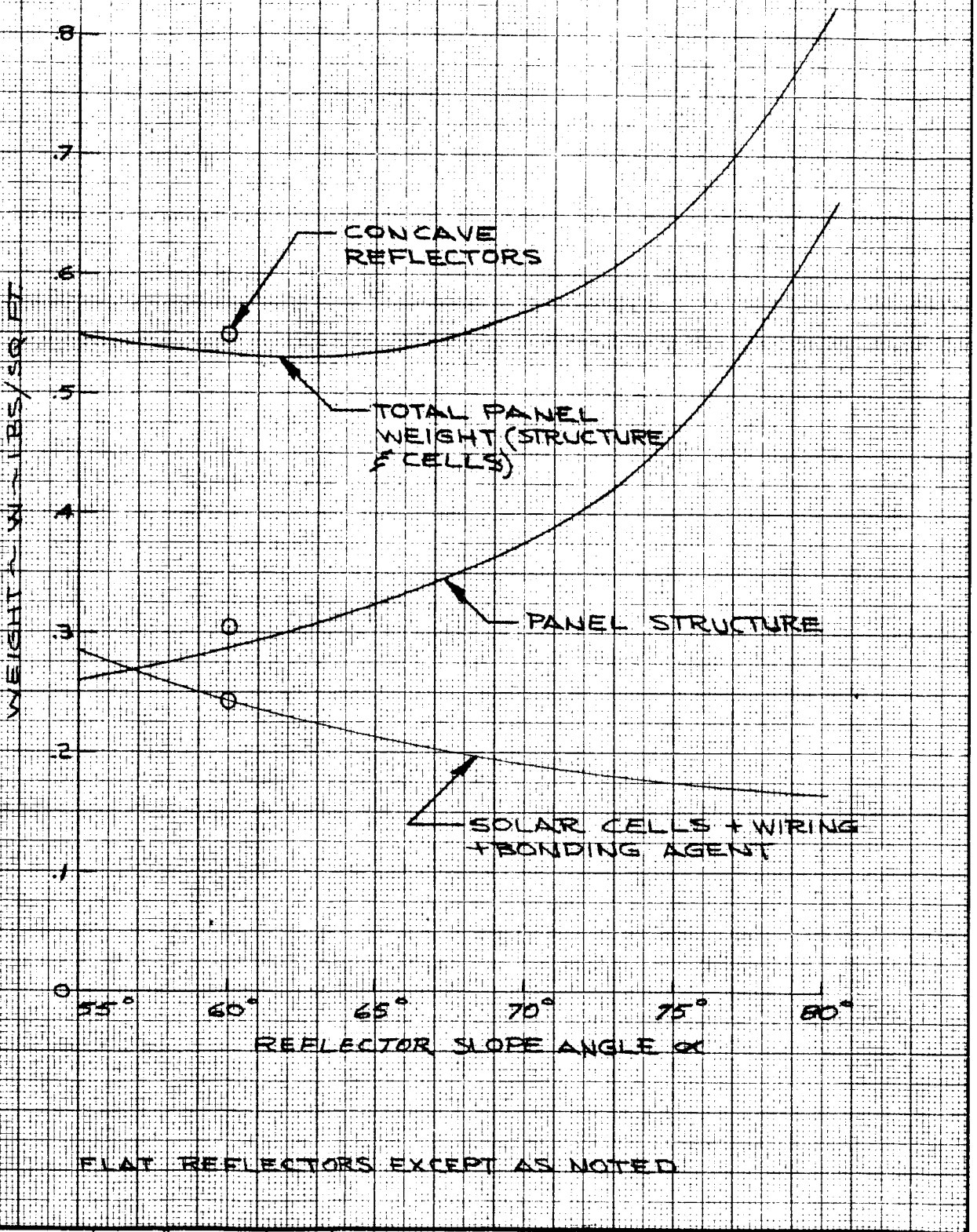

FLAT REFLECTORS EXCEPT AS NOTED

CALC			REVISED	DATE	CALCULATED WEIGHTS FOR V-RIDGE CONCENTRATORS
CHECK					
APR					
APR					

FIG. 6

D2-90041-A

BOEING AIRPLANE COMPANY

PAGE 15

where: A_r = projected active area of the reflectors
A_c = area of solar cells
S = solar intensity
η = conversion efficiency of solar cells
R = reflectance of reflectors

The power output (P_o) of a flat non-concentrating structure covered with solar-cells having the same stacking density is

$$P_o = A_o S \eta \qquad (15)$$

where A_o = area of the flat structure.

For equivalent power output, equations (14) and (15) are equated:

$$A_o S \eta = (A_c + R A_r) S \eta \qquad (14)$$

$$A_o = A_c + R A_r \qquad (16)$$

The ratio (A*) of concentrating structure area to non-concentrating structure area for equivalent power output is

$$A^* = \frac{A_c + A_r}{A_o} = \frac{A_c + A_r}{A_c + R A_r} \qquad (17)$$

$$= \frac{1 + \frac{A_r}{A_c}}{1 + \frac{R A_r}{A_c}} \qquad (17)$$

Values of A* are plotted in Figure 7.

The efficiency coefficient (C_E) includes the effects of reflectance and stacking density, and consequently represents the real power increase from a given number of solar cells due to the increased incident radiation per cell from the reflectors.

Use of the area requirement curve (Fig. 7) is illustrated by the following example:

> A flat panel design requires 100 sq. ft. of panel area to supply the required power for a given mission. The concentrator design has flat reflectors with base angles of 60 degrees. The measured C_E is 1.90 and A* is found to be 1.053. Then 105.3 sq. ft. of concentrator panel will be required to replace 100 sq. ft. of flat panel.

Normalized Weight Calculation

The weight requirement curves (Fig. 8) were based upon the area requirement curves and the weight/sq. ft. curve for the concentrator structure including solar cells and wiring. Auxiliary supporting structure weight is not included.

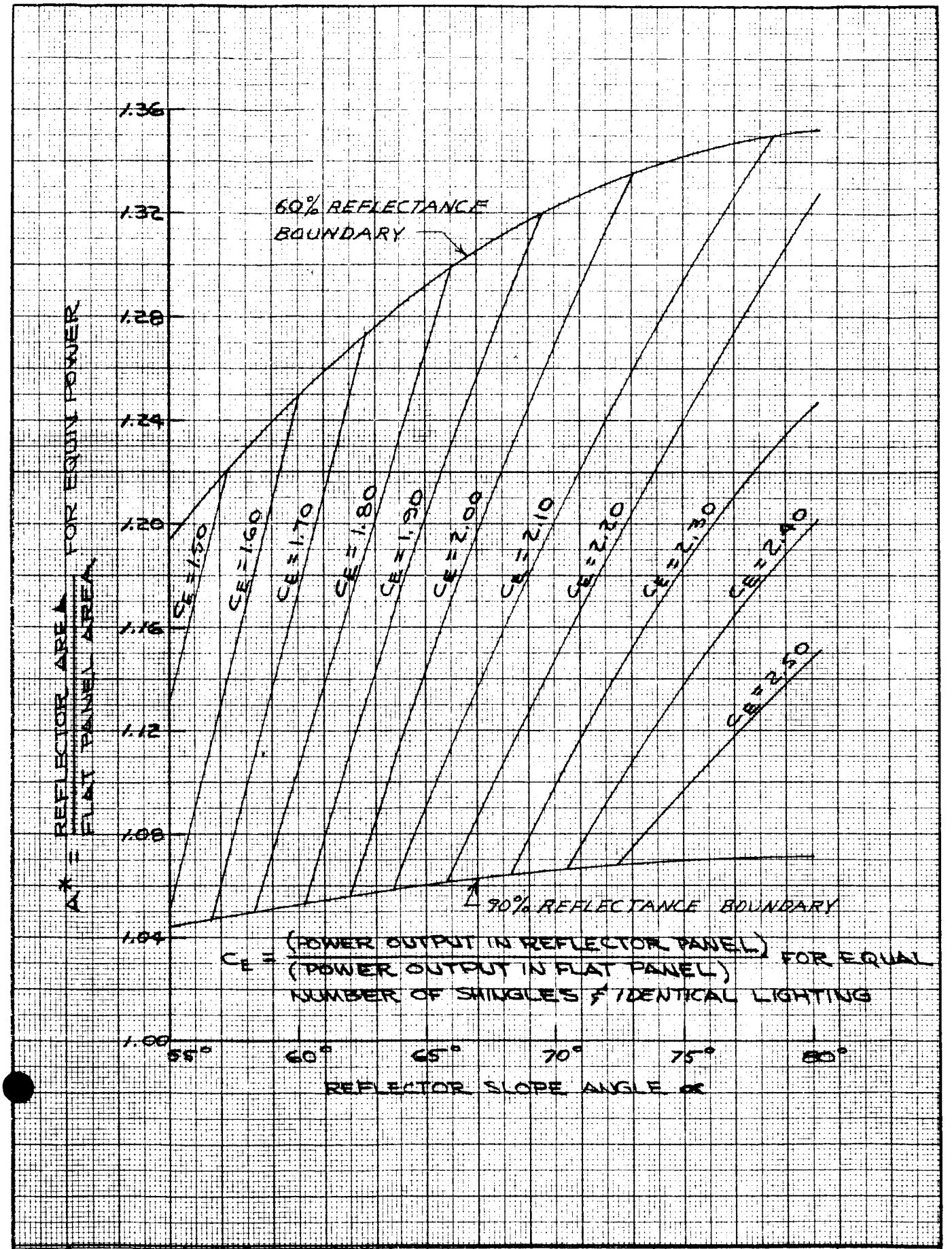

CALC			REVISED	DATE
CHECK				
APR				
APR				

AREA REQUIREMENTS FOR V-RIDGE PANELS

FIG. 7

D2-90041-A

BOEING AIRPLANE COMPANY

PAGE 17

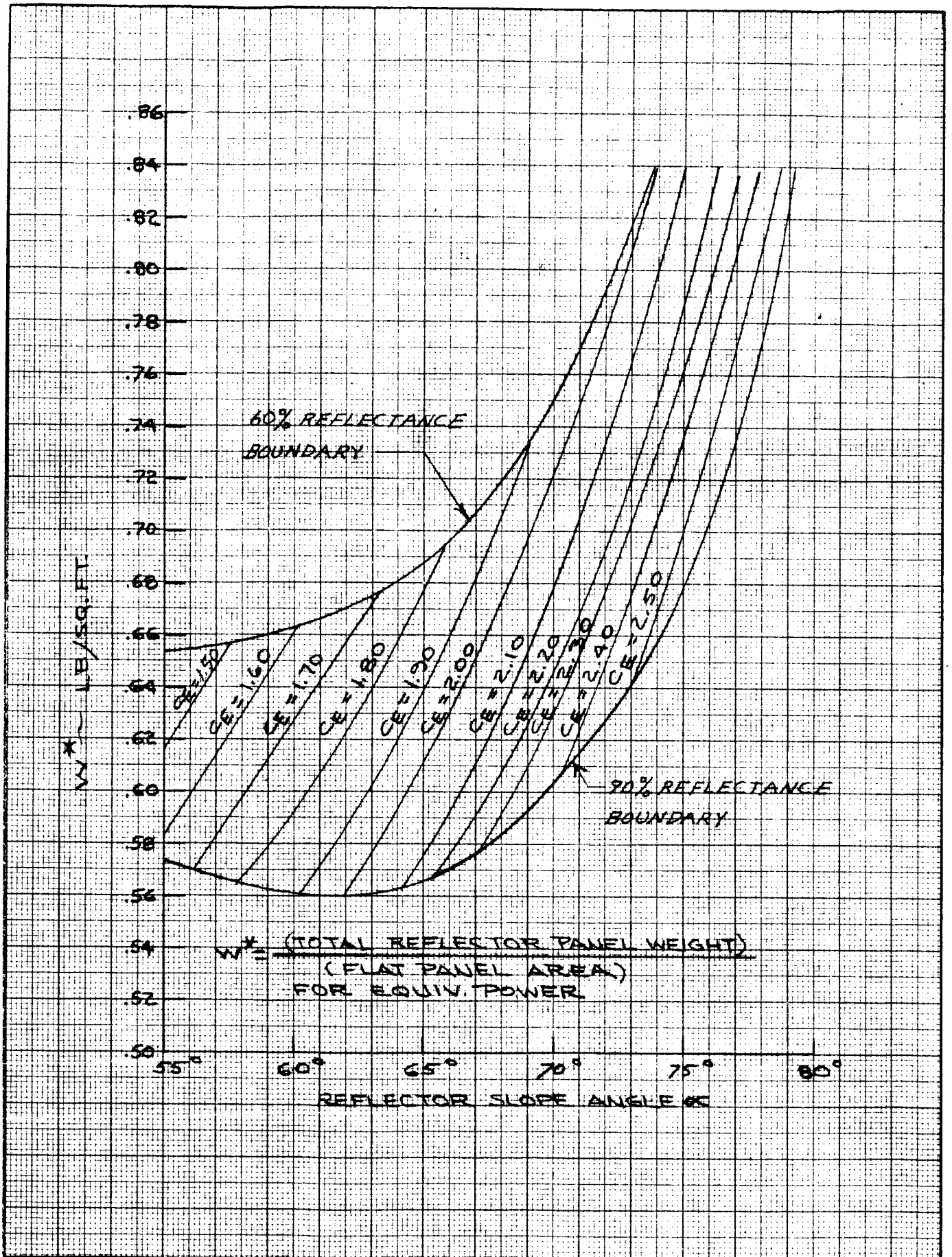

			REVISED	DATE
CALC				
CHECK				
APR				
APR				

WEIGHT REQUIREMENT FOR V-RIDGE PANELS WITHOUT AUXILIARY BEAMS

FIG. 8

D2-90041-A

BOEING AIRPLANE COMPANY

PAGE 18

The total weight (W_{cp}) of the concentrating panel producing the power output (P) is

$$W_{cp} = W(A_c + A_r) \tag{18}$$

From equation (17),

$$A^* A_o = A_c + A_r$$

Where A_o = total area of non-concentrating panel producing the power output (P).

Substituting this in equation (18),

$$W_{cp} = W A^* A_o \tag{19}$$

W* is defined as the ratio of total concentrating panel weight to non-concentrating panel area for equivalent power outputs:

$$W^* = \frac{W_{cp}}{A_o} \tag{20}$$

Substituting equation (19) in equation (20):

$$W^* = \frac{W A^* A_o}{A_o} \tag{21}$$

$$W^* = W A^*$$

The use of these curves is illustrated in a calculation using the same constants as the previous A* example.

Assuming C_E = 1.90 and α = 60 degrees

Then, W* = 0.56 lbs/sq. ft.

Thus the concentrator panel design total weight will be (0.56) (100)-56 lbs.

Limiting Strain on Solar Cells

The maximum allowable panel length without solar cell failure under static loading was calculated from the following classical equation for flexural strain:

$$\epsilon = \frac{My}{IE} = \frac{w''g''L_y^2}{8IE} \tag{22}$$

The resulting maximum panel lengths for various "g" loadings are plotted in Fig. 9.

The limiting value for ϵ was found by test to be 0.0003 inches/inch strain.

Thus $L^2 = (0.0003)\ \frac{8EI}{w''g''y}$ (23)

This was evaluated point by point since I, w, and y are all functions of the reflector angle (α). For example, if the loading is to be 10 "g" and the base angle for the reflector is 65 degrees, the maximum allowable simply supported length of corrugation is 75 inches, from the standpoint of solar-cell strain. However, such an unsupported length would be too long from a resonant frequency standpoint. Therefore resonant frequency considerations rather than solar-cell strain limits will determine panel sizes.

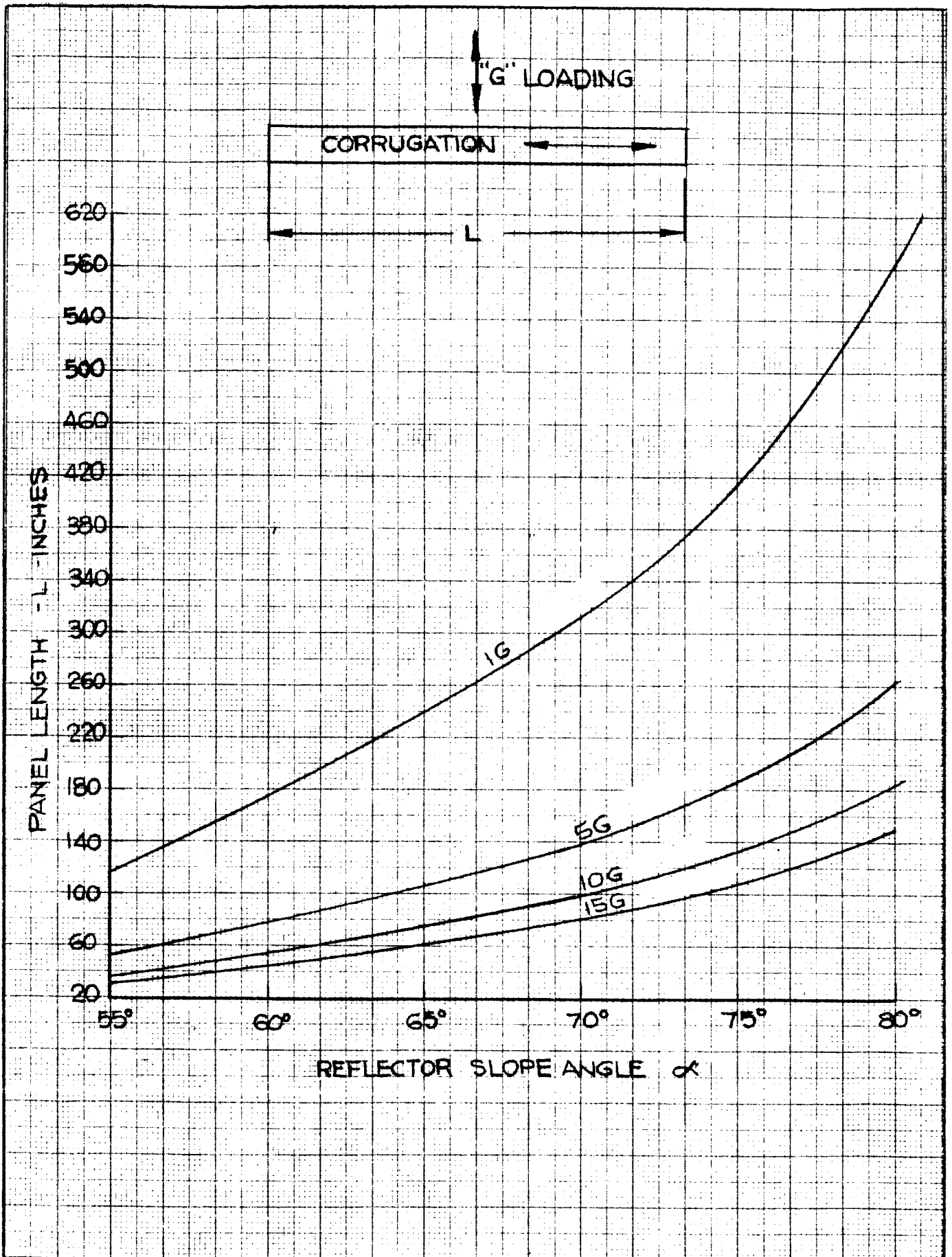

CALC			REVISED	DATE	MAXIMUM ALLOWABLE SIMPLY-SUPPORTED PANEL LENGTH WITHOUT SOLAR CELL FAILURE
CHECK					
APR					
APR					

FIG 9

D2-90041-A

THE BOEING COMPANY

PAGE 20

K-E ALBANENE 1951 50629

C. Thermal Analysis

The steady-state temperature of solar cells and a concentrating structure in space environment was estimated by a simple energy balance equating the incoming and outgoing heat fluxes.

$$\sum q_{in} = \sum q_{out} \tag{24}$$

The incoming flux, q_{in}, is that due to solar radiation incident on a unit area. The outgoing flux is comprised of the energy reflected back into space q_r, that converted by the cell to electrical energy q_e, and to heat q_h, plus that absorbed by the reflecting surfaces of the concentrator q_α, which also must be rejected as heat. Energy balance equation (24) becomes:

$$q_{in} = q_r + q_e + q_h + q_\alpha \tag{25}$$

The assumption that all radiating surfaces of the cell and structure are in an isothermal condition permits a first approximation of cell temperature by substitution of the sum of fluxes which are rejected as heat in Stefan's equation;

$$Q = \sigma \sum A E T^4 \tag{26}$$

The assumed values of emissivity, E , and fractions of radiating surface per unit area, A, are given in the Table below. T is the radiating surface temperature and σ is the Stefan-Boltzmann constant.

	Assumed Constants		
Surface	Emissivity	Absorptivity	Fraction of Unit Area (A)
Cell cover glass	0.84	0.78	0.25
Back coating	0.85	–	0.25 (back of cell) 0.25 (back of reflectors)
Reflecting surfaces	0.75	0.20	0.25

Thermal Conductivity (Cal/cm-sec-°C) - silicon 0.2; aluminum 0.4.

Solar Radiation (Milliwatts/cm^2) - Mars 47; Earth 140.

Cell Conversion Efficiency - 10 percent.

From these values the cell temperature, T, was computed. It was found to be approximately 49°C in a near-Earth space environment and -23°C in a near-Mars space environment.

An approximation of the temperature difference, ΔT, across the cell thickness was made using the Fourier equation for steady-state unidirectional heat flow,

$$Q = K \frac{A}{L} \Delta T \qquad (27)$$

In this equation K is the thermal conductivity of the silicon material, A is the area and L the thickness of the silicon layer. The application of Stefan's equation to find the heat radiated from the cell at the temperature determined by the first approximation, indicates that about 75 percent of q_h must be transmitted by conduction from the cell to the supporting structure. This portion of q_h would cause an insignificant temperature difference of 0.006°C across the cell.

To obtain an approximate structure temperature for a heat rejection computation, the temperature drop along the concentrator reflecting surfaces from root to apex was calculated with Eq. (27). The assumption that the heat rejected from each reflecting surface is directly proportional to its fraction of the projected unit area causes the distribution of 25 percent of q_h to each reflecting surface. The actual value of this ΔT obtained by calculation was 4.2°C. The mean effective reflector temperature using the first approximation of cell temperature is then about 47°C in the near-Earth environment and -25°C in the near-Mars environment.

A re-calculation of cell temperature using these reflector temperatures in Eq. 26 is then made to determine by difference, the portion of q_h which must be radiated from the cell itself. Re-use of Eq. 27 for calculating the temperature difference from the root to apex of the concentrator indicates the temperature of the cell would be approximately 50°C near Earth or -22°C near Mars. This result is nearly the same as that obtained in the first approximation.

The resulting cell temperature in the concentrator is only about 10°C [illegible]ve that expected in a conventional panel. To reduce the cell temperature in the concentrating panel one would try to increase the emissivities of the radiating surfaces and attempt to reflect away infrared radiation at the cover glass.

D. Application of Design Factors

The contract specifies the design objectives, in order of emphasis, as follows:

(1) Electrical-optical efficiency (high concentration ratio)

(2) Minimum weight

(3) Maximum structural rigidity

(4) Reliable electrical connections

It is further required that the specific power ratio be 90 percent or higher. The specific power ratio requirement is controlling and, for a given type of reflecting surface, dictates the required concentration ratio.

The illumination in watts falling upon the solar cells in a concentrating panel (I_c) has two components, the light energy received directly from the sun (I_d) and the light energy received from the reflectors (I_r). The relation between these components is

$$I_c = I_d + I_r \tag{28}$$

The power output (P) of the concentrating panel is

$$P = \eta_1 I_d + \eta_2 I_r \tag{29}$$

Where: η_1 = conversion efficiency of solar cells applicable to direct-light power output;

η_2 = conversion efficiency of solar cells applicable to reflected-light power output.

The reflected-light efficiency term (η_2) includes three factors that alter the direct-light conversion efficiency (η_1), so that

$$\eta_2 = \eta_1 \cdot \eta_c \cdot \eta_t \cdot \eta_a \tag{30}$$

Where: η_c = factor to account for a change in conversion efficiency resulting from an increase in the light intensity on the solar cells.

η_t = factor to account for a change in conversion efficiency resulting from a higher equilibrium solar-cell temperature.

η_a = factor to account for a change in conversion efficiency resulting from the reflected light striking the solar cells at an angle.

The direct illumination falling upon the solar cells is

$$I_d = A_c S \tag{31}$$

Where: A_c = active area of solar cells = $F_1 A_t$ (32)

S = solar intensity in milliwatts per sq. cm.

F_1 = factor to account for inactive area in the cell trough due to wiring and cell mounting allowances

A_t = gross area of cell trough.

Substituting equation (32) in equation (31):

$$I_d = F_1 A_t S \tag{33}$$

The illumination falling upon the reflectors (I_R) is

$$I_R = A_r S \tag{34}$$

Where: A_r = projected area of reflector

Illumination reflected to the active solar-cell area is

$$I_r = F_2 K R I_R \tag{35}$$

Where: F_2 = factor to account for loss in reflector area due to bending radii, cell height and inactive space between cells in trough;

K = factor to account for light scatter resulting from manufacturing variations;

R = reflectance of reflector surface.

Substituting equation (34) in equation (35):

$$I_r = F_2 K R A_r S \tag{36}$$

Substituting equations (33) and (36) in equation (29):

$$P = \eta_1 F_1 A_t S + \eta_2 F_2 K R A_r S \tag{ }$$

$$= S\left[\eta_1 F_1 A_t + \eta_2 F_2 K R A_r\right] \tag{ }$$

$$= A_t S\left[\eta_1 F_1 + \eta_2 F_2 K R \frac{A_r}{A_t}\right] \tag{37}$$

The power output of a conventional flat panel (P_o) having the same total projected area as the concentrating panel ($A_t + A_r$) is

$$P_o = \eta_1 S F_3 (A_t + A_r)$$

$$= \eta_1 S F_3 A_t (1 + \frac{A_r}{A_t}) \qquad (38)$$

Where: F_3 = factor to account for wiring and cell mounting allowances. This was set at 85 percent by the contract.

The specific power ratio (SPR) by definition is

$$SPR = \frac{P}{P_o} \qquad (39)$$

Substituting equations (37) and (38) in equation (39):

$$SPR = \frac{A_t S \left[\eta_1 F_1 + \eta_2 F_2 K R \frac{A_r}{A_t}\right]}{\eta_1 S F_3 A_t (1 + \frac{A_r}{A_t})}$$

$$= \frac{\eta_1 F_1 + \eta_2 F_2 K R \frac{A_r}{A_t}}{\eta_1 F_3 (1 + \frac{A_r}{A_t})} \qquad (40)$$

The power concentration ratio (C_p) is defined as the ratio of the power output (P) of a concentrating panel to the power output of the solar cells without concentration, i.e., with reflectors shaded:

$$C_p = \frac{\eta_1 F_1 A_t S + \eta_2 F_2 K R A_r S}{\eta_1 F_1 A_t S}$$

$$= 1 + \frac{\eta_2 F_2 K R A_r}{\eta_1 F_1 A_t} \qquad (41)$$

To design concentrators, it is necessary to establish values for the design factors. Some of these factors had to be evaluated by special tests which are described in Section IV. Others were determined by calculation or estimated.

η_1 = direct-light conversion efficiency of the solar cells at space-level solar intensity, which was established to be 10 percent from the manufacturer's rating at 140 milliwatts per sq. cm.

η_c = 100 percent, since preliminary tests showed that the quantum efficiency of gridded cells does not decrease as the light intensity is increased within the applicable range of light intensities. (See Figs. 12 and 14)

η_t = 100 percent, since the temperature effects are not to be considered in this contract.

η_o = 98 percent, since tests showed that the quantum efficiency is reduced by 2 percent for oblique light at a 60° angle of incidence.

η_2 = reflected-light conversion efficiency, which equation (30) specifies to be the product of the above four factors:

$$\eta_2 = (0.10)\ (1.00)\ (1.00)\ (0.98) = 9.8 \text{ percent}$$

The area factors F_1 and F_2 must be calculated. The sketch shows the parameters which affect these area factors. The overall dimensions of a 5-cell shingle are 0.788 by 1.80 inches, while the active portion of the shingle is in effect 0.788 by 1.75 inches. Since the cells are interconnected on the back side of the panel, a spacing of 0.10 inch between shingles is adequate for the wiring. Thus, a 5-cell shingle with wiring will occupy 1.90 inches of trough length. Because of concentrator and cell tolerances, it is necessary to make the trough somewhat wider than the shingle. A trough width of 0.8 inch was found to be adequate. With these data F_1 can be evaluated from equation (32) on a per-shingle basis:

$$F_1 = \frac{A_c}{A_t} = \frac{(0.788)(1.75)}{(0.80)(1.90)} = 0.91$$

The spacing factor for the reflectors (F_2) is more involved. A bending radius of 0.010 inch was used in forming the aluminum sheet. It was assumed that the reflector area at the bend lines is ineffective. With the 0.010 inch bending radius, each of the two bends required for a facet will consume about 0.009 inch of the projected width of the reflector.

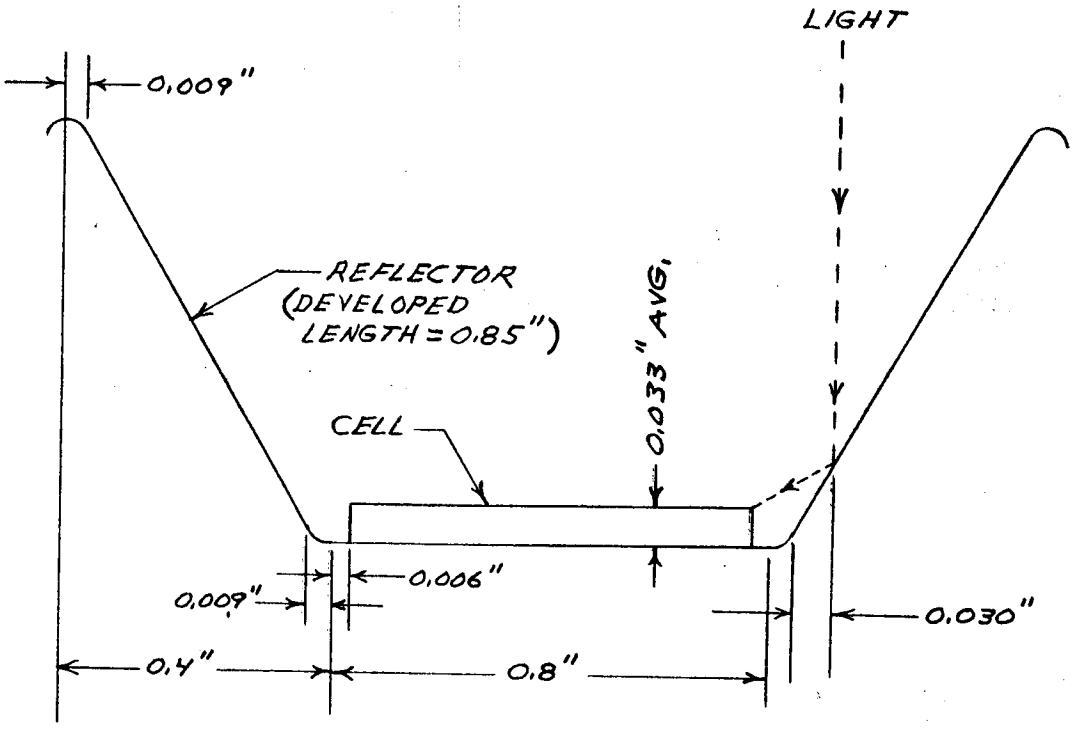

Another loss results from the cell surface being above the trough. With a bonding layer 0.003 inch thick, the cell surfaces will be at an average of 0.033 inch above the trough. The light reflected into the crevice between the cell and reflector will be lost. This will reduce the projected width of each reflector by 0.030 inch.

The loss in usable projected width of each of the 0.4 inch wide reflectors is therefore 0.018 + 0.030 = 0.048 inch. The ratio of usable projected reflector width to actual projected reflector width is:

$$\frac{0.400 - 0.048}{0.400} = 0.88$$

The reflector will illuminate the complete trough length, although active cell area occupies 1.75 inches of each 1.90 inch illuminated. The ratio of usable reflector length to actual reflector length is therefore:

$$\frac{1.75}{1.90} = 0.92$$

The reflector area factor (F_2) is the product of the width and length ratios:

$$F_2 = (0.88)(0.92) = 0.81$$

The reflectance (R) of an aluminized lacquer surface was found by measurement to be 0.82 in the part of the spectrum in which the solar cell is sensitive.

The scatter factor (K) was estimated to be 0.97, since it was not possible to determine this factor until after the models were built.

Substituting the above values into equation (40) for specific power ratio gives

$$SPR = \frac{(0.10)(0.91) + (0.098)(0.81)(0.97)(0.82)\left(1 + \frac{A_r}{A_t}\right)}{(0.10)(0.85)\left(1 + \frac{A_r}{A_t}\right)}$$

$$= \frac{0.091 + (0.063)\frac{A_r}{A_t}}{(0.085)\left(1 + \frac{A_r}{A_t}\right)} \qquad (42)$$

Equation (42) can be solved for A_r/A_t by setting SPR = 0.90, which is the contract requirement for CS-1. It will be found that with the above constants, an SPR of 0.90 can be obtained only with an A_r/A_t of 1.08 or less. Once the A_r/A_t ratio is established, the power concentration ratio can be computed from equation (41).

$$C_p = 1 + \frac{(0.098)(0.81)(0.97)(0.82)(1.08)}{(0.10)(0.91)}$$

$$= 1.75$$

An A_r/A_t ratio of 1.0 was chosen for EOM and CS-1 concentrators. An A_r/A_t of 1.0 corresponds to a reflector angle of 60° which is close to the optimum as is shown in Section III-A.

The above analysis was performed at the beginning of the contract period using available information and some approximations in order to arrive at an A_r/A_t ratio for prototype and EOM concentrators. Subsequent tests and observations suggest changes in some of the factors. For example, JPL has observed that 92 percent would be more realistic for the area utilization factor (F_3). Also, recent tests on the gridded 10-percent efficient blue-sensitive cells used in the concentrators show an increase of 6 percent in conversion efficiency for the applicable increase in intensity. This makes factor (η_c) = 1.15. Furthermore, improved wiring techniques developed for the CS concentrator allow a closer spacing of the solar-cell shingles in the troughs. This changes factor (F_1) to 0.93 and factor (F_2) to 0.83.

IV. BASIC INVESTIGATIONS

It was necessary to develop certain design criteria before the analytical design could be made. These design criteria were developed partly in the course of Boeing research prior to the award of this contract, and partly during the contract duration. The development of design criteria involved investigations into the performance of solar cells in high light intensities, the performance of solar cells and cover glasses under non-normal incident light, the effect of curved reflectors, and the reflectances of possible reflecting surfaces.

A. Solar-Cell Performance at High Light Intensities

The efficiency of solar cells irradiated at illumination levels from 50 to 500 milliwatts/sq. cm. and at temperatures from 17 to 45°C was measured. Both gridded 13-percent nominal efficiency and 10-percent non-gridded solar cells of the conventional type were tested. Also, the efficiency of Hoffman blue-sensitive solar cells under different light intensities has been measured in Boeing research.

Illumination was provided with a light source (Fig.10) which employed a diffusion screen for controlling illumination intensity. Cell temperature was controlled with a water-cooled cell holder. Accessory equipment included variable cell-output resistors, instruments for measuring cell current and voltage, an X-Y plotter for tracing voltage-current curves, and a precision potentiometer for monitoring the cell temperature-sensing thermocouple.

The uniformity of the illumination at the cell holder was measured with a cell fragment. The results of this check are shown in Fig. 11 where relative flux as represented by short-circuit cell current is shown at three levels of illumination. The illumination variations over the cell holder area which is normally occupied by the test cells were quite small, especially at the lower illumination intensities. It should be noted that the lamp and diffusion screen arrangement is not a collimated light source. However, since the flux was uniform within one percent at the lower levels of illumination and in the order of 10 percent at high intensities, the results were considered to be as significant as if a collimated source had been used.

The distance between the diffusion screen and the light source was adjusted to achieve the desired illumination at the test cell. The cell temperature was established with constant-temperature water circulating through the cell-holder. After equilibrium conditions were reached, the cell-output resistance was varied from zero to infinity to obtain a voltage-current (V-I) curve. Fluxes from 50 to 500 milliwatts per sq. cm. were used in increments as small as 25 milliwatts/cm^2.

The point of maximum power on each V-I curve was established with the aid of a transparent overlay on which curves of constant power versus current and voltage had been plotted.

The data obtained from the V-I curves were reduced to plots of efficiency at maximum power output versus illumination intensity (Figs. 12 and 13). It is interesting to note that the maximum efficiency points of the gridded cells occurred at higher illumination levels than maximum-efficiency points of the non-gridded cells. Maximum efficiencies were achieved for gridded cells at illumination levels greater than direct sunlight in a near-Earth space environment. The efficiency of gridded cells is consistently high through the illumination range up to and above a concentration ratio of two. The non-gridded cells show a definite drop in efficiency for illumination levels experienced in a near-Earth space environment as compared to the efficiencies obtained with Earth-surface intensities. The effect of temperature on cell efficiency agrees with published data.

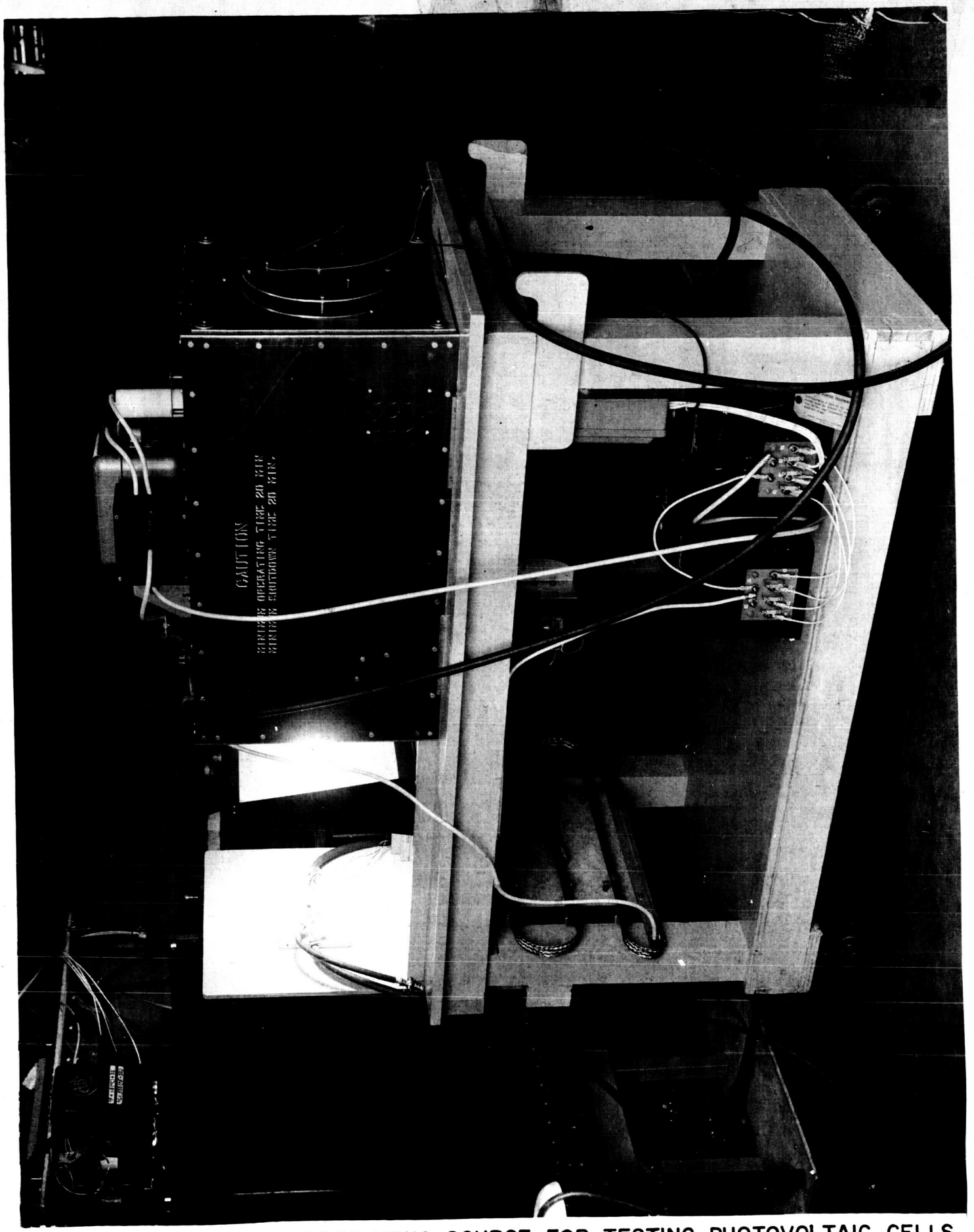

XENON-ARC SOLAR SIMULATING SOURCE FOR TESTING PHOTOVOLTAIC CELLS

FIG. 10

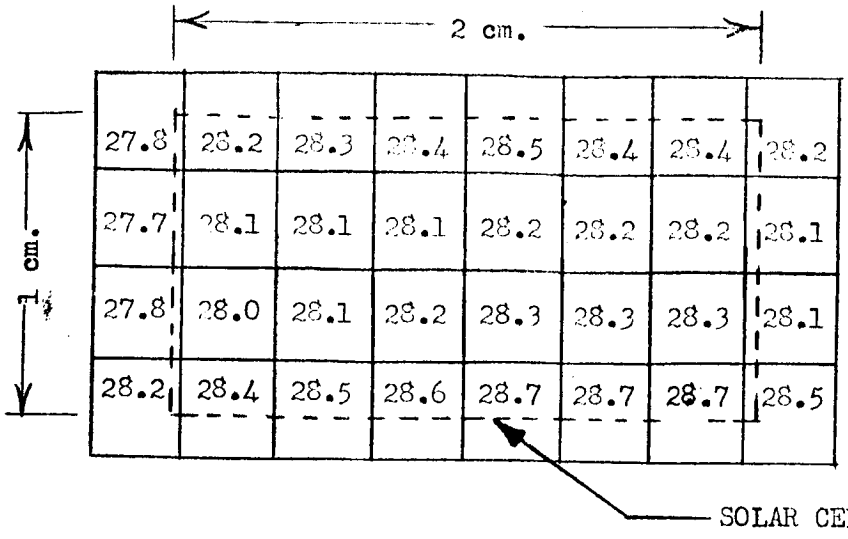

55.4	56.4	57.2	57.7	57.9	58.2	58.1	58.1
55.2	56.6	57.3	57.7	57.9	57.9	57.6	59.3
55.2	56.2	57.0	57.5	57.8	57.9	57.7	57.1
55.2	55.9	56.8	57.2	57.5	57.4	57.2	56.6

200 MW/CM2

7 percent variation

104.7	109.1	112.3	114.7	115.7	115.7	114.1	111.3
105.7	109.5	112.3	114.6	115.6	115.3	114.0	111.3
105.4	100.3	112.1	114.2	114.6	114.5	113.1	110.9
103.8	107.3	110.5	113.1	113.7	113.4	111.7	118.7

400 MW/CM2

10 percent variation

PLOT OF THE RELATIVE FLUX DENSITY AT THE CELL HOLDER WHEN ILLUMINATED AT VARIOUS INTENSITIES WITH THE XENON LAMP.

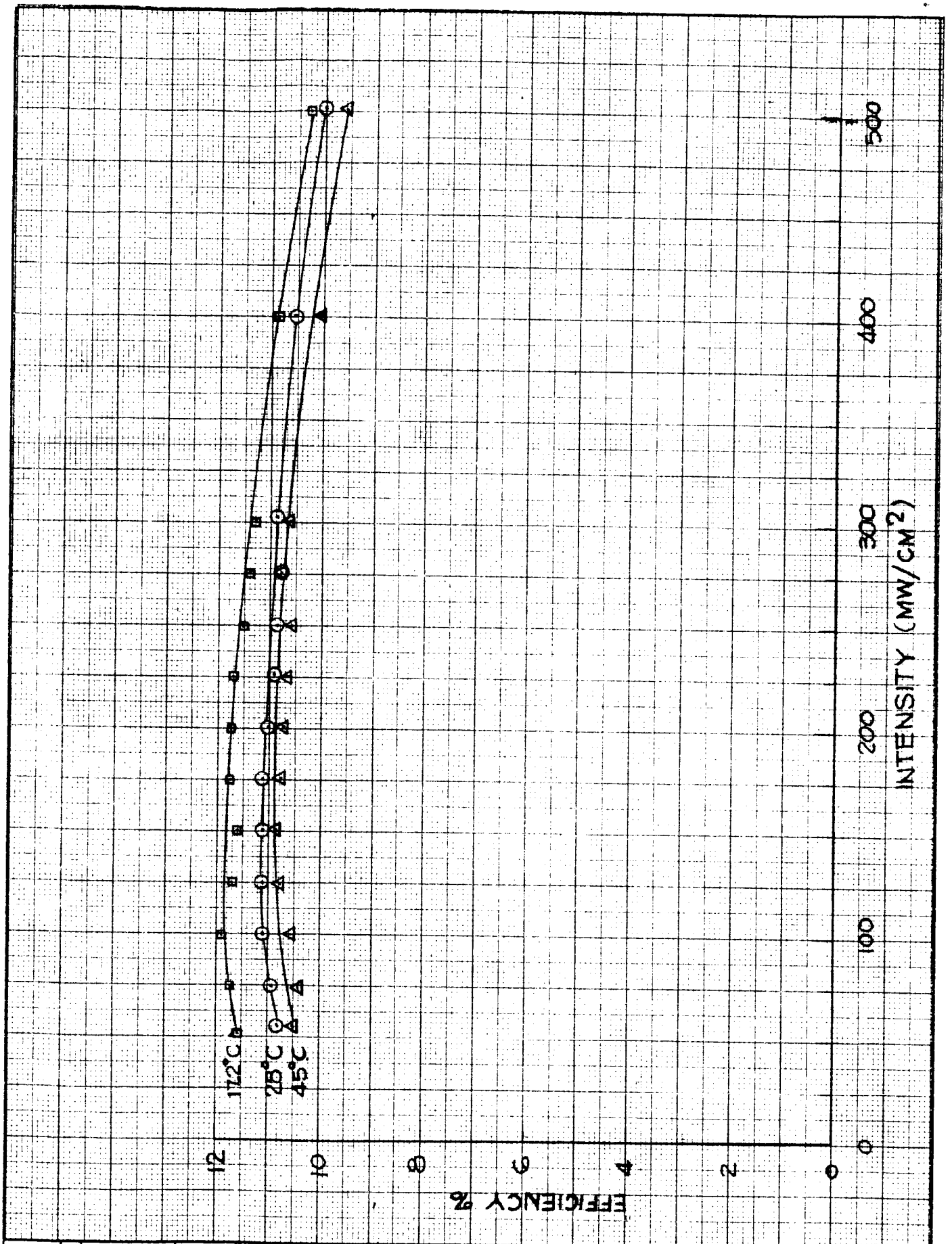

CALC			REVISED	DATE	EFFICIENCY AS A FUNCTION OF INTENSITY & TEMPERATURE FOR HOFFMAN P-N 13% CELL (COVERED)
CHECK					
APR					
APR					
					THE BOEING COMPANY

FIG 12

D2-90041-1

PAGE 32

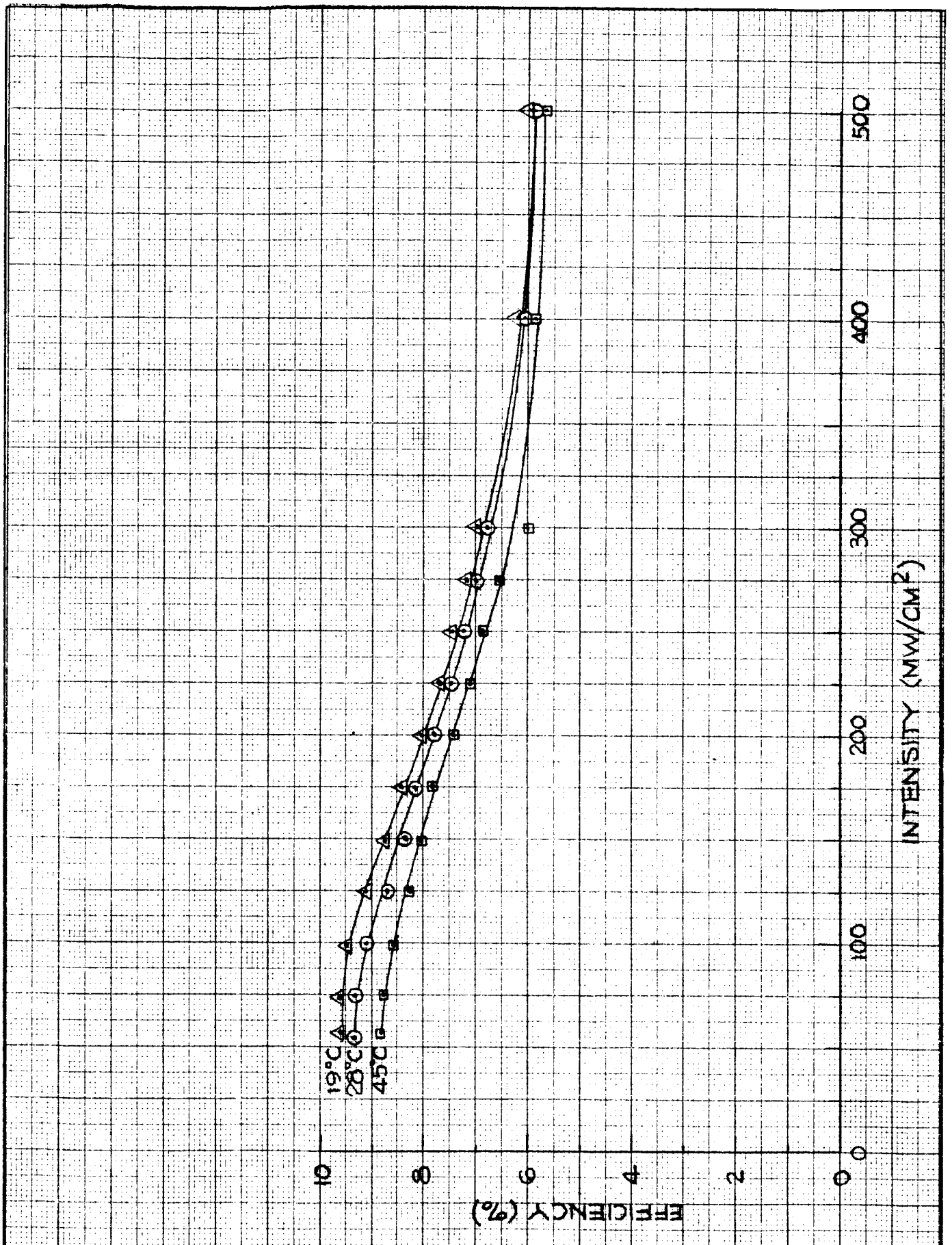

CALC			REVISED	DATE	EFFICIENCY AS A FUNCTION OF INTENSITY & TEMPERATURE FOR HOFFMAN P-N 10% CELL
CHECK					
APR					
APR					
					THE BOEING COMPANY

FIG 13

D2-90041-A

PAGE 33

It is necessary to compare conventional solar cells with the new blue-sensitive cells from the standpoint of efficiency as a function of light intensity. In Fig. 14 is plotted the efficiency of a blue-sensitive cell as a function of light intensity. This is representative of data obtained in recent tests. It will be noted that the efficiency improves with light intensity up to 300 milliwatts per sq. cm., and that the drop in efficiency as light intensity is increased from 300 milliwatts per sq. cm. to 500 milliwatts per sq. cm. is not significant. The blue-sensitive cells appear to be definitely better than conventional solar cells for application to concentrating photovoltaic power sources.

From these test results it is apparent that the use of gridded cells is feasible for concentration ratios of two and higher if cell temperatures can be kept low.

B. Solar-Cell Performance with Non-Normal Incident Light

A solar cell in a V-ridge concentrator is illuminated by both normal incidence light from the sun and non-normal incidence light from the reflectors. The performance of a cell under normal incidence light is well understood. On the other hand, no usable data on the performance of a solar cell and cover-glass combination using non-normal incidence light could be found in the literature. Since the V-ridge concentrator depends upon reflected light to increase solar-cell output, the relation between incidence angle of the illumination and conversion efficiency of the cell is important.

Initial investigations were directed toward determining the cover-glass transmittance and the solar-cell output as a function of angle of incidence of the incoming light. For example, spectral cover-glass transmittance was measured to confirm data furnished by Optical Coating Laboratory, Inc. (OCLI) (Fig. 15), and Bausch and Lomb.

It soon became apparent that independent measurements of cover glass and solar-cell performance were of little value. For example, the installation of an OCLI cover glass on a 13-percent efficient solar cell illuminated by a zirconium lamp caused an 8-percent drop in solar-cell output. A drop in output of about 16 percent would be expected based on a 92 percent transmittance of the cover glass in air, and an 8 percent loss in short-circuit current due to the reflection of wavelengths shorter than the cutoff (0.45 microns). The failure to observe the expected loss suggests that the transmittance of a cover glass in air does not apply when the glass is bonded to the cell.

This observation was confirmed in tests with 4-percent efficient solar cells. Here, the presence of an OCLI cover glass resulted in a reduction in output of less than 2-1/2 percent. This low loss of output can be explained by the fact that these low-efficiency cells have little response to radiation of less than 0.450 microns wavelength.

It appears that while the cover glass has a first surface reflection loss at wavelengths greater than 0.450 microns wavelength, the bare solar cell also has a surface reflection loss of about the same magnitude. However, in the assembly, the cover glass, epoxy bonding cement, and cell surface were apparently well matched in index of refraction and the only significant reflection loss in the combination occurred at the surface of the cover glass.

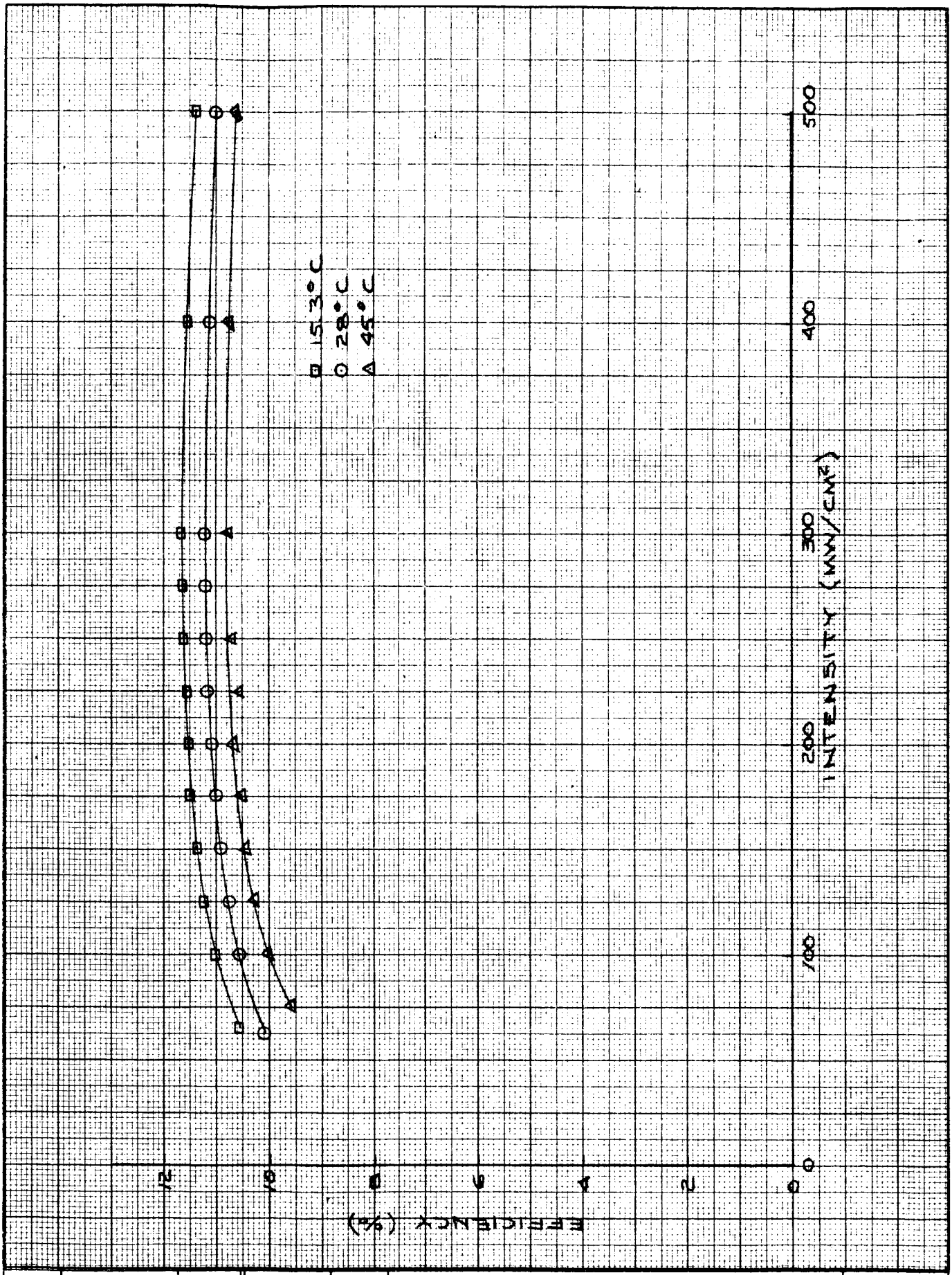

CALC			REVISED	DATE	EFFICIENCY AS A FUNCTION OF INTENSITY AND TEMPERATURE FOR HOFFMAN 10% BLUE CELL
CHECK					
APR					
APR					BOEING AIRPLANE COMPANY

FIG. 14

D2-90041-A

PAGE 35

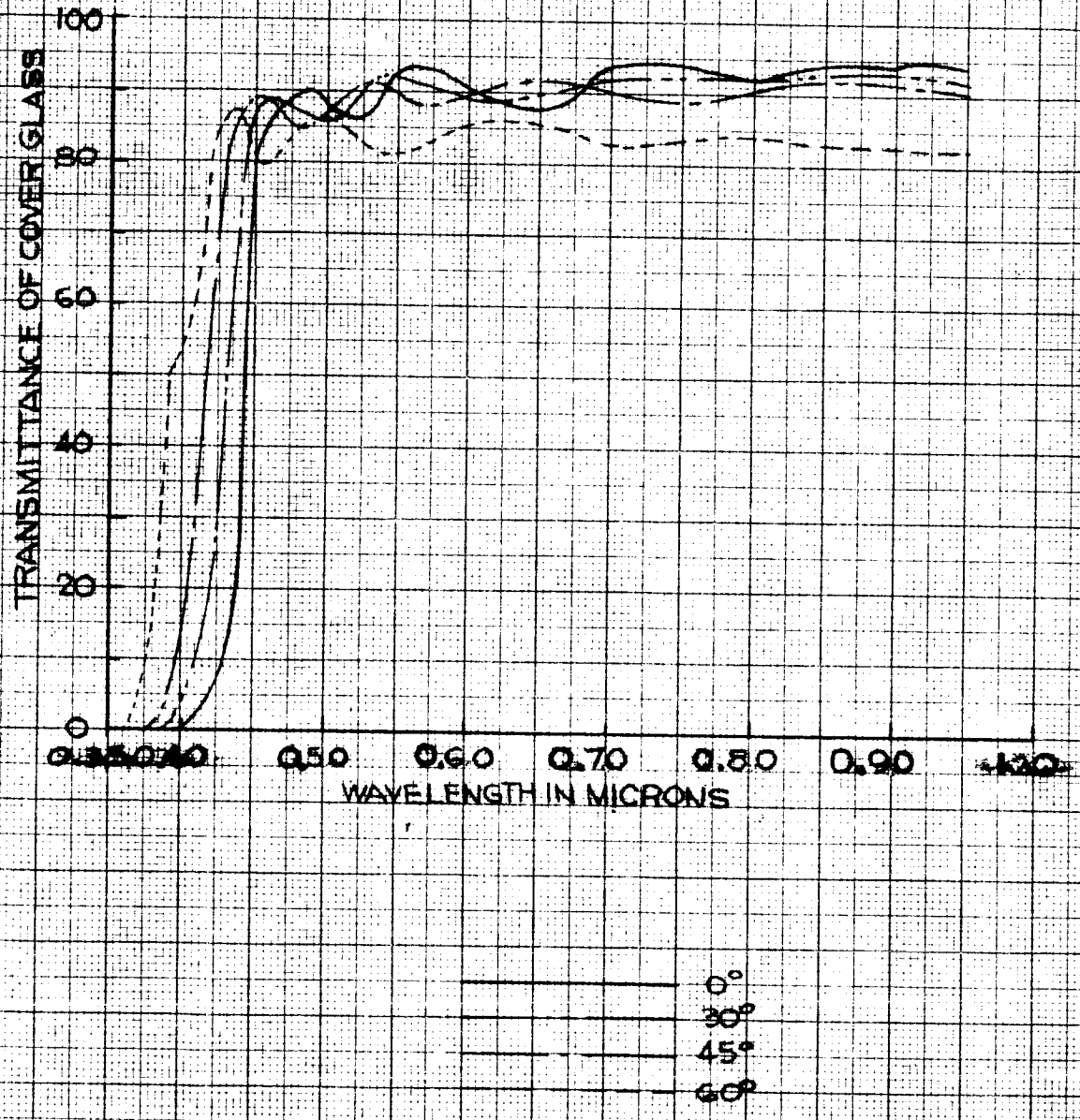

CALC			REVISED	DATE	SPECTRAL TRANSMITTANCE OF OCLI COVER GLASS AS A FUNCTION OF ANGLE OF LIGHT INCIDENCE
CHECK					
APR					
APR					
					THE BOEING COMPANY

FIG 15

D2-900/1-A

Attempts to confirm this supposition directly have been frustrated by the difficulty of measuring the index of refraction of the solar-cell surface.

In subsequent tests, solar-cell output was measured as a function of angle of incidence of the uniform-intensity incoming light. These measurements were made with cells having nominal efficiencies of 4 and 13 percent, and with and without 0.006 inch thick cover glasses.

The test setup is shown in Fig. 16. The light source was a 25-watt zirconium-arc lamp located at the focus of an achromatic lens. The lens was stopped down to insure that the beam was collimated and uniform in intensity. The cell was mounted on a rotatable test stand having an engine-divided quadrant.

The results of these tests are shown in Fig. 17, 18, 19, and 20. Note that in general the short-circuit current of an uncovered cell approximated a cosine curve, as is generally reported in the literature. With three of the four cells tested, the short-circuit current was about 2 to 30 percent less than the cosine curve. The larger deviations occurred at the larger angles of incidence. In one cell (No. 4) the short-circuit current was coincident with the cosine function until the incidence angle reached 55 degrees and became less than the cosine function for larger angles.

It should be noted that cell output was measured in terms of short-circuit current. It is a well established fact that in a given cell each short-circuit current defines a volt-ampere curve, and hence a maximum power point. Thus a higher short-circuit current in a given cell indicates that a higher maximum-power point is available.

The installation of an OCLI cover glass (No. 207-SCC450-2) on a solar cell produced an interesting effect. At normal incidence, the presence of the cover glass resulted in a 2 to 6 percent decrease in short-circuit current. As explained above, this decrease is caused by the reflection of radiation having wavelengths less than 0.450 microns by the cover glass. However, as the incident angle increases, the OCLI cover glass has the effect of increasing the output of the cell relative to the output of an uncovered cell. The two curves cross between 20 and 50 degrees angle of incidence. At larger angles, the short-circuit current of the covered cell more closely approximates the cosine function. For example, at 60 degrees the short-circuit current of the uncovered 13-percent cell is 10 percent less than the cosine function. However, the same cell when covered with an OCLI glass has a short-circuit current that is only 2 percent less than the cosine function. This is significant because it means that the conversion efficiency of the covered cell, illuminated with oblique light having a given energy-content, is only slightly less than it is with the same light energy at normal incidence. The cause for this behavior has not been fully established, but it appears to be a result of the anti-reflectance film.

The Bausch and Lomb cover glass (#3722) did not exhibit this behavior. The output of a cell with this glass was reduced 6 percent at normal incidence and remained about 6 percent below that of the uncovered cell for all angles of incidence.

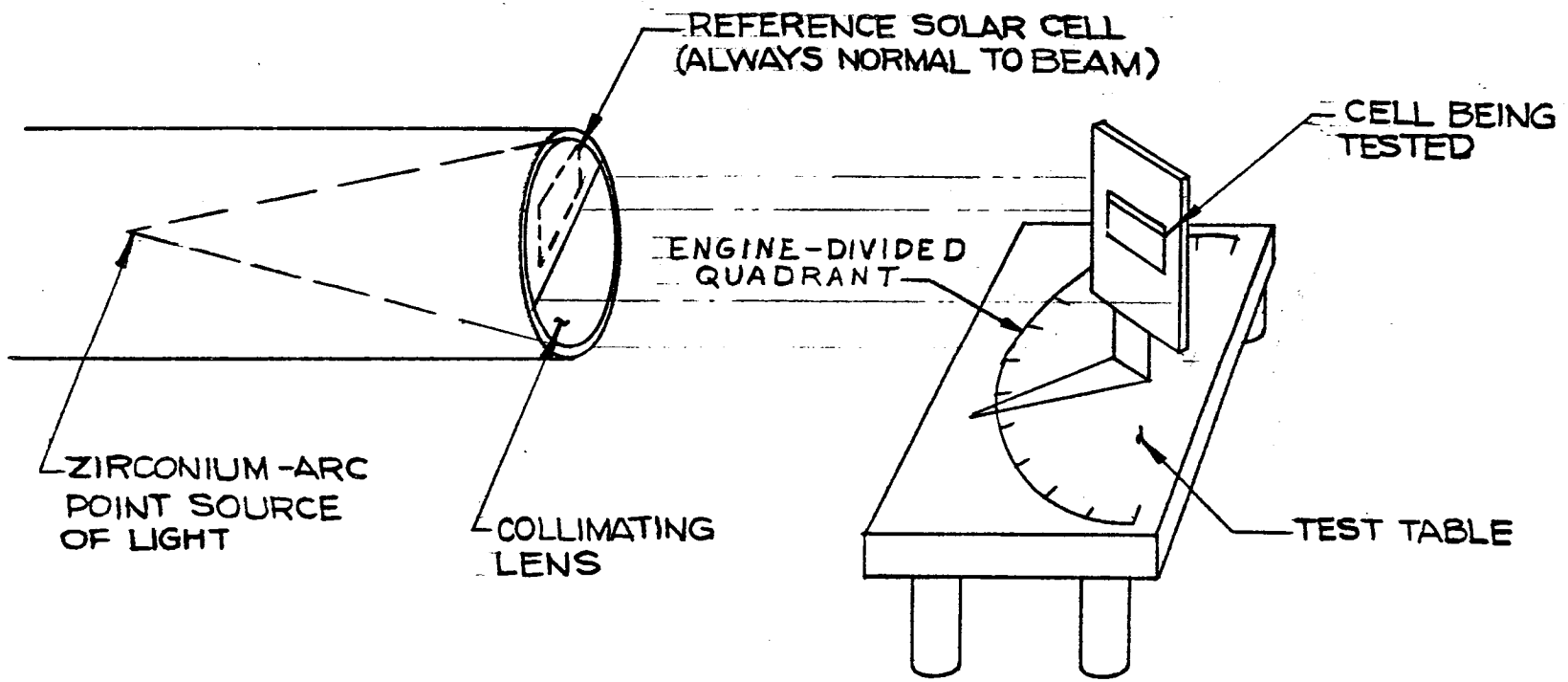

EXPERIMENTAL APPARATUS FOR DETERMINING SOLAR CELL OUTPUT AS A FUNCTION OF INCIDENT ANGLE OF LIGHT

FIG 16
Page 38
M2-9004-1-A

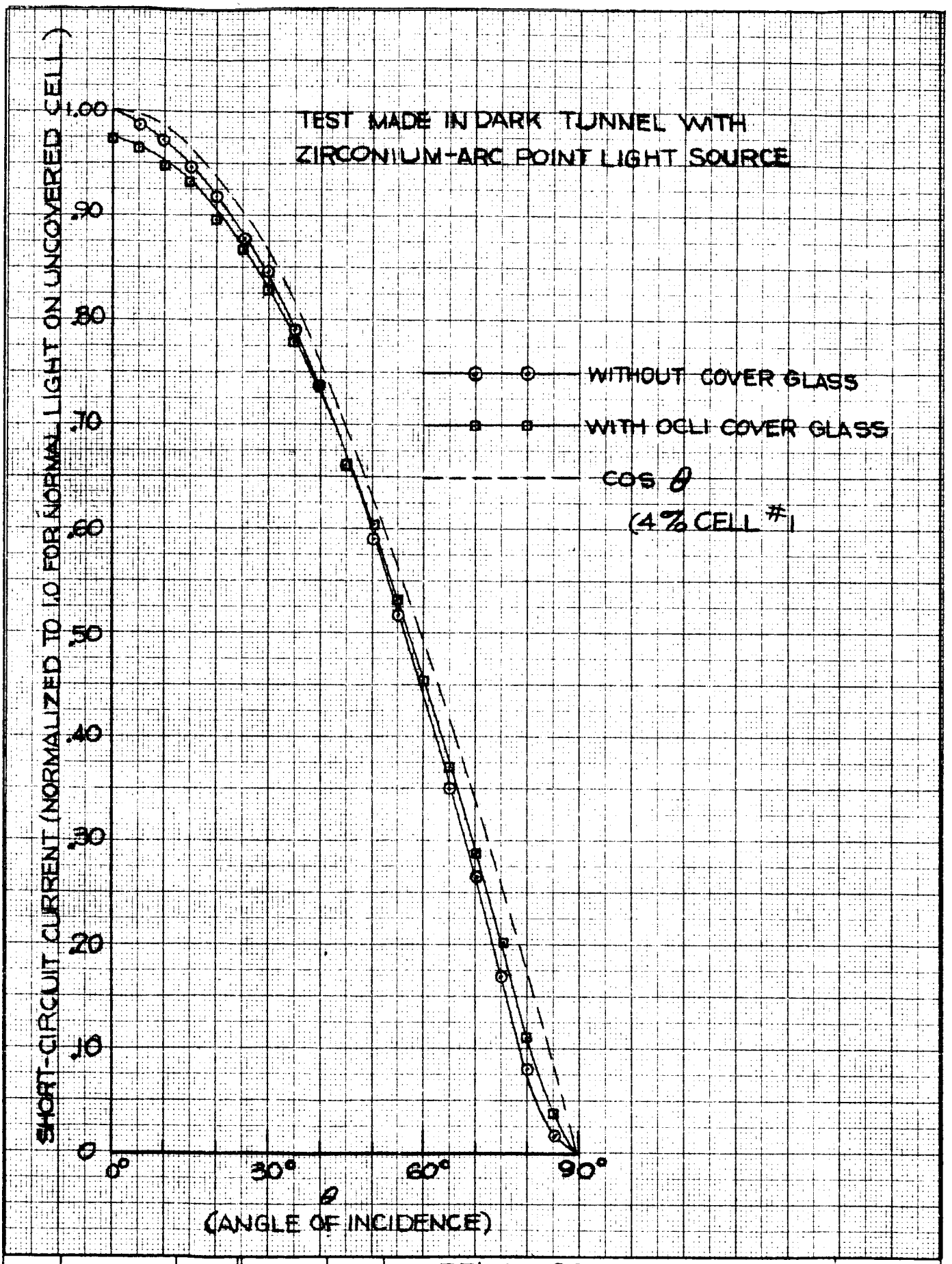

			REVISED	DATE
CALC				
CHECK				
APR				
APR				

HOFFMAN SOLAR CELL OUTPUT VS ANGLE OF INCIDENT LIGHT

FIG 17

D2-90071-1

THE BOEING COMPANY

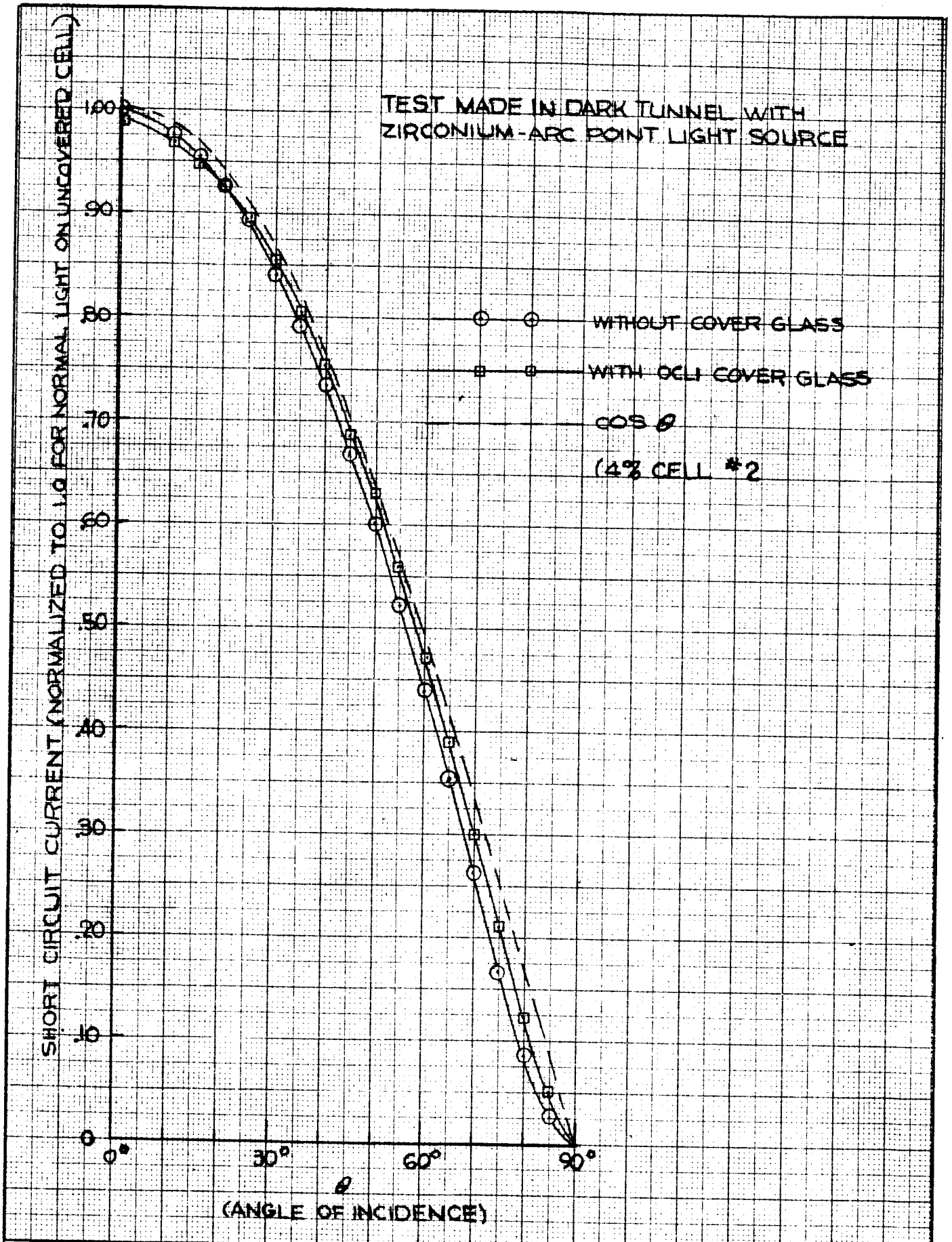

CALC			REVISED	DATE	HOFFMAN SOLAR CELL OUTPUT VS ANGLE OF INCIDENT LIGHT
CHECK					
APR					
APR					
					THE BOEING COMPANY

FIG 18

D2-90041-1

PAGE 40

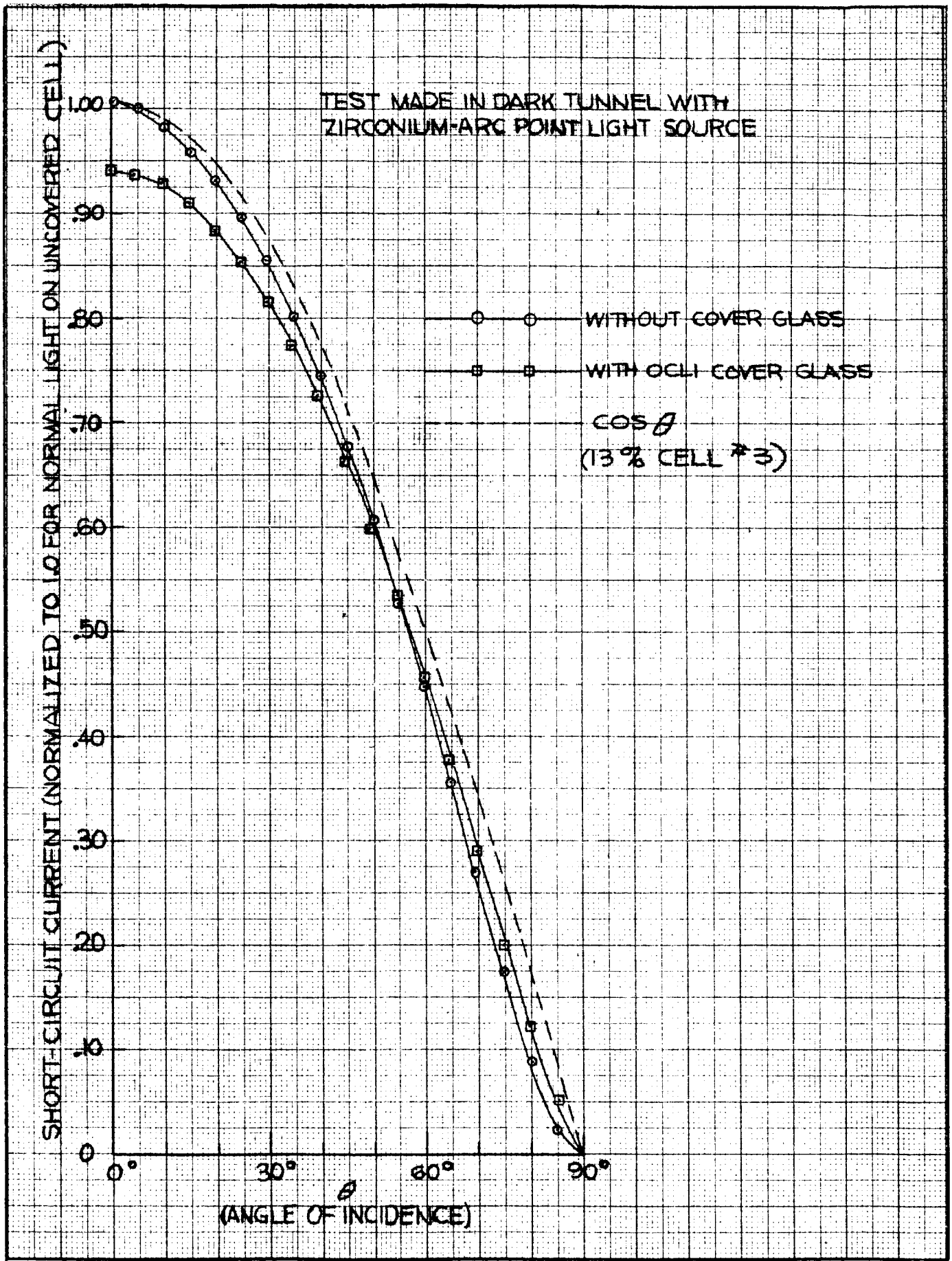

CALC			REVISED	DATE	HOFFMAN SOLAR CELL OUTPUT VS ANGLE OF INCIDENT LIGHT
CHECK					
APR					
APR					
					THE BOEING COMPANY

FIG 19

D2-20041-A

PAGE 41

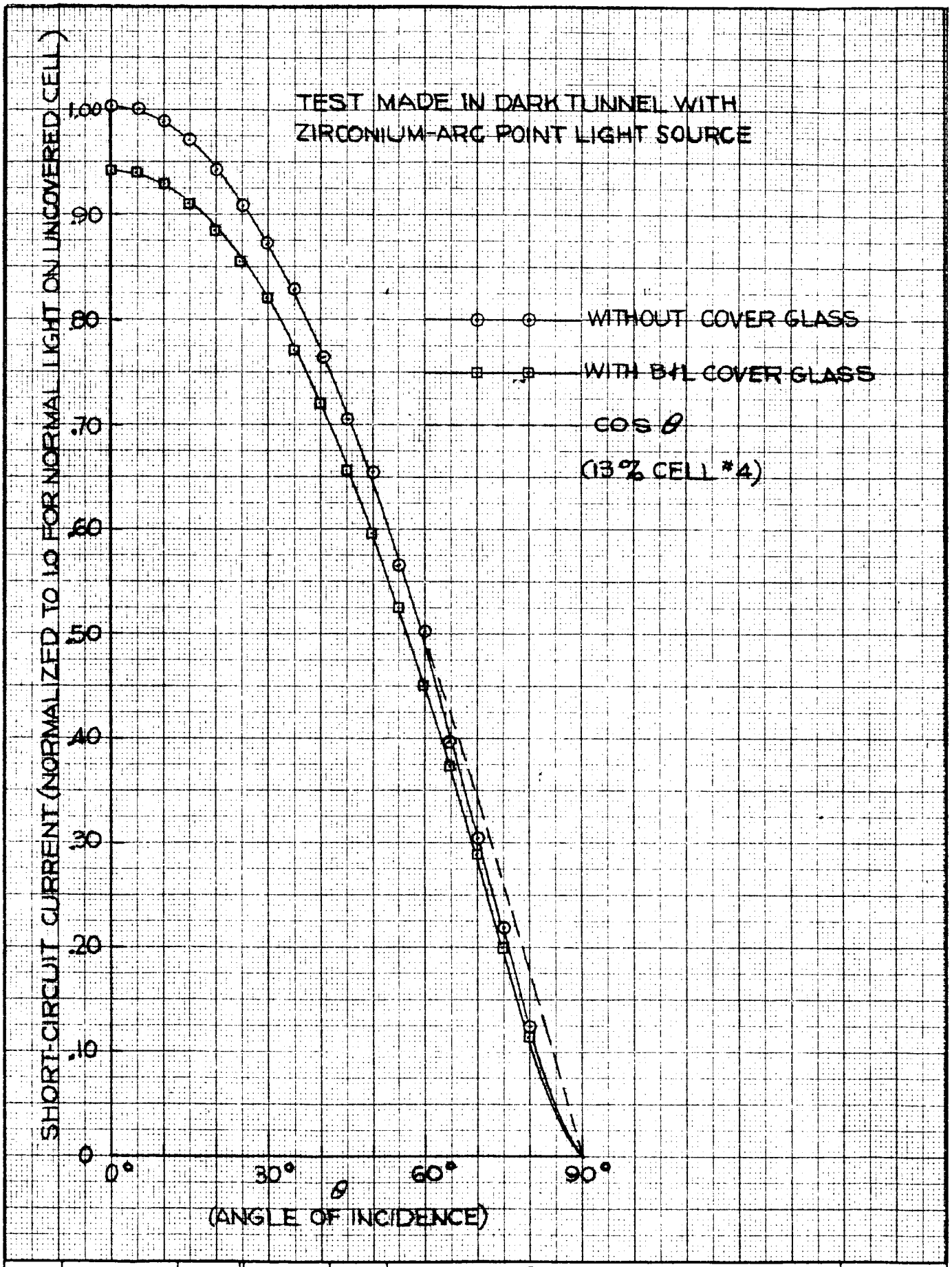

CALC			REVISED	DATE	HOFFMAN SOLAR CELL OUTPUT VS ANGLE OF INCIDENT LIGHT
CHECK					
APR					
APR					
					THE BOEING COMPANY

FIG 20

D2-[illegible]-1

PAGE 42

The results of this test are important because they show that with a multiple dielectric coated cover glass such as the OCLI No. 207-SCC450-2, the cell can utilize obliquely incident light with only a small penalty in conversion efficiency. However, with an OCLI cover glass the cutoff point shifts to a shorter wavelength for oblique light (Fig. 15). For example, the cutoff-point wavelength is 0.440 microns at normal incidence and 0.390 microns at 60 degrees angle of incidence. This shift could cause degradation in the bonding cement under space illumination since more ultraviolet will reach the epoxy. However, according to OCLI, a cover glass coating which will not have this shift could be specially designed for application in concentrating structures. The cost of developing such a new coating is nominal.

C. Curved-Reflector Analysis

The limiting concentration ratios obtainable with a V-ridge concentrator having flat reflectors are well understood and are discussed in the Appendix. There is also the possibility of using curved reflecting surfaces. An example of a curved surface is an off-axis parabolic cylinder. Such curved surfaces could produce higher concentration ratios, and hence higher output from each solar cell. With careful thermal design it would be possible to keep cell temperatures low by utilizing the increased concentrator area for heat radiation.

The concentration ratios possible with different reflecting surface shapes have been calculated. The surfaces investigated were parabolic, hyperbolic, and circular cylinders, and combinations of these curvatures with a flat surface. The restrictions placed on each shape were that it illuminate the entire solar cell and that the reflector height be 2 inches. The reflector height was arbitrarily chosen.

The results of this analysis are summarized below:

Reflector Shape	Maximum Theoretical Concentration, Two Reflectors, 2 Inches High
Flat	2.60
Parabolic Cylinder	3.60
Combination, flat surface and parabolic cyliner	3.65
Circular Cylinder	3.69
Combination, flat surface and circular cylinder	3.70

It should be noted that the above concentration ratios are based on ideal surfaces having 100 percent reflectance. The reflector height was not optimized to give a maximum concentration ratio-to-weight ratio. The circular cylinder appears to be the best shape since it is easiest to fabricate and gives nearly the maximum concentration ratio. The dimensions of a circular-cylinder concentrator which would have a concentration ratio of 3.65 under ideal conditions are shown below:

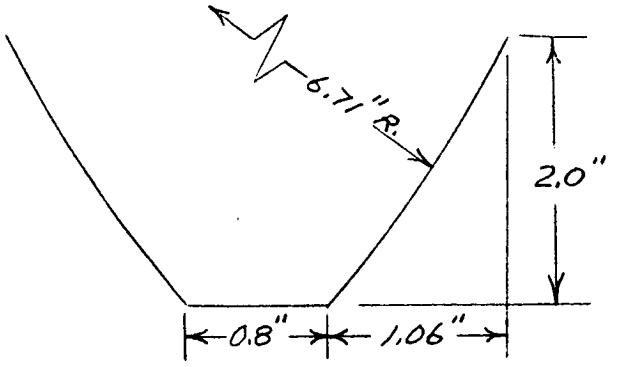

The limited duration of this contract does not permit further investigation of curved-surface concentrators. The techniques and tools developed for bending flat-surface concentrators obviously would not be usable for curved-surface concentrators.

D. Reflecting Surface Selection

Forty-eight samples of reflective surfaces were tested in an evaluation program. Two types of tests were performed, with some samples receiving only one type of test and others receiving both types of tests.

In one test, the specular reflectance was measured at various angles of incidence with a monochrometer and goniometer (Fig. 21). The resulting data were in the form of spectral reflectance. Typical results are shown in Figs. 22 and 23. In order to use these data, they must be expressed in terms of a total specular reflectance as seen by the solar cell. This total reflectance is defined as the ratio of the radiant energy reflected from the surface to that incident upon the surface---both quantities being measured with a solar cell located normal to the impinging light. Since the spectral response curve of a solar cell is not a constant, but instead varies with wavelength, the total reflectance will be a function of both the reflecting surface and light source.

To provide data that could be used to predict the performance of the various surfaces in sunlight, the total reflectance was calculated with terrestrial sunshine as the light source. This value was obtained by computing the short-circuit current produced by the sunlight reflected onto the cell by a sample surface and dividing this by the short-circuit current produced by non-reflected sunlight. The short-circuit current produced by the reflected light was calculated by a "step by step" integration of the product of the spectral response of the solar cell (Fig. 24), spectral reflectance of the coating (example-Fig. 23), and spectral energy distribution of terrestrial sunshine in Seattle (Fig. 25). The short-circuit current produced by the non-reflected sunlight was calculated in a similar manner except that the spectral reflectance was taken to be unity for all wavelengths. The resulting reflectances do not include the effect of non-normal light on the cell and this effect must be considered separately when analyzing the performance of the various surfaces in the concentrating structure.

The foregoing test provides data from which the performance of various reflecting samples in any light source can be predicted. However, the method

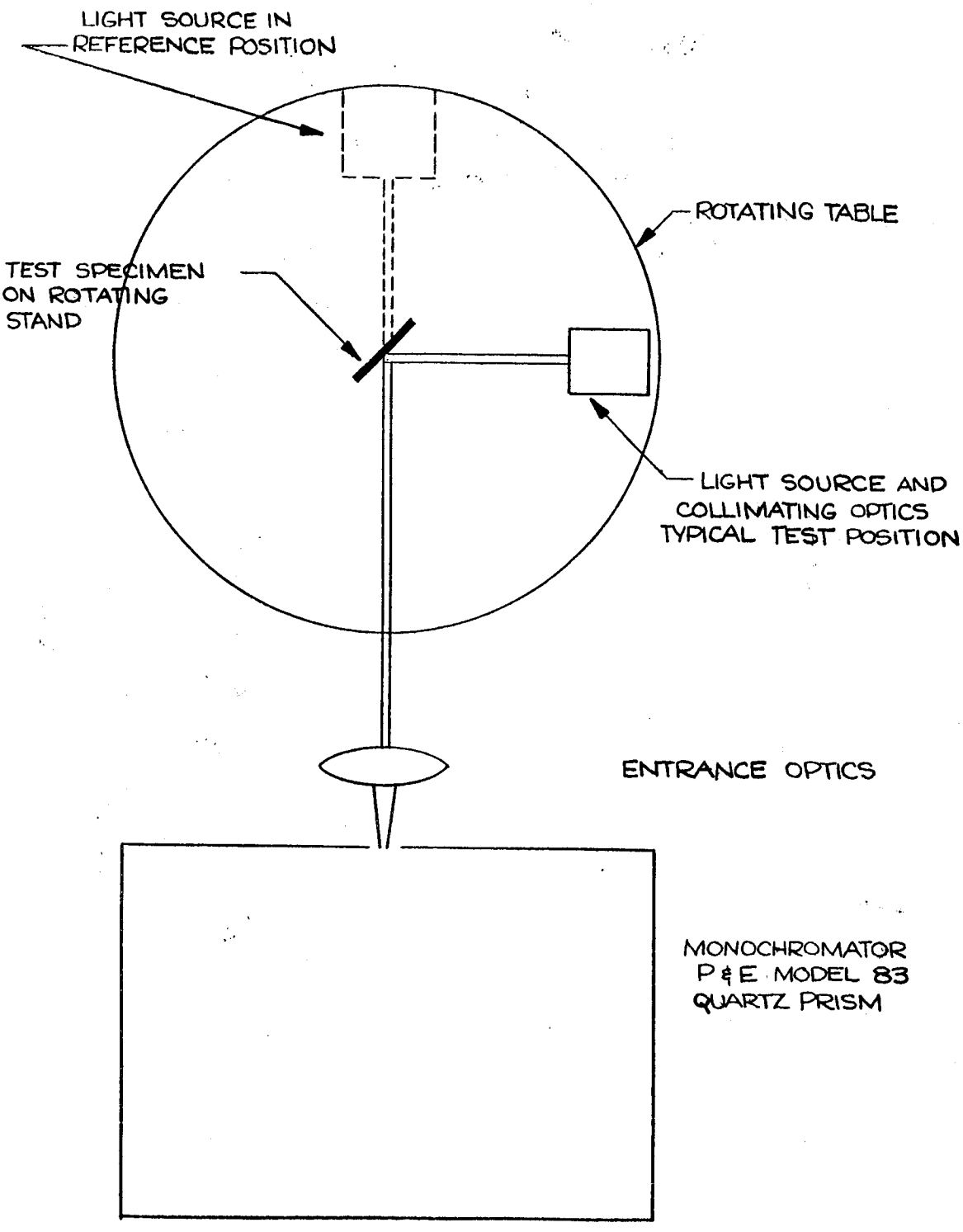
LIGHT SOURCE IN REFERENCE POSITION
ROTATING TABLE
TEST SPECIMEN ON ROTATING STAND
LIGHT SOURCE AND COLLIMATING OPTICS TYPICAL TEST POSITION
ENTRANCE OPTICS
MONOCHROMATOR P & E MODEL 83 QUARTZ PRISM
GONIOMETER

FIG. 21

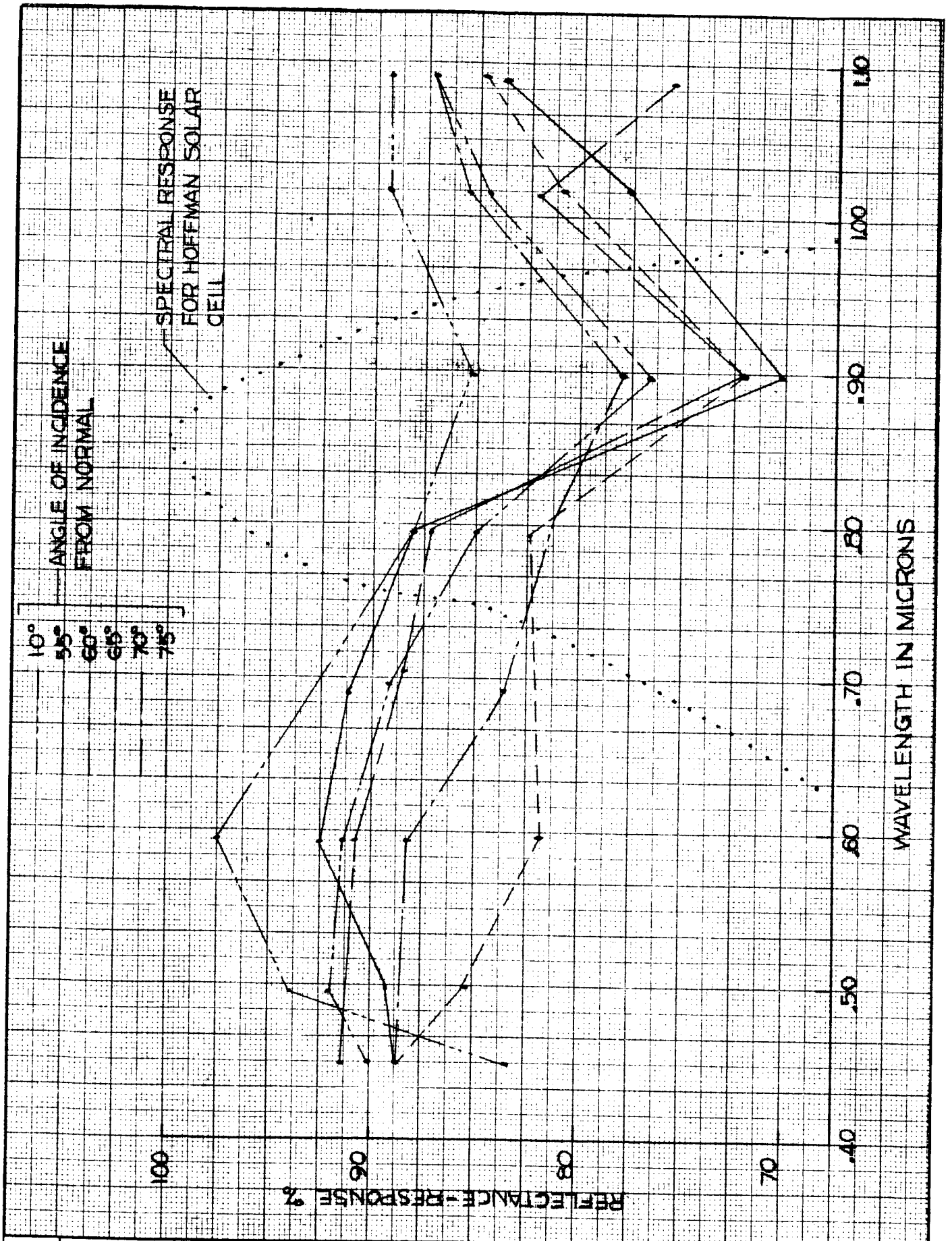

CALC			REVISED	DATE	REFLECTANCE vs WAVELENGTH SAMPLE OCLI #1 ALUMINUM & THREE DIELECTRIC INTERFERENCE COATINGS ON GLASS
CHECK					
APR					
APR					
					THE BOEING COMPANY

FIG 22

D2-90071-A

PAGE 46

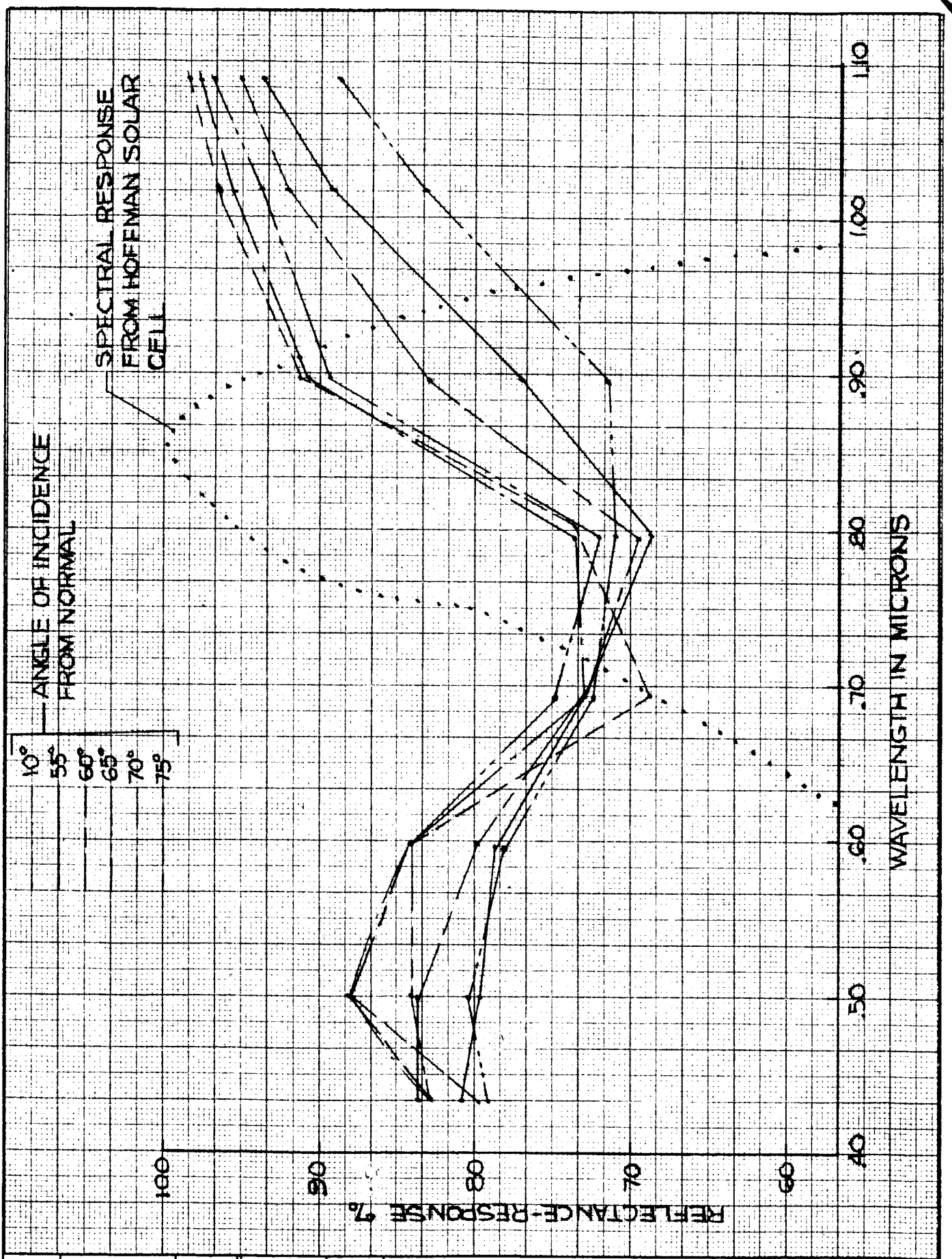

CALC			REVISED	DATE	REFLECTANCE vs WAVELENGTH SAMPLE BAC #1 VAPOR DEPOSITED SLO-Al ON POLISHED GLASS
CHECK					
APR					
APR					THE BOEING COMPANY

FIG 23

D2-90042-A

PAGE 47

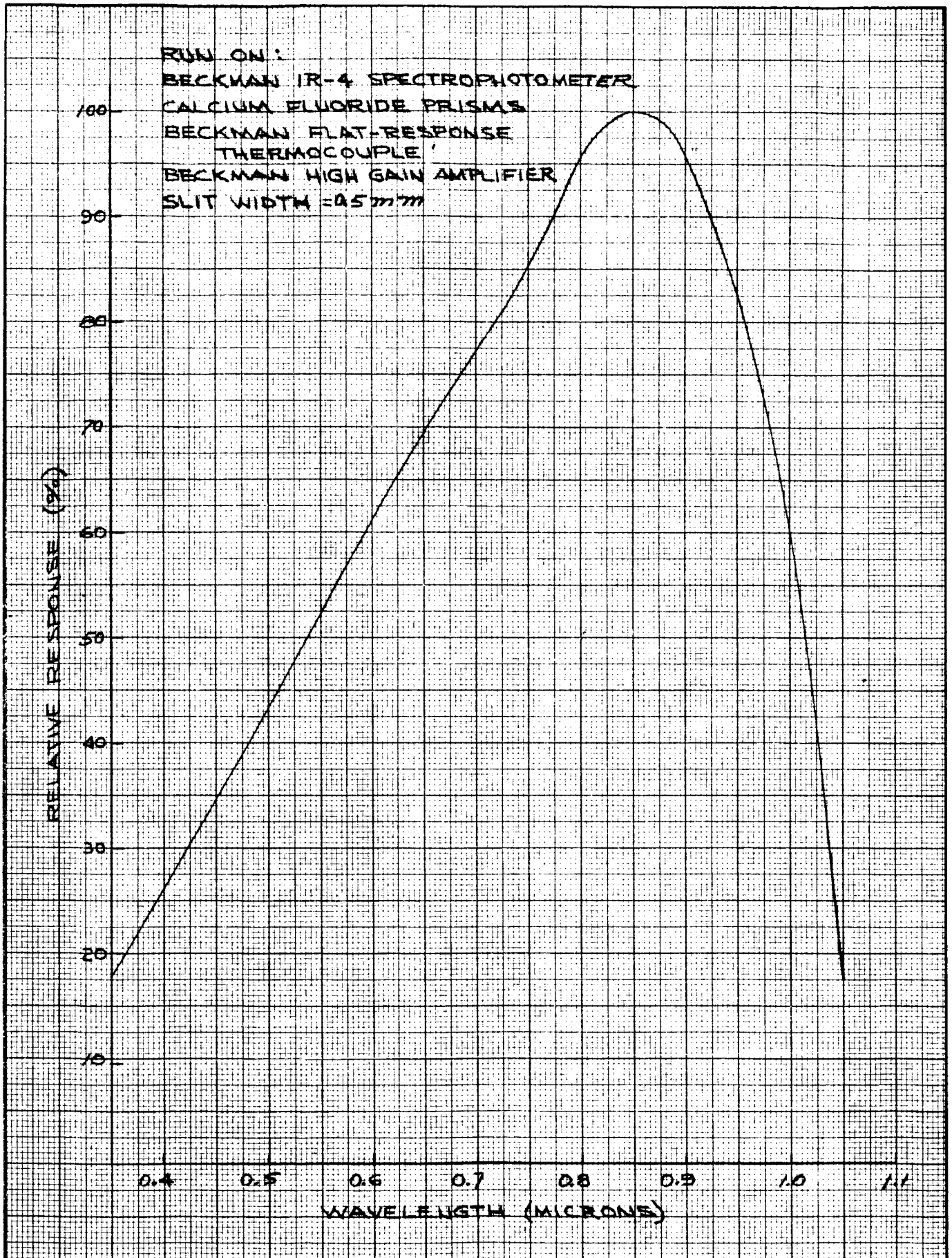

CALC			REVISED	DATE	TYPICAL SPECTRAL RESPONSE CURVE HOFFMAN 10% NON-GRIDDED CELL
CHECK					
APR					
APR					
					BOEING AIRPLANE COMPANY

FIG. 24

D2-90041A

PAGE 48

is very tedious and is not suitable for evaluating large numbers of samples. To overcome this difficulty, a second method was devised. In this method, the sample is placed in a Somor-type test fixture, in which the parameters can be varied (Fig. 26). A 5-cell shingle in the fixture is illuminated by both direct sunshine and reflected light from a reflecting-surface sample. The short-circuit current is observed both without the sample and with the sample placed at various angles. Actual concentration ratios are then calculated from the observed short-circuit current readings. The apparent reflectance is calculated from these ratios by considering the relation between the projected area of the active reflective surface and the reflector angle. The apparent reflectance obtained from these measurements includes the effect of non-normal incident light on the cover glass and cell. However, supplemental tests described in Section IV-B have shown that this effect is small - about 2 percent at 60 degrees - so the reflectance values will be very close to actual.

The reflective surfaces tested in the evaluation program included samples from the following sources:

1. Kaiser Aluminum and Chemical Corp. - several samples of 5252 alloy with reflective surfaces obtained by various methods of buffing, polishing, dipping and anodizing.

2. Reynolds Metals Company - several samples of 5657 alloy with reflective surfaces obtained by various methods of buffing, polishing, and anodizing.

3. Aluminum Company of America (ALCOA) - several samples of ALZAK (a commercially available reflector material), with various finishes and one sample of unprocessed lighting sheet.

4. Optical Coating Laboratory, Inc. (OCLI) - one sample consisting of aluminum and 3 proprietary coatings deposited on polished glass.

5. Boeing - several samples of clad 7075 alloy and 6061 alloy with reflective surfaces obtained by various methods of buffing and polishing; several samples of vapor-deposited SiO-Al on polished glass, and several samples of aluminum vapor-deposited on lacquered 6061 aluminum alloy.

Six samples showed up considerably better in the reflectance tests than any of the remaining samples evaluated. Test results for these samples are shown in Fig. 27.

The OCLI surface performed very well in the reflectance tests, but the specimen was on a glass plate. OCLI has now deposited a similar surface on aluminum, and this new surface is being evaluated. The OCLI surface could not be obtained on aluminum in time to be used in the concentrators for the JPL contract.

It was not possible to purchase polished Kaiser 5252 aluminum sheet because Kaiser's entire production of this material is committed to the automobile industry.

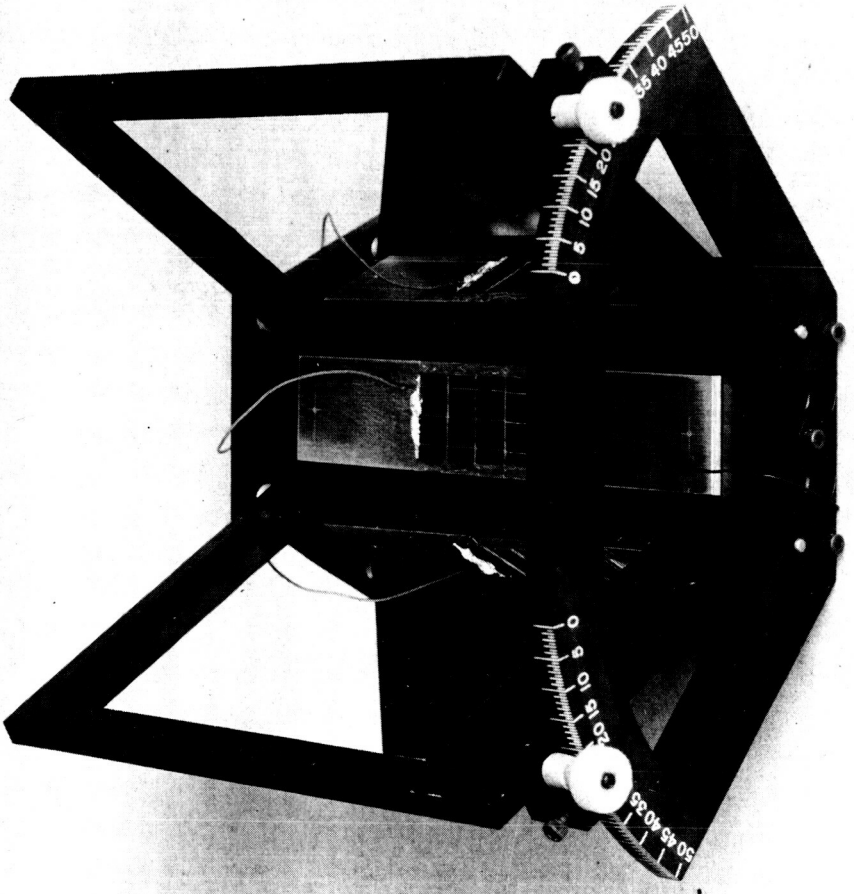

CONCENTRATOR TEST FIXTURE FOR EVALUATING REFLECTIVE SURFACES

FIG. 26

SPECIMEN	SOURCE	DESCRIPTION	ANGLE degrees	REFLECTANCE percent	CONC. * ratio	SPECIFIC POWER RATIO** percent
K-3-1	Kaiser	Alloy 5252 - buffed and bright-dipped in "R-5"	55	73.2	1.504	89.3
			60	80.2	1.802	90.2
			65	83.1	2.080	87.3
			70	82.9	2.276	87.1
K-4-3	Kaiser	Alloy 5252 - bright-dipped in "R-5" only	55	76.5	1.527	90.3
			60	82.7	1.827	91.4
			65	84.0	2.091	90.0
			70	82.4	2.269	89.4
OCLI	Optical Coating Lab	High purity aluminum and 3 proprietary coatings deposited on polished glass	55	78.1	1.538	91.0
			60	84.0	1.840	91.0
			65	89.5	2.165	94.3
			70			
ALCOA	Aluminum Company of America (ALCOA)	Unprocessed lighting sheet. 99.85% Al clad to 1100 alloy and rolled with polished rollers.	55	75.5	1.520	89.8
			60	81.9	1.819	90.0
			65	84.0	2.092	90.9
			70	83.8	2.290	90.3
BAC 6	Boeing	Vapor-deposited aluminum over Dupont RK-5752 lacquer on 6061 alloy	55	74.2	1.51	89.5
			60	82.0	1.82	91.0
			65	85.5	2.11	92.1
			70	82.5	2.27	89.8
BAC 7	Boeing	Vapor-deposited aluminum over Dupont RK-5752 lacquer on 6061 alloy	55	71.3	1.49	88.4
			60	82.0	1.82	91.0
			65	83.9	2.09	91.2
			70	83.8	2.29	90.5

* Short-circuit current concentration ratio.

** Based on 85 percent coverage of solar cells in both concentrating and non-concentrating panel.

Calc.			REVISED	DATE	RESULTS OF REFLECTANCE TESTS ON HIGHLY REFLECTIVE SURFACES.	Fig. 27
Trac						D2-90041-1
Chk					BOEING AIRPLANE COMPANY SEATTLE 24, WASHINGTON	Page 52
Appr.						
Appr.						

BAC 360 C 61

DATA SHEET

ALCOA unprocessed lighting sheet was purchased for a prototype concentrator, but it was found to lack the reflectance that the tested sample had shown. This sheet had been custom rolled to the 10-mil thickness specified by Boeing, and the rolling process had degraded the surface finish. This material still remains very promising, but high-quality sheets could not be obtained in time to use in the concentrators for the JPL Contract. However, quotations are being obtained for high-quality unprocessed lighting sheet in quantity sufficient for future concentrator fabrication.

The Boeing aluminized lacquer surface (see Section VI) on 6061 alloy was used in the EOM-1A and EOM-2A concentrators. The same surface on the ALCOA unprocessed lighting sheet described above was used in both the EOM-1B, EOM-2B and CS-1 concentrators delivered to JPL.

V CONCENTRATOR DESIGN

The contract requires that three concentrators be designed, built, tested, and delivered. Two of these concentrators are called "Electrical-Optical Models" and are designated EOM-1 and EOM-2. The third concentrator is called "Type Approval Model" and is designated CS-1. The design of these three concentrators is described in this section. In addition, a design approach to a larger 20-sq. ft. concentrator is presented.

A. EOM Concentrators

Each of the two 9-inch by 9-inch EOM concentrators has 45 silicon solar cells. The EOM-1 concentrator has nine 5-cell shingles, installed in three troughs. The other concentrator is designated EOM-2 and it has three 15-cell shingles installed in three troughs.

The EOM concentrator design was based on the analysis of design factors discussed in Section III, and experience with 9-inch by 9-inch prototype concentrators. From these considerations the following design criteria were established:

1. Nominal obtuse angle between plane of solar cells and reflecting surface - 120 degrees.
2. Bending-brake setting for obtuse angle between plane of solar cells and reflecting surface - 120 degrees.
3. Apex angle, nominal - 60 degrees.
4. Bending-brake setting for apex angle - 53 degrees.
5. Number of troughs - 5
6. Structural material - ALCOA unprocessed lighting sheet, H-25 temper.
7. Thickness of structural material - 0.010 inch.
8. Reflecting surface - aluminized lacquer.
9. Type of solar cells - Hoffman, blue-sensitive silicon solar cells, 10-percent efficient when illuminated with the solar spectrum and intensity present with zero intervening air mass.

The reason for making the apex angle and the angle between solar cells and reflecting surface other than nominal was to avoid convex reflecting surfaces. With a convex reflecting surface it is possible that manufacturing tolerances will cause some of the reflected light to miss the solar cells. On the other hand, with a slightly concave reflecting surface all of the reflected light will be directed to the solar cells.

The material thickness was established by structural considerations. It was also the minimum thickness in which unprocessed lighting sheet could be obtained from ALCOA, the supplier. The reflecting surface selection was based on the test results described in Section IV.

The resulting EOM concentrator design is shown in Fig. 28 .

B. CS-1 Concentrator

The contract requires that the CS-1 concentrator be 10 inches by 18 inches in size and contain 100 high-efficiency solar cells. The remaining solar-cell area is to be filled with material that closely simulates the solar cells in mass. Actually, low-cost, low-efficiency solar cells were used to fill this remaining area.

The CS-1 concentrator design was based on EOM concentrator experience and test results. The final design, as approved by JPL, is shown in Fig. 29 and incorporates the following features:

1. Nominal obtuse angle between plane of solar cells and reflecting surface - 120 degrees.

2. Bending-brake setting for obtuse angle between plane of solar cells and reflecting surface - 118 degrees.

3. Apex angle, nominal - 60 degrees.

4. Bending-brake setting for apex angle - 56 degrees.

5. Number of troughs - 10

6. Number of cells in each trough - 25, arranged in shingles of 5 cells per shingle.

7. Number of troughs with high-efficiency cells - 4

8. Type of high-efficiency solar cells - Hoffman blue-sensitive silicon solar cells, 10-percent efficient when illuminated with the solar spectrum and intensity present with zero intervening air mass.

9. Number of troughs with low-efficiency cells - 6

10. Solar-cell connections - each of the high efficiency shingles is connected in series with the other shingles in its trough, and in parallel with shingles in the other active troughs. The low-efficiency shingles are electrically inactive and are not connected for power purposes. They are used for structural evaluation.

11. Structural material - ALCOA unprocessed lighting sheet, H-25 temper.

12. Thickness of structural material - 0.010 inch.

13. Reflecting surface - aluminized lacquer.

14. Actual size - 10.67 by 18 inches.

15. Actual weight of concentrator, without solar cells, cover glasses, adhesive or wiring - 0.451 pounds or 0.339 pounds per sq. ft.

BLER
1 X 9.30 ALUMINUM (1)

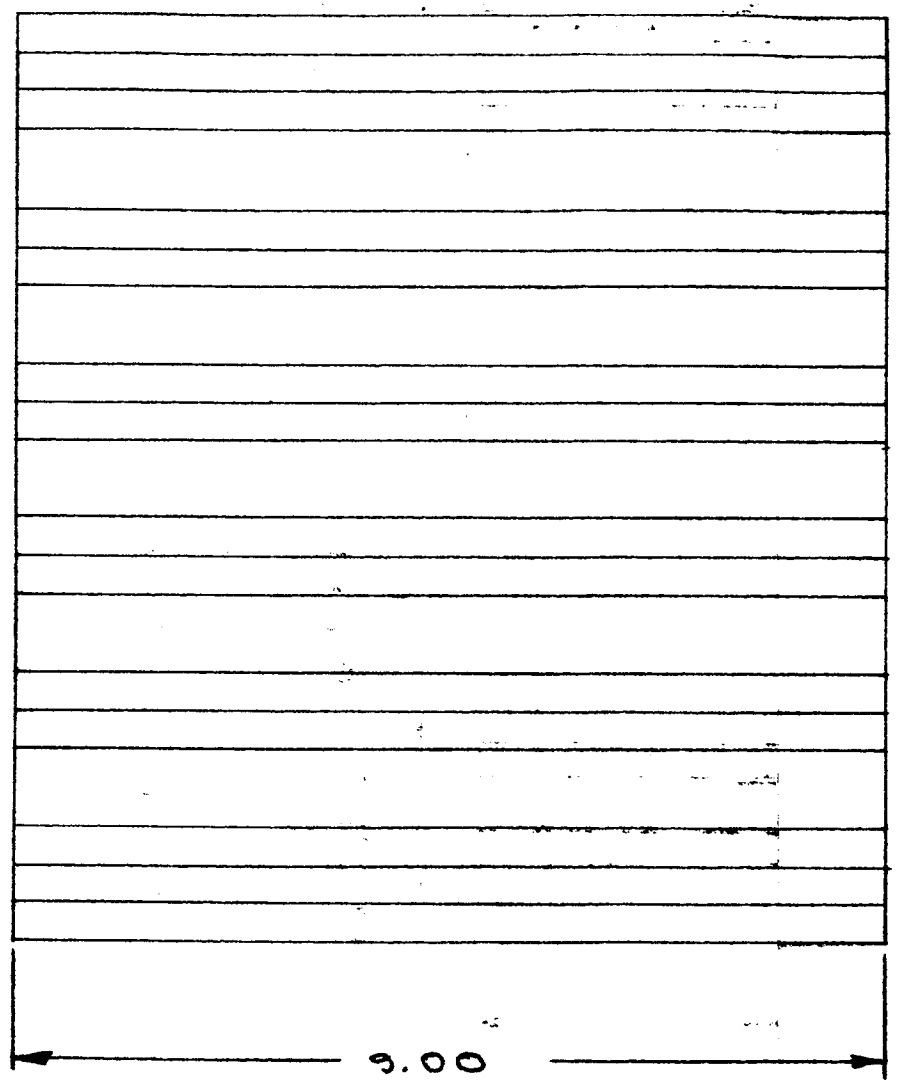

-5 REFLECTOR
.010 9.0 X 14.40 ALUMINUM (1)

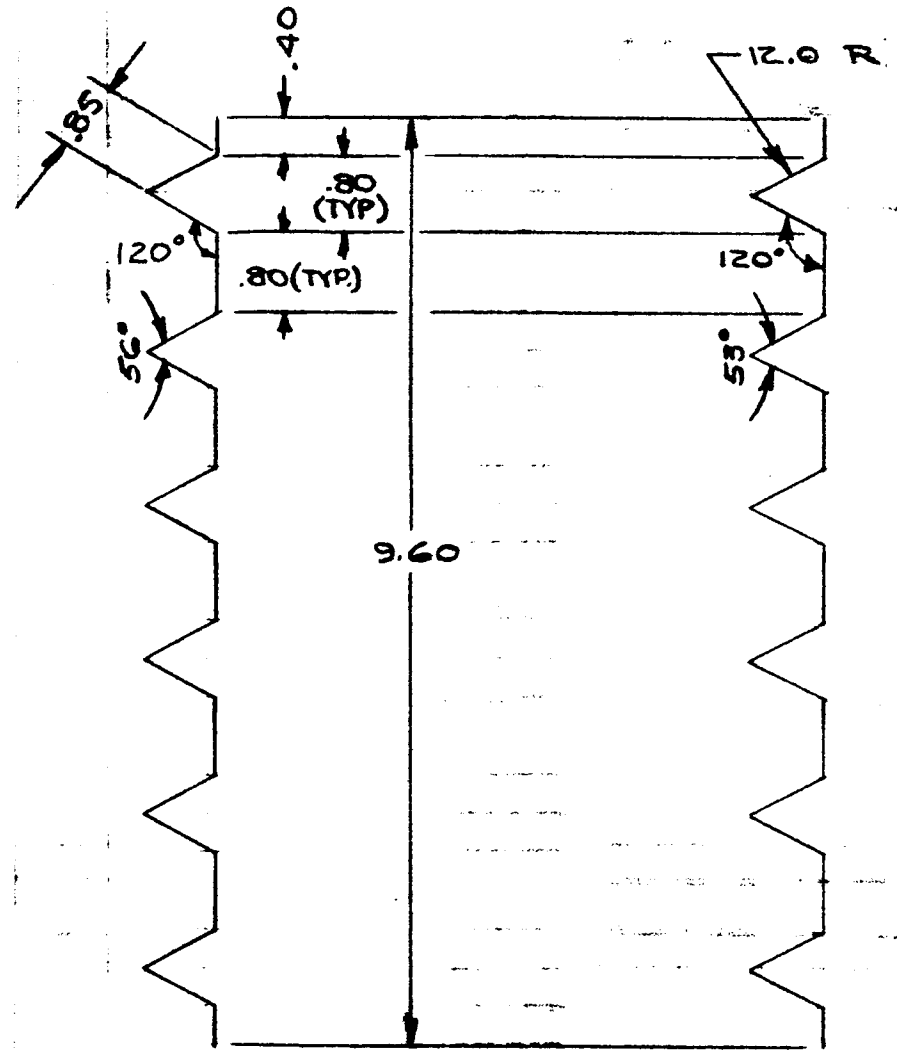

TYPICAL FOR PROTOTYPES #1 THRU #9 AND EOM 1A & 2A

TYPICAL FOR PROTOTYPES #10 AND #11 AND EOM 1B AND 2B

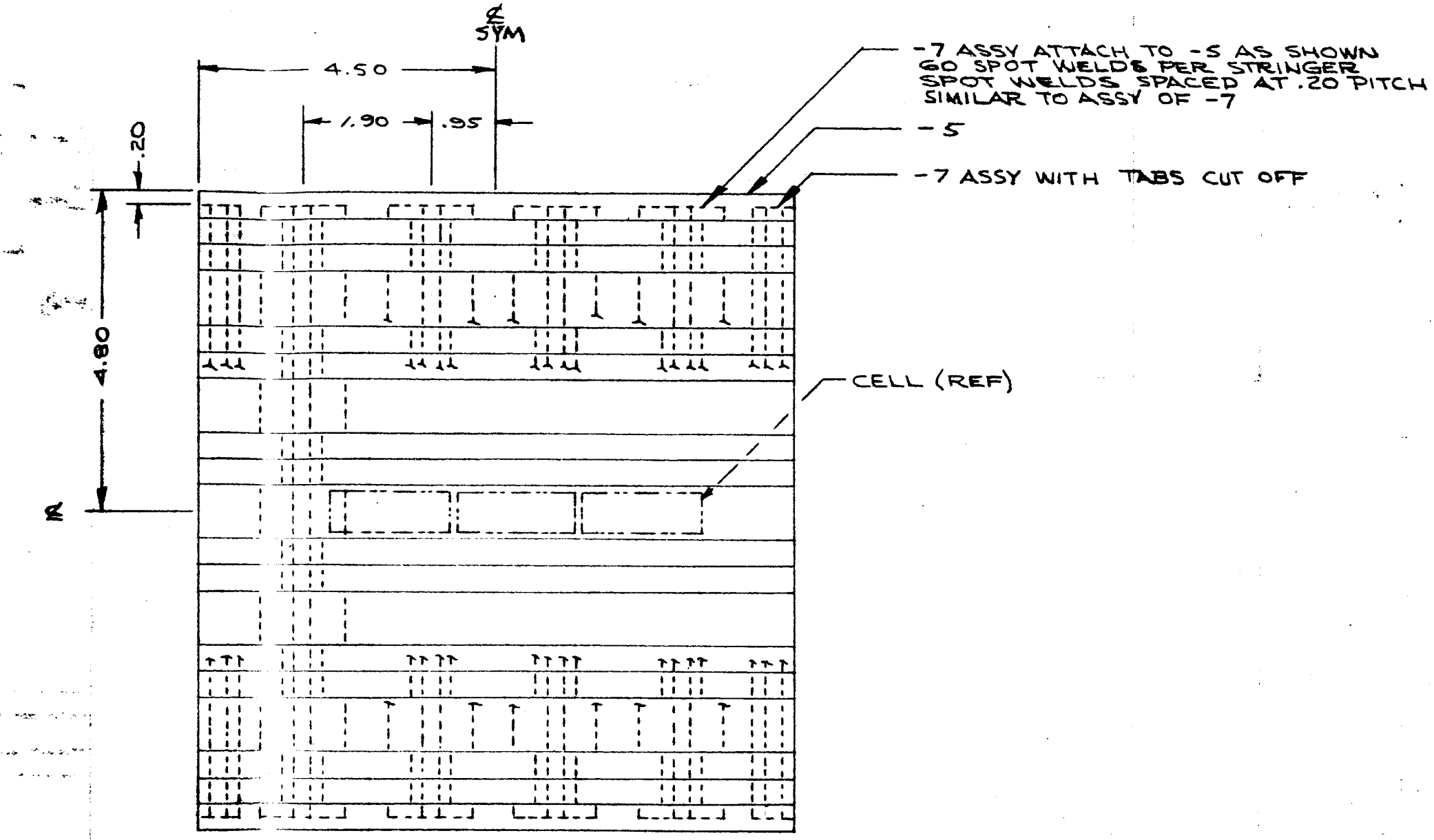

-8 PANEL ASSY

(1) 606I-T3 FOR PROTOTYPES #1 THRU #9 AND EOM 1A & 2A UNPROCESSED LIGHTING SHEET (1100 H 25) FOR PROTOTYPES 10 AND 11 AND EOM 1B AND 2B

NOTE: DOUBLERS (-6) WERE OMITTED FROM PROTOTYPES 10 AND 11 AND EOM 1B AND 2B

SCALE: HALF SIZE EXCEPT AS NOTED

ELECTRO-OPTICAL MODEL
PROTOTYPES 1 THRU 11 AND EOM 1 AND 2
JPL CONTRACT 950122

DWG NO. 25-16005-B

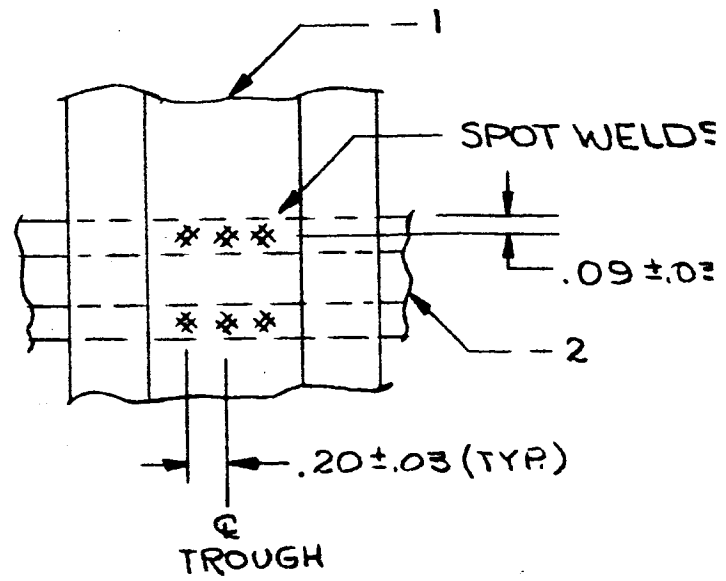

DETAIL A
(FULL SIZE)
ATTACHMENT DETAILS -1, TO -2

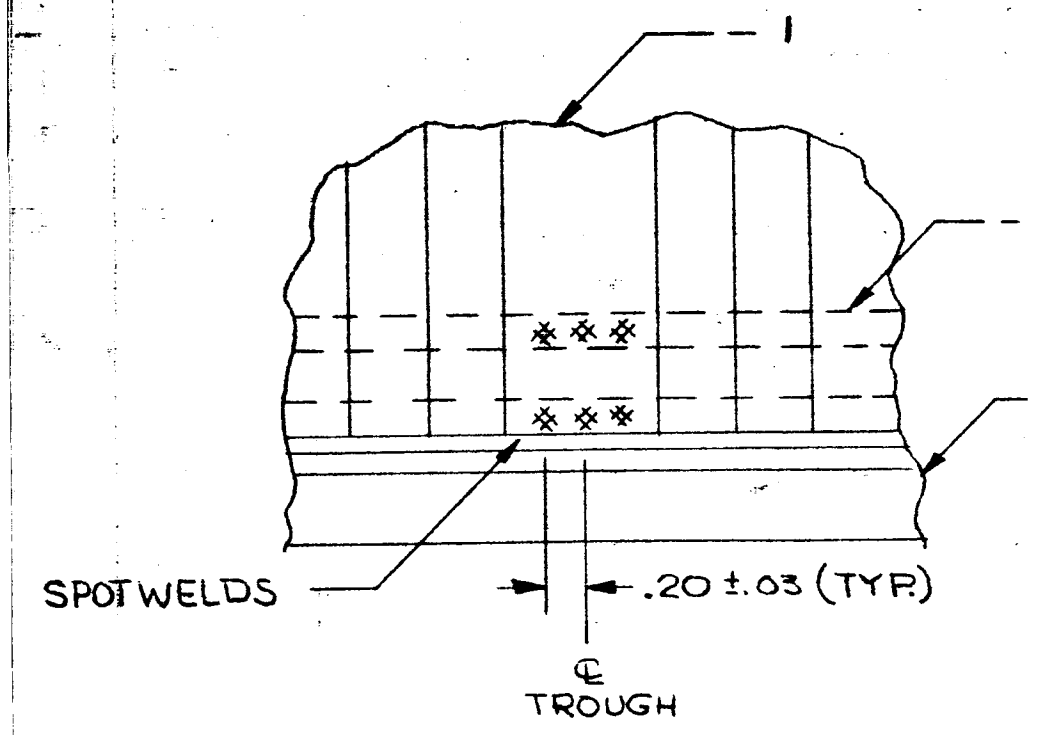

DETAIL B
(FULL SIZE)
ATTACHMENT DETAILS -3 TO

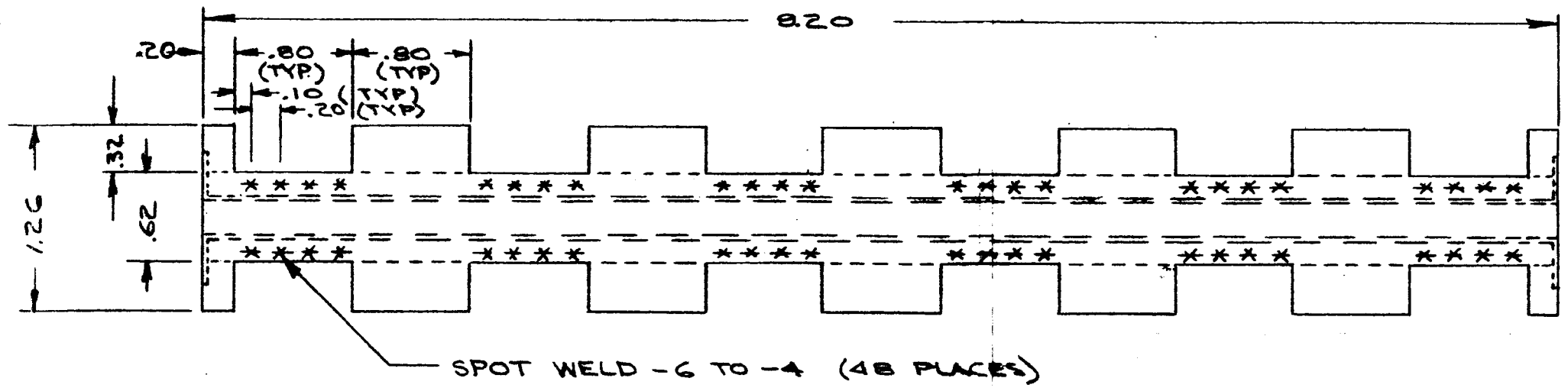

-7 STRINGER ASSY
SCALE : FULL SIZE

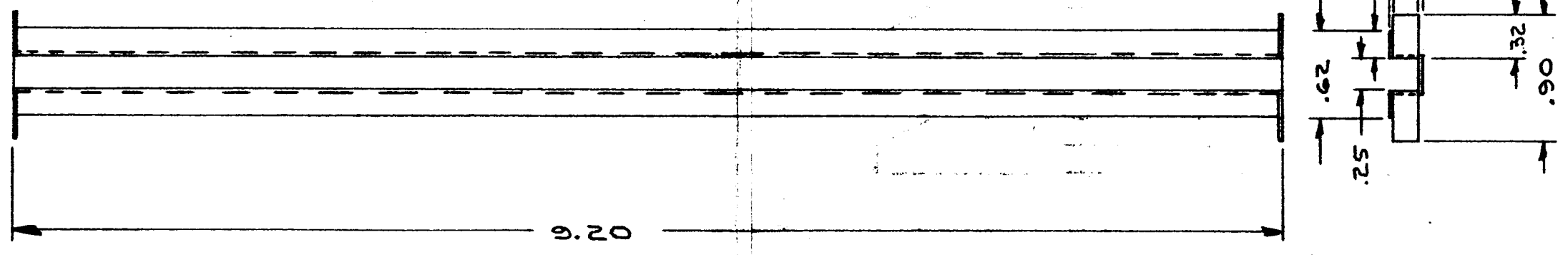

-4 STIFFENER
.010 X 1.3 X 9.9 ALUMINUM 1
SCALE: FULL SIZE

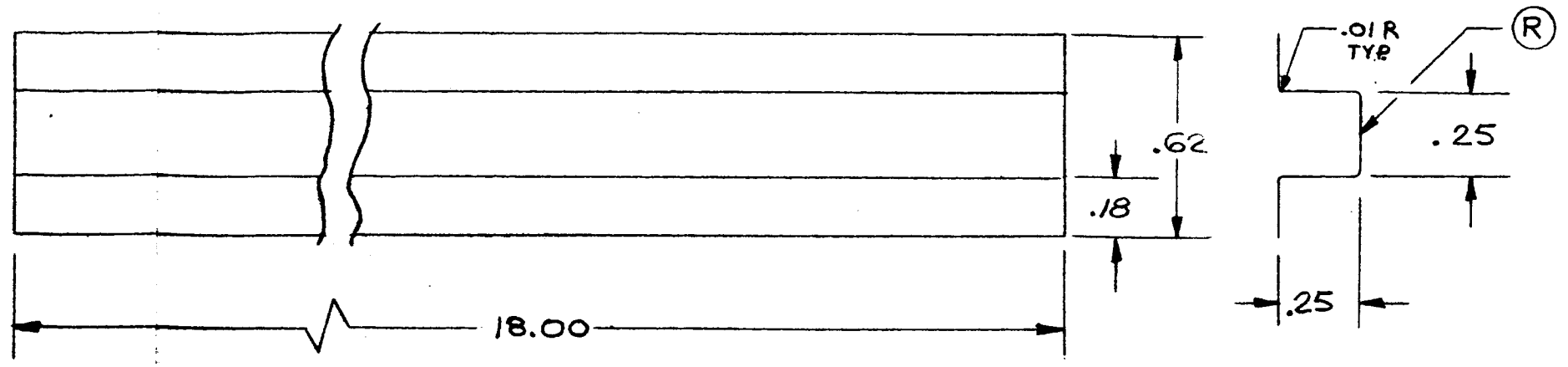

-2 STIFFENER (TWICE SIZE)

MAT'L: .01 x 1.20 x 18.00 ALZAK HEAT TREAT H-25

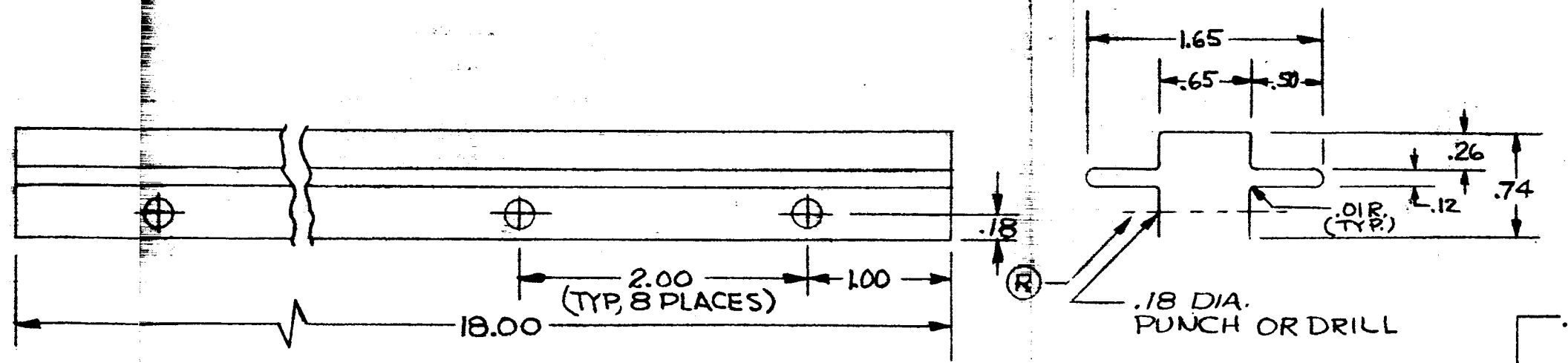

-3 CLIP (FULL SIZE)

MAT'L: .01 x 4.20 x 18.00 ALZAK HEAT TREAT H-25

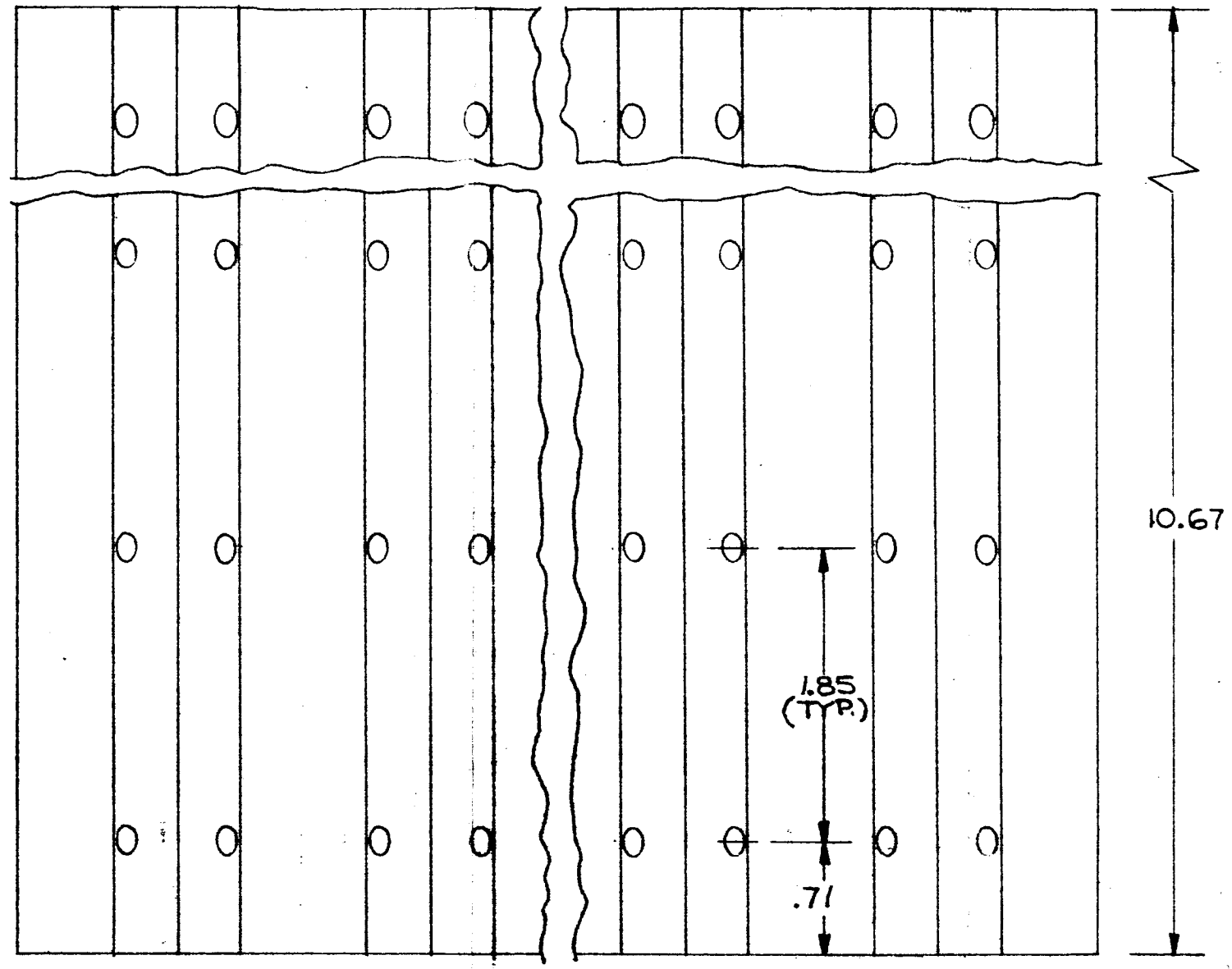

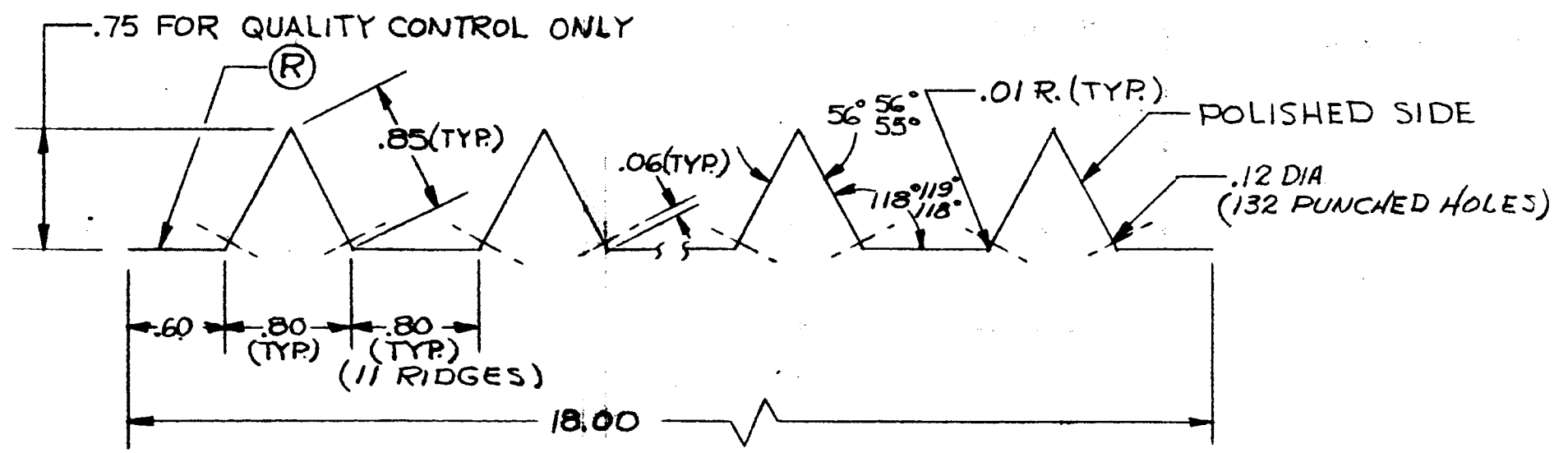

-1 REFLECTOR (FULL SIZE)

MAT'L: .01 x 10.70 x 28.00 ALZAK HEAT TREAT H-25

16. Actual weight of concentrator, with cells, cover glasses, adhesive, wiring, and strippable protecting lacquer coating - 0.768 pounds or 0.575 pounds per sq. ft.

The angle between solar cells and reflecting surfaces and the apex angles were altered from the EOM design because it was found with other experimental concentrators that the 56-degree and 118-degree angles were more satisfactory. The angles used in the EOM concentrator actually resulted in each reflector illuminating about two-thirds of the solar-cell area. This non-uniform illumination apparently does not affect solar-cell efficiency. However, more uniform illumination could be obtained with the angles selected for the CS-1 concentrator, and the resulting reflecting surface was still slightly convex.

The structural material and reflecting surface selections were based on EOM concentrator experience and availability. Alternate reflecting surfaces could not have been obtained in time to permit manufacture, test, and delivery of the CS-1 concentrator on schedule.

The weight of the CS-1 concentrator without solar cells, cover glasses, adhesive or wiring exceeds the contract requirement of 0.4 pounds. The excess weight is attributable in part to the weight of the film-forming lacquer, and in part to the excess of hat-section stiffeners that resulted from a stiffener spacing of 1.85 inches. This close spacing was adopted because the stiffener sides formed an excellent support for the paralleling strips which are further described in Section VI, and hence a stiffener was located approximately at each point where two solar-cell shingles were abutted, and also at each end of the rows. The dimensions of the concentrator were such that two stiffeners had to be located very close together at the edge of the concentrator. The result was that the CS-1 concentrator had more stiffeners than were structurally necessary. In a larger concentrator it would probably not be necessary to parallel the solar cells at the end of every shingle, so the number of stiffeners could be reduced.

C. Larger Concentrators

The studies and tests described in this report provide criteria with which larger concentrating photovoltaic structures can be designed. It is interesting to explore the preliminary design of a concentrator that would produce as much power as would be produced by a non-concentrating solar-cell panel which is trapezoidal in shape with outside dimensions of 52 inches by 68 inches, and having an area of 20.5 sq. ft.

Example of Larger Concentrator Design

From Section III-B it can be established that the minimum weight concentrating panel design incorporates a 63-degree angle between the plane of the solar cells and the reflecting surfaces. The attainable coefficient of efficiency C_E is at least 2.00, giving a value of 0.560 for W* from Fig. 8. Therefore, the concentrating panel weight will be:

$$W^*A = (0.560)\ (20.5) = 11.5 \text{ lbs.}$$

The panel area will be:

$$A^*A = (1.057)\ (20.5) = 21.7 \text{ sq. ft.}$$

The resultant panel can be 52 inches wide by 60 inches long. It is assumed that the panel will be supported from the vehicle by hinges along the 52-inch dimension. Thus, the spars of the panel should terminate at the 52-inch edge, and should extend in the 60-inch direction of the panel as shown in Fig. 29-A. The panel corrugations will then lie in the 52-inch direction.

For structural integrity, the resonant frequency of the subpanels within the main 52-inch by 60-inch panel should be higher than 250 cps. Therefore, the maximum overhang of the corrugations beyond the two outer side spars (L_1) will be approximately:

$$L_1^2 = \epsilon C_f/250 = (0.54)(111)/_{250} = 0.240 \qquad (43)$$

$$L_1 = 0.50 \text{ ft.}$$

On the other hand, the maximum span across which the corrugations can extend as fully fixed end beams will be:

$$L_2^2 = 4 \epsilon C_f/250 = 960/_{250} = 3.84 \qquad (44)$$

$$L_2 = 1.96 \text{ ft.}$$

Thus, two interior spans and two cantiler spans are needed. The total possible width is

$$2 \times 1.96 \text{ ft.} + 2 \times 0.50 \text{ ft.} = 4.92 \text{ ft.}$$

The assumed panel width is 52 inches or 4.33 ft. The span lengths proportioned down to the 4.33 ft. width are:

$$\text{Interior: } 1.96 \times \frac{4.33}{4.92} = 1.72 \text{ ft.}$$

$$\text{Cantilever: } 0.50 \times \frac{4.33}{4.92} = 0.44 \text{ ft.}$$

The loading on the spars will be unequal because the middle spar supports 1.72 ft. of panel width while the exterior spars support only 1.30 ft. of panel width each. Therefore, the stiffness of the central spar must be greater than the stiffness of either of the exterior spars.

The load on the interior spar will be:

$$1.72 \times 0.530 = 0.910 \text{ lb/ft. of panel length}$$

For the exterior spars, the load will be:

$$1.30 \times 0.530 = 0.689 \text{ lb/ft. of panel length.}$$

The spars will be supported by an actuator mechanism at 24 inches from the inboard end. The resonant frequency (from Eq. 9) is defined by:

$$f = \frac{\beta^2}{2\pi} \sqrt{EI/m}$$

where the parameter β is evaluated from considerations of boundary conditions.

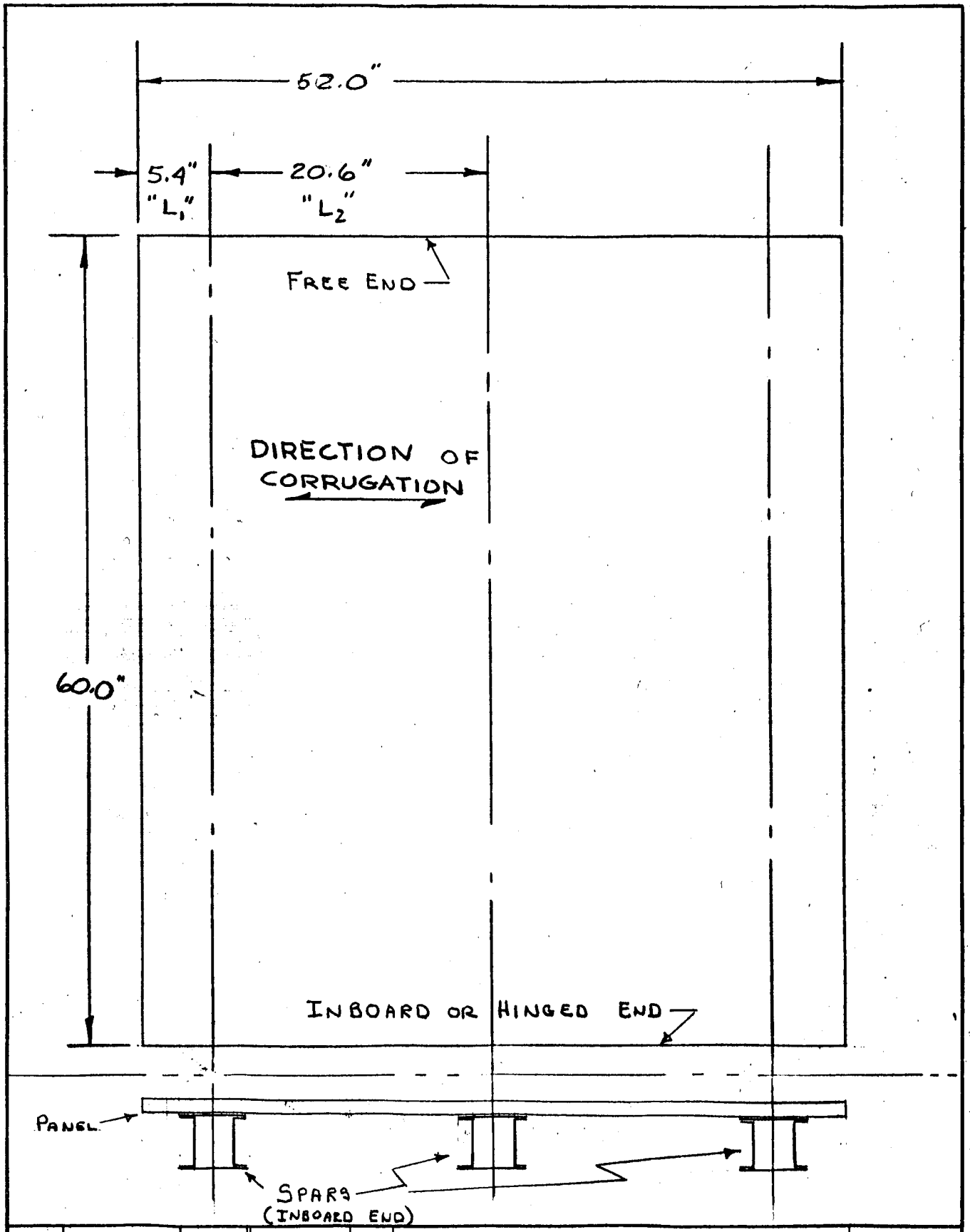

CALC			REVISED	DATE	AN EXAMPLE OF A LARGE CONCENTRATOR PANEL - PLAN & END VIEW -
CHECK					
APPD					
APPD					

FIG 29A

D2-90041-A

BOEING AIRPLANE COMPANY

PAGE 59A

For the propped cantilever with the support at 2/5 of the length, the parameter β has a value of 8.00/L.

Therefore,

$$f = \frac{64}{2\pi L^2} \sqrt{EI/m}$$

Assuming a design resonant frequency of 4 cps,

$$EI/m = \frac{f^2 \pi^2 L4}{(32)^2} = \frac{16 \pi^2 (60)4}{(32)^2} \qquad (45)$$

For the grade of aluminum proposed, $E = 10^7$. Then

$$I = \frac{m (16 \pi^2)(36)(36)}{(32)(32) \times 10^3}$$

$$= m \times 194 \times 10^{-3} = 0.2\ m$$

It is now necessary to assume the mass of the spar and load at some value per unit length. For the interior spar this mass is assumed to be:

$$m = \frac{0.910}{12 \times 386} + \frac{0.509}{12 \times 386} = \frac{1.419}{12 \times 386} \text{ slugs/inch.}$$

Then: $I = \frac{1.419}{12 \times 386} \times 0.2 = 6.11 \times 10^{-5}$ in.^{4}

The above calculation based on a 4 cps resonant frequency establishes a moment of inertia so small that it is not the significant criteria of spar design. Therefore, the supporting spars need be designed to the criteria of having enough torsional stiffness to limit rotations at the panel-to-spar joints.

A reasonable torsional rigidity would be 10 times the flexural rigidity of the total number of corrugations between the point on the spar and the free end. Therefore, the torsional rigidity of the spars should be 10 x 26,000 in.^{2} lb. at the free ends and 10 x 39 x 26,000 in.^{2} lb. at the inboard ends.

$$\text{Torsional rigidity} = GI\rho = \frac{EI\rho}{2(1+\mu)} = \frac{EI\rho}{2.6} \qquad (45a)$$

$I\rho$ at free end should be:

$$I\rho = \frac{26{,}000 \times 2.6 \times 10}{10^7} = 0.0675 \text{ in.}^4$$

$I\rho$ at the inboard end should be:

$$I\rho = \frac{39 \times 26{,}000 \times 2.6 \times 10}{10^7} = 2.64 \text{ in.}^4$$

The sections shown below were assumed:

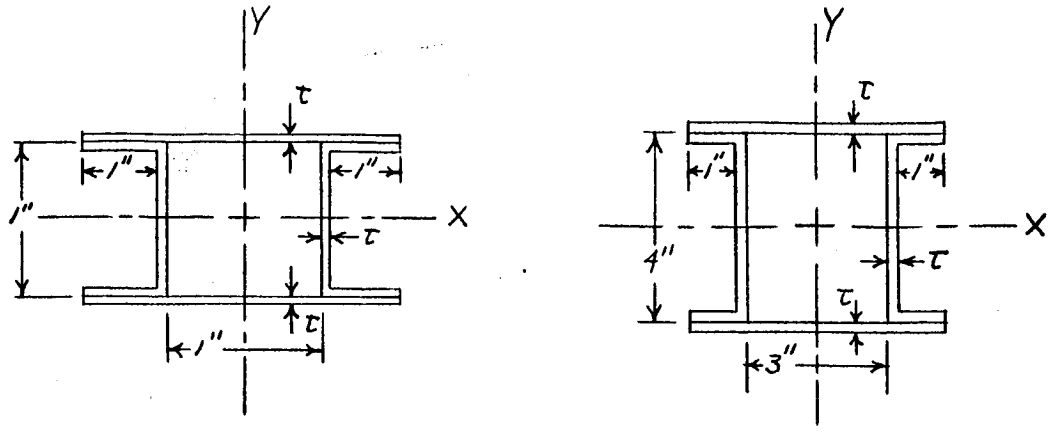

FREE END

I_{xx}	2.66 t
I_{yy}	7.0 t
$I\rho$	9.66 t

INBOARD END

I_{xx}	66.7 t
I_{yy}	55.8 t
$I\rho$	122.5 t

($I\rho$ is rotational moment of inertia)

The thickness of the metal in this formed spar should be:

$$t = (2.64)/122.5 = 0.021 \text{ inches}$$

The nearest standard metal thickness is 0.020 inch.
Then, the weight of each spar will be:

$$W_s = (0.097)(0.020)(60)\left[\text{Mean Area}\right]$$

$$= 0.117\left[\frac{12 + 22}{2}\right] = 1.98 \text{ lbs.}$$

The total weight will be approximately:

$$W_t = \text{Panel weight} + \text{spar weight}$$

The panel weight is a product of the panel area, 21.7 sq. ft., and the specific panel weight of 0.53 lb. per sq. ft. from Fig. 6.

$$W_t = \left[0.530 \times 21.7\right] + \left[3 \times 1.98\right]$$

$$= 17.46 \text{ pounds.}$$

Thus, it appears that the use of the concentrator offers not only an approximately 50 percent cost reduction because of fewer solar cells, but also a construction that is about 40 percent lighter when compared with a nonconcentrating solar-cell panel. The concentrating panel will require 5.2 percent more area than the nonconcentrating panel for a given power output.

VI. MANUFACTURING

The concentrating structures are fabricated in four major steps: (1) the parts are formed from aluminum sheet stock, and spot-welded together, (2) the reflecting surface is applied, (3) the solar-cell shingles are cemented to the panel, and (4) the shingles are wired in series-parallel. These steps are described in respective order.

1. Forming and Welding

Each panel is composed of hat-section stiffeners and the sheet of aluminum which forms the trough and reflecting facets. In early panels a strip of aluminum was welded to each hat section to form a box beam. This reinforcement was abandoned after vibration tests showed the concentrators were rigid enough without it.

The hat sections are made from the same aluminum and thickness that is used for the rest of the panel. The flanges of the hat section are made by a hydroform and brake die operation as shown in the following sketch:

The first step is to hydroform the flanges as shown. The second step with the brake die forms the channel shape. The tools used for the hat section are shown in Fig. 30.

The reflecting facets and troughs are formed by brake forming a continuous sheet of aluminum. A precision jig is used for marking the bend lines with punch marks. The V-ridge surfaces are then formed in a precision, hand-operated brake die as shown below:

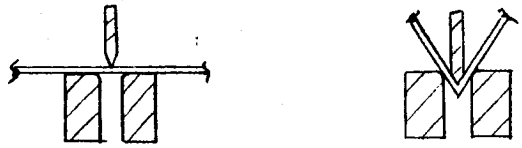

The bend angle is controlled with accurate stops on the brake die. The brake tool contacts the aluminum only about 0.05 inches on each side of the bend, thus minimizing the damage to the reflecting-surface substrate. The brake die is shown in Fig. 31.

The bends are made one at a time, progressively across the sheet. Care is taken in the forming and handling to avoid contact with the reflecting surfaces. Following these forming operations, all parts are chemically cleaned to remove dirt and surface oxide. The hat-section stiffeners are then spot-welded to the back of the concentrator as shown in Fig. 32. In this operation a special weld-jig holds the reflecting surfaces in proper position.

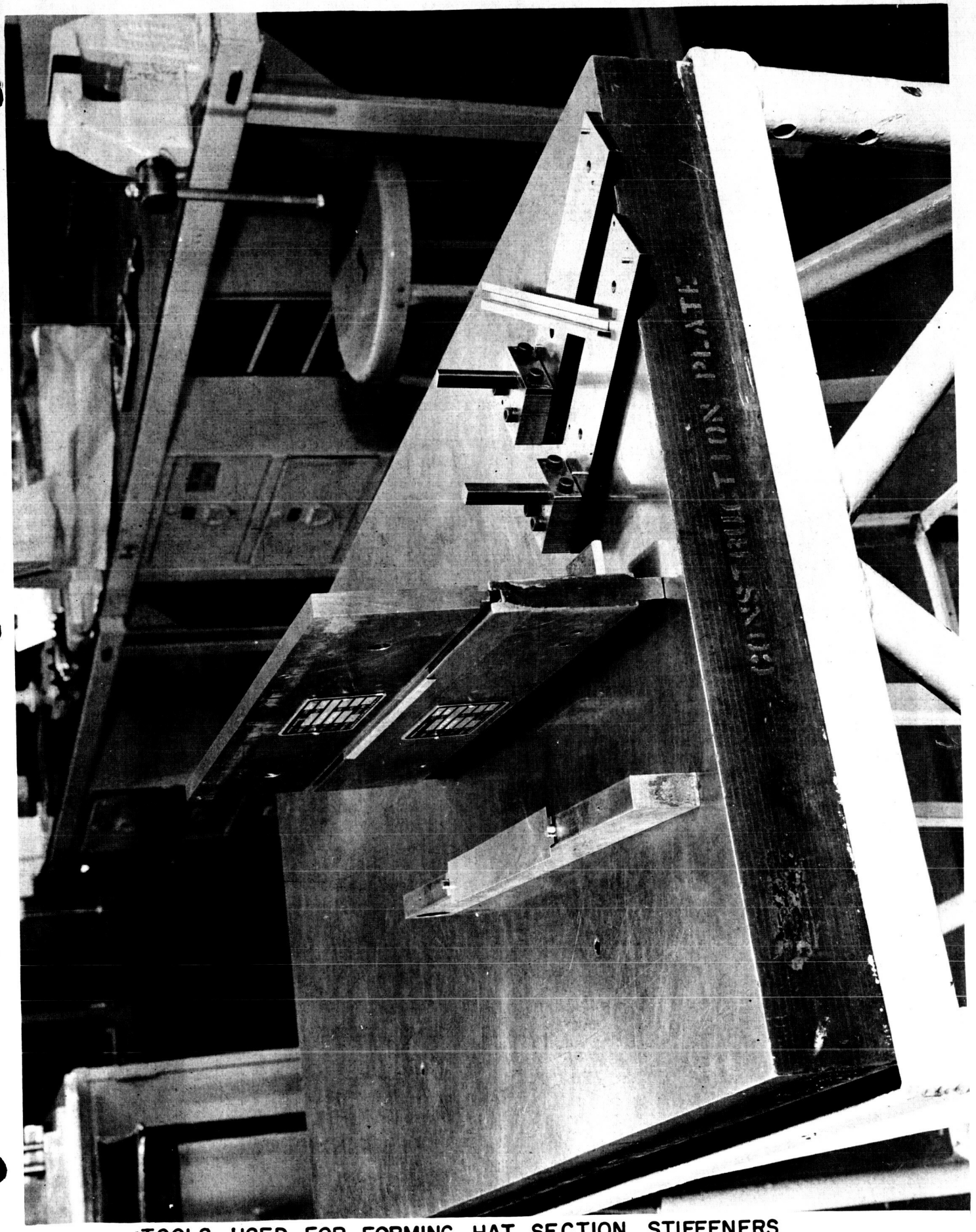

TOOLS USED FOR FORMING HAT SECTION STIFFENERS

FIG. 30

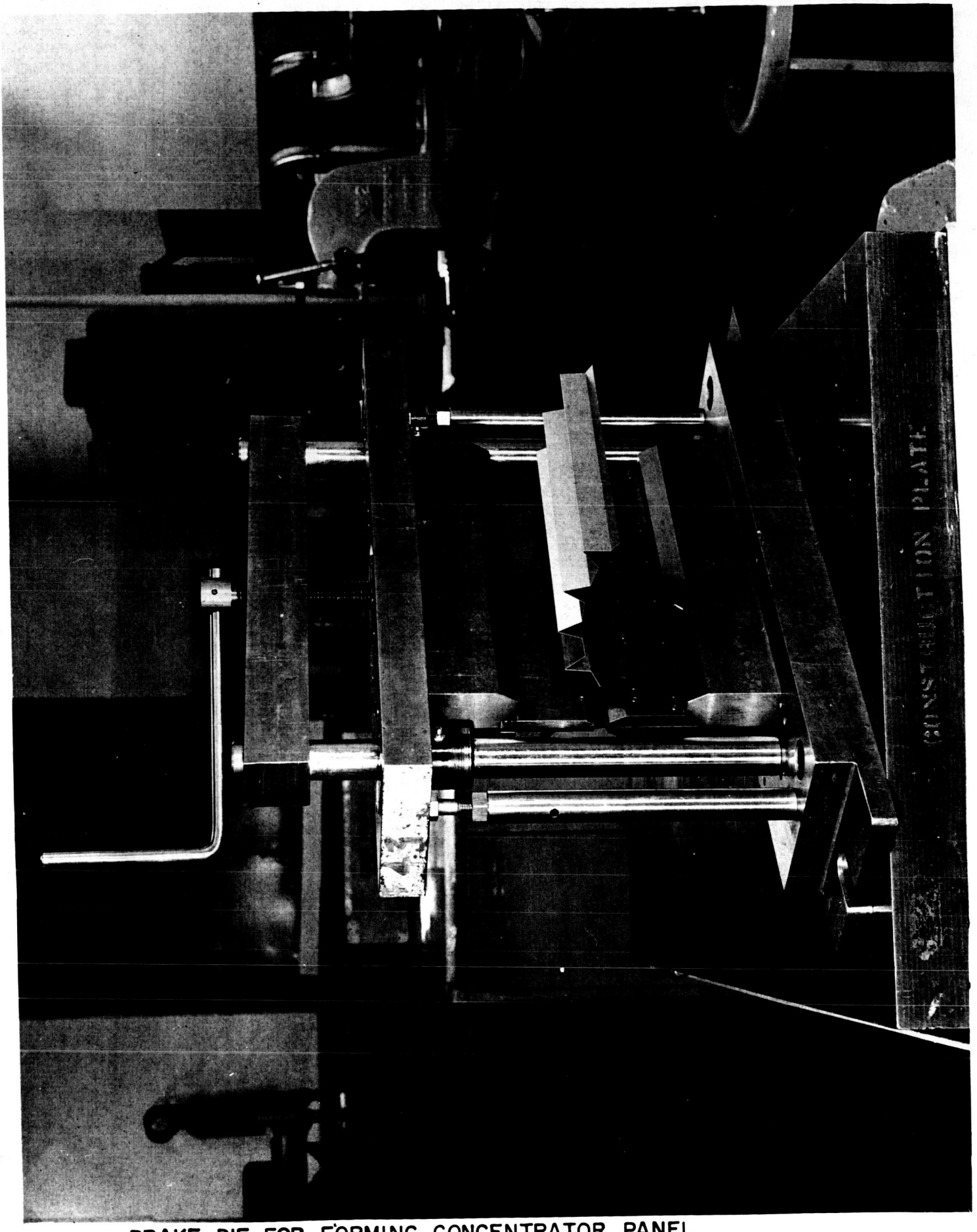

BRAKE DIE FOR FORMING CONCENTRATOR PANEL

FIG. 31

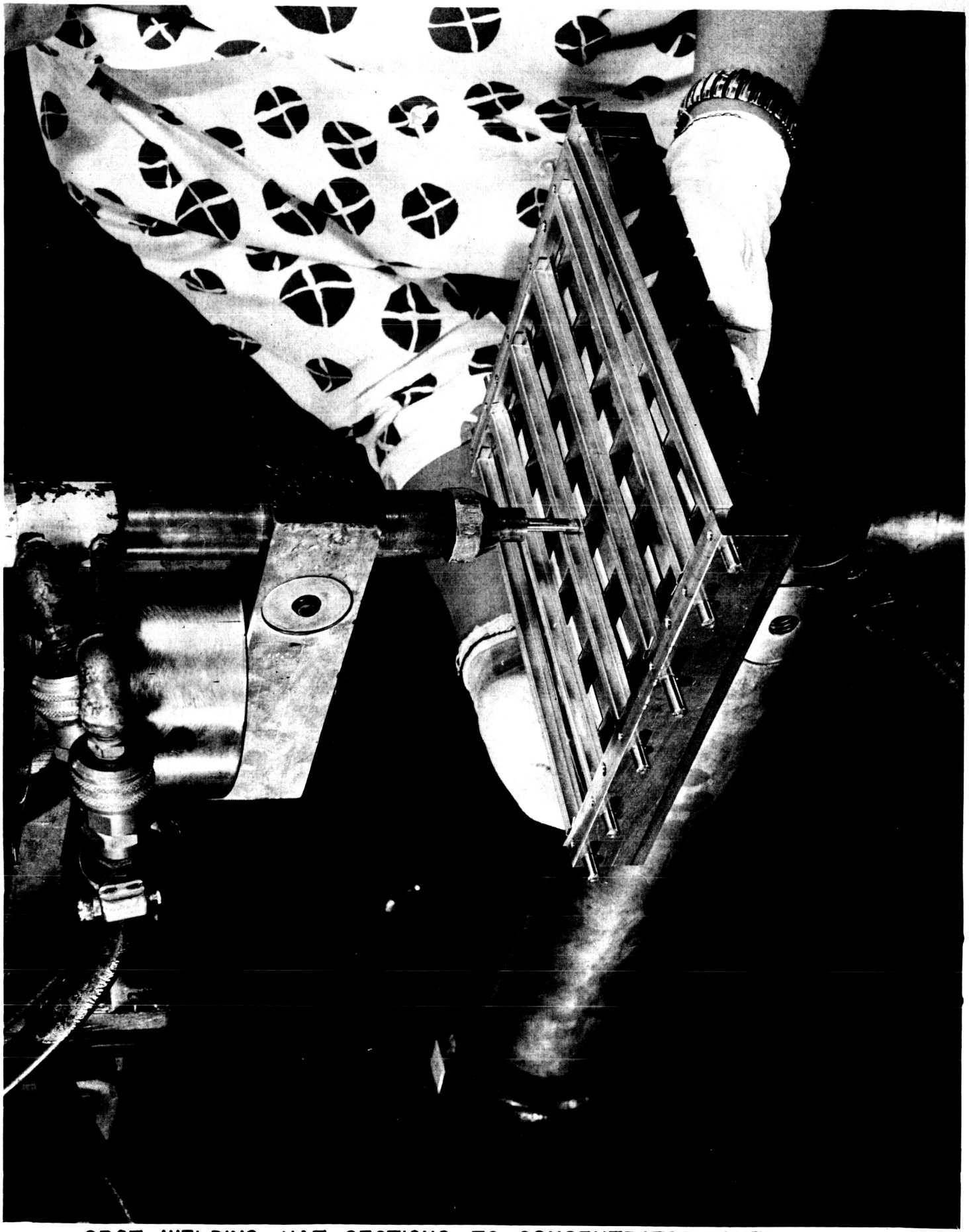

SPOT WELDING HAT SECTIONS TO CONCENTRATOR PANEL

FIG. 32

Reflective Surface Preparation

The steps in preparing an aluminized lacquer coating are:

1. The aluminum panel surface is thoroughly degreased, and flushed with solvents such as acetone and toluene to wash off all dust and foreign particles.

2. The lacquer (DuPont Dulux Clear Metal Finish RK-5752) is carefully filtered to eliminate dust and other particles. A solution of 2 parts RK-5752 to 1 part thinner (DuPont T-8911) is prepared.

3. A thin film of this lacquer is applied to the aluminum reflecting surfaces. The concentrator is placed with the trough nearly vertical and the thinned lacquer is flowed over the reflective surfaces with an eye dropper from the top edge.

4. The panel is kept vertical and in a clean environment until the lacquer is dried.

5. A second coat of lacquer is applied by the same procedure.

6. After the lacquer has dried, the panel is baked in an oven at 280° F for 30 minutes.

7. The panel is then placed in a vapor-deposition chamber and coated with aluminum.

8. A strippable lacquer (3-M EC968) is sprayed on the concentrator to protect the reflecting surfaces during subsequent cell installation.

The most difficult problems have been keeping dust particles out of the film and minimizing the roughness of the aluminum substrate.

The strippable lacquer has been found to be useful for temporary protection of the reflecting surfaces during manufacturing. However, it may not be satisfactory for protection during long-term storage. ALCOA reports that EC968 is not satisfactory for anodized sufaces because within a few days a tenacious bond is developed between the anodic suface and strippable lacquer. Alternate protective treatments are being investigated in Boeing research.

The aluminized lacquer surface is a simple and fast method of applying a specular surface to the rolled aluminum. The technique can easily be used on panels of larger size. However, alternate reflecting surfaces need to be investigated.

Solar-Cell Shingle Assembly

Hoffman Semi-Conductor Division was unable to supply assembled shingles of solar cells in time for the EOM concentrators. It was possible to obtain a supply of single solar cells without cover glasses that were rated 10 percent efficiency in space-level solar intensity and spectrum.

In previous research Boeing had developed procedures for testing the individual cells, assembling matched cells into shingles, and installing cover glasses. The 5-cell and 15-cell shingles required for the EOM concentrators were assembled in the Boeing Solar Systems Laboratory using these procedures. The data required for cell-matching are obtained under a xenon light source with the intensity adjusted to the equivalent of 100 milliwatts/sq. cm. of terrestrial sunshine. A voltage-current curve is recorded and current at maximum power noted. The cells having nearly equal current at maximum power are assembled into shingles.

Cells are soldered together to form shingles by preheating the cells on a copper plate held at a temperature of 175° to 180°C. Then they are locally heated at the joint to the melting point of solder (186°C) with two strokes of the fine point of a small soldering iron. A very thin coat of soldering flux is applied to one surface of the joint before the solar cells are laid in place on the preheat plate. The terminal surfaces of the solar cells contain enough solder to insure a good joint without additional solder.

The assembled shingles are cleaned with a solvent to remove all soldering flux, fingerprints, and dust. Cover glasses are then cemented in place with an epoxy adhesive, Furane E15. OCLI No. 207-SCC450-2 cover glasses are used.

Solar cells for the CS-1 concentrator were assembled into shingles by Hoffman, the supplier.

Attachment of Shingles to Panel

The solar-cell shingles are attached to the concentrator panel in the following manner:

> The concentrator trough and backs of the shingles are first cleaned with acetone until all traces of grease and dirt are removed. The trough and shingles are then painted with General Electric XS 4004 Silicone primer. This primer is allowed to dry for one hour. A 0.001 inch thick mylar strip, the length and width of a concentrator trough is cleaned with acetone and then painted on both sides with the Silicone primer.
>
> A layer of General Electric RTV-60 Silicone adhesive, approximately 0.004 inch thick, is spread in the concentrator trough after the primer has thoroughly dried. The thickness of the adhesive is controlled by a scraper with a depth-gauge attachment.

A thin layer of RTV-60 is also spread on the back side of the solar-cell shingle. The mylar film is placed in the trough on top of the 0.004-inch thick RTV-60 and worked into position. All of the trapped air between the mylar and RTV-60 is carefully forced out. A 0.016-inch thick layer of RTV-60 is then spread on top of the mylar film. The solar-cell shingles are then pressed firmly into the trough, working out the air trapped beneath each shingle and mylar.

The concentrator panel is left to dry at room temperature for five or six hours.

Wiring Technique

A unique method of interconnecting the solar-cell shingles has been developed and tested. All the cells in a given trough are connected in series and these shingles are connected in parallel with shingles in the adjacent troughs, as shown below. This circuit was chosen because it minimizes power loss resulting from any cell failure with very little extra wire weight.

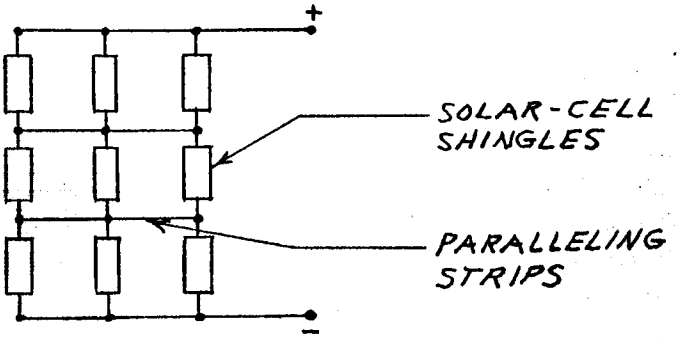

The concentrator structure is reinforced in the back by hat-section stiffeners which run the full length of the concentrator perpendicular to the direction of the V-ridges and troughs (Fig. 33). These stiffeners are located 1.85 inches apart and are spot-welded into place. The 1/4-inch faces of the stiffeners form areas on which paralleling strips can be bonded. The paralleling strips are made from copper-plated plastic sheet which is used in the manufacture of printed circuits.

The 1/32-inch thick printed board material is cut into 1/4-inch wide strips. A 1/8-inch wide tape is placed down the center of the copper side of the strip. The strip is then submerged in a ferric chloride solution to etch away the 1/16-inch of exposed copper on each side of the tape. Removing this copper provides assurance that no short-circuits will occur between the copper strip and the concentrator structure. Details of the paralleling strip are shown in Fig. 33 and in the following sketch.

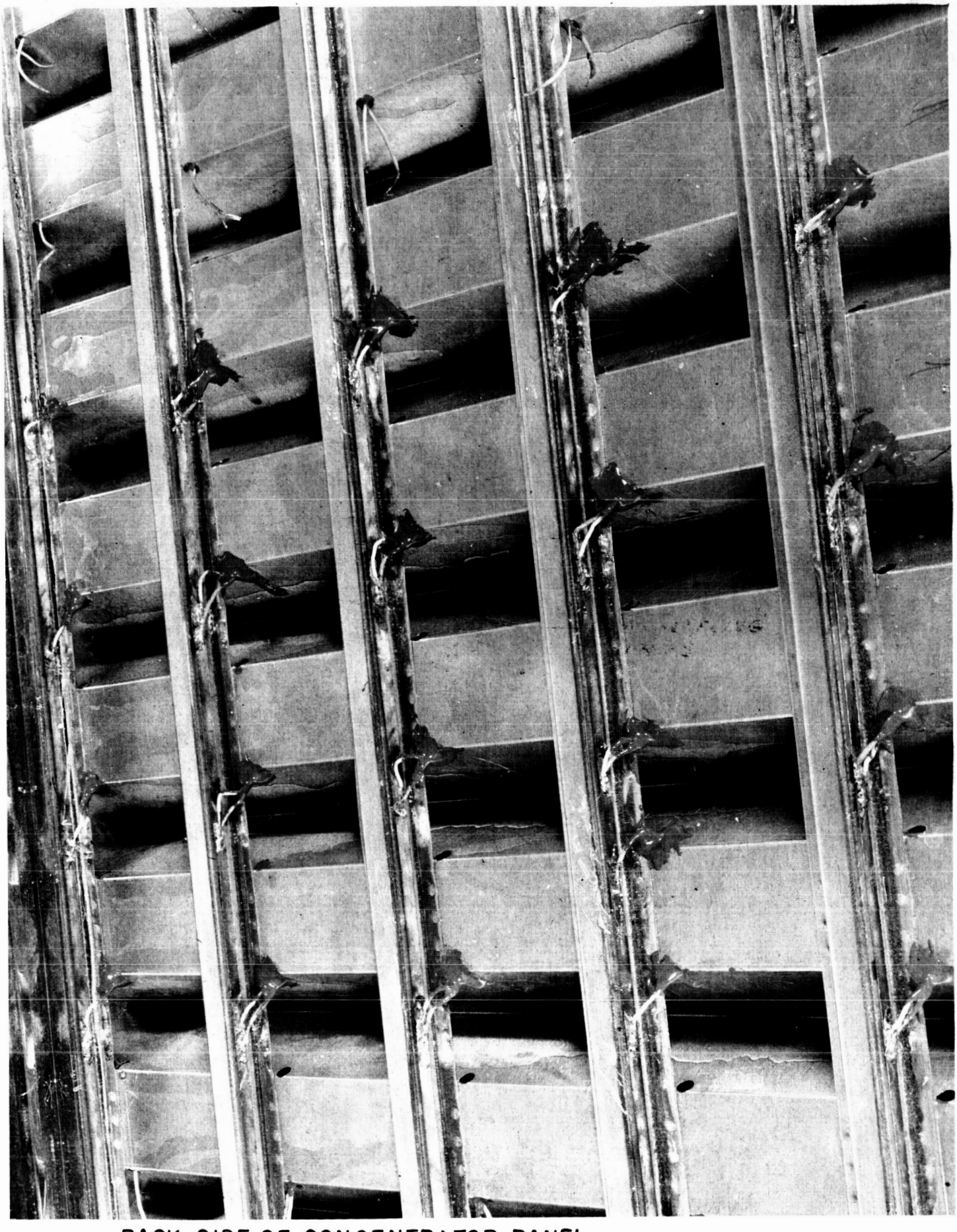

BACK SIDE OF CONCENTRATOR PANEL
SHOWING WIRING DETAILS

FIG. 33

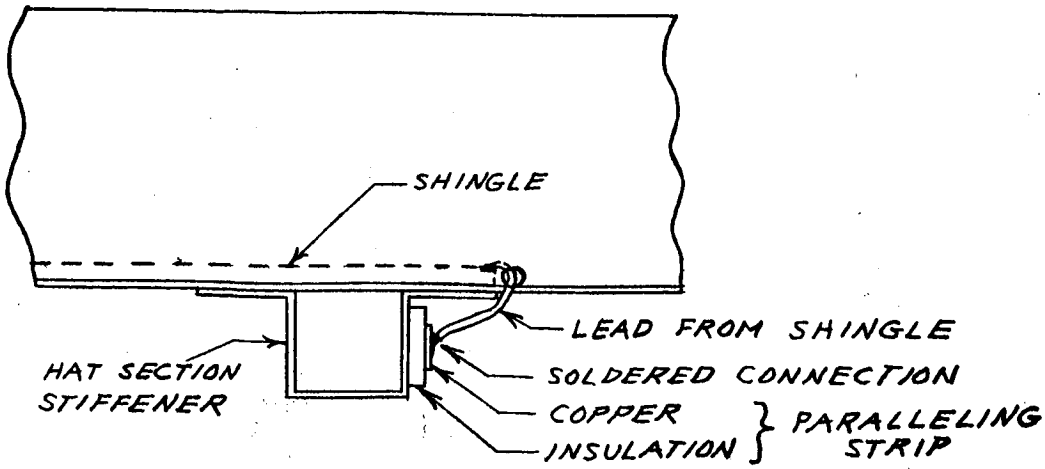

In attaching the paralleling strip one side of the cleaned hat-section is coated with a mixture of Epon 815 and Versamid 125. The back side of the paralleling strip is coated with the same mixture and then the two surfaces are clamped together firmly for 16 hours. One copper strip is bonded on each hat section for the parallel connections between the shingles. These strips also serve as convenient terminals for making the series connections between shingles.

The concentrator has 1/8-inch diameter holes 1.85 inches apart at the edges of the troughs for solar-cell pigtail leads. Each hole is located 1/4-inch from the hat-section face having the paralleling strip.

Each solar-cell shingle has a piece of Number 28 Teflon-insulated stranded wire soldered to each end. The positive lead from one shingle and the negative lead from the next shingle are brought through the same hole and both leads are soldered to the same paralleling strip. This establishes the series connections as well as the parallel connection between the shingles.

A paralleling strip on one edge of the concentrator has only negative leads soldered to it, and one paralleling strip on the opposite edge has only positive leads soldered to it. Terminals mounted on these strips constitute the power outlet of the concentrator.

VII. TESTING

Prototype, EOM, and CS-- concentrators were subjected to solar and mechanical tests and physical measurements. Solar and mechanical tests are described, followed by an analysis of test results.

A. Prototype and EOM Concentrator Tests

Prototype Concentrator Solar Tests

Nine prototype concentrators were tested for optical-efficiency to evaluate various materials and processes for manufacturing the EOM concentrators. The tests also established the variation in efficiency within a given concentrator.

The setup for solar tests is shown in Fig. 34. A portable equatorial mount is used to track the sun. The test concentrator, reference solar cell, pyrheliometer, and a sun alignment indicator are mounted on a plywood platform which is attached to the polar axle of the equatorial mount. Shade tubes are placed over the reference cell and the concentrator to eliminate nearly all the diffuse sky radiation.

It was found in early tests on solar-cell concentrators that considerable experimental error resulted when shade tubes were not used. The reason was that light reflected from surrounding objects and diffuse sky radiation can change during a run, while the direct radiation intensity is relatively constant. The diffuse component of sunlight would normally not be present in space conditions. Furthermore, diffuse radiation contributes more to the output of the cells without the concentrators, than it does to cells in a concentrator.

Care must be taken in use of shade tubes., The test area on the concentrator must be small to minimize the amount of sky this area can see. Preferably, only one shingle and its adjacent reflector walls should be illuminated at a time. The shade tube arrangement is shown in the following sketch:

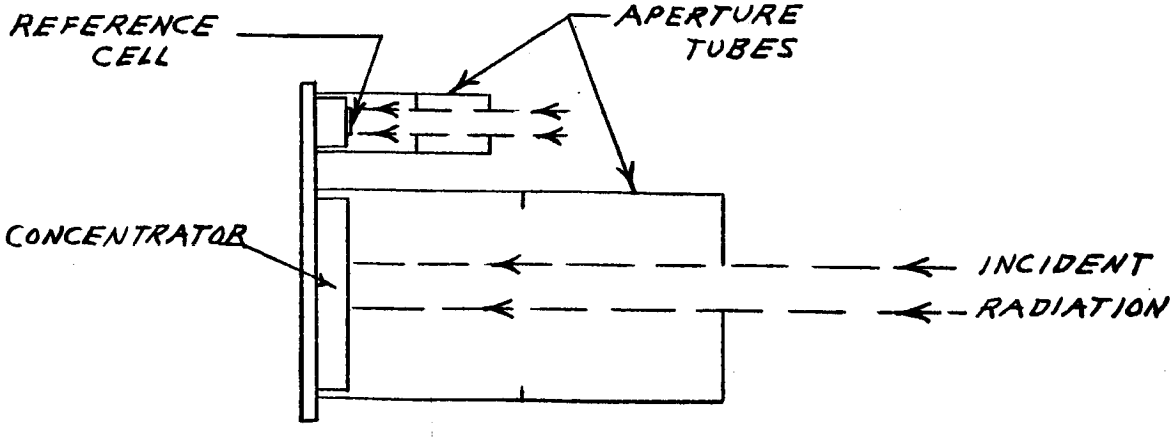

SOLAR TEST APPARATUS

D2-GC043-A

FIG. 34

The shade tube and concentrator must be accurately aligned towards the sun. The inside walls of the shade tube are covered with an optically black cloth which absorbs light at grazing angles. This prevents diffuse sky radiation from being reflected off the walls onto the cells.

In evaluating a concentrator the short-circuit current of a 5-cell shingle of solar cells is measured both with and without concentration. Simultaneously, the short-circuit current of the reference cell is recorded. The readings from the shingle are then corrected for any change in solar intensity indicated by the reference cell. The ratio of the corrected short-circuit current with and without concentration gives the concentration ratio (C) of the concentrator.

The best technique for the short-circuit current measurement without concentration is to remove the concentrator from the shade tube and lay the cells directly on the plywood platform. Then the short-circuit current of each test shingle is measured with illumination through the same aperture as used with the concentrator. However, this technique can only be used for preliminary evaluation of the concentrators before solar cells are bonded in the troughs.

Three 5-cell shingles of 10-percent efficiency cells with cover glasses were used in prototype concentrator tests. These shingles were placed at equally spaced intervals along a given trough. After the measurements in one trough were completed, the three shingles were removed and placed in another trough.

The temperature of the shingles was kept low (20 to 30°C) by exposing the cells to sunlight only when readings were taken.

Typical test data are shown in the following tabulation for concentrator No. 4. The positions of the shingles in the concentrator are shown in the sketch.

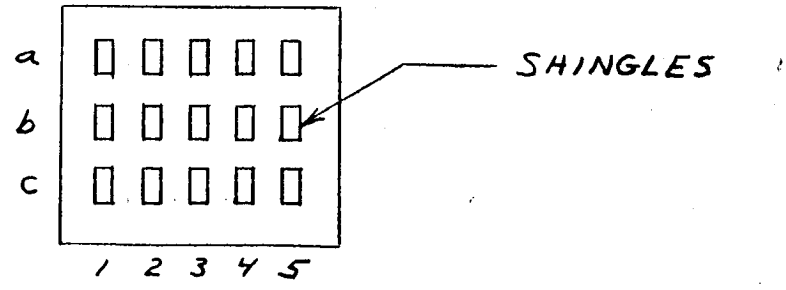

Cell Position In Concentrator	Current with concentrator / Current without concentrator
1a	1.70
1b	1.68
1c	1.75
2a	1.70
2b	1.74
2c	1.76
3a	1.71
3b	1.71
3c	1.74
4a	1.74
4b	1.74
4c	1.78
5a	1.74
5b	1.70
5c	1.77
Average	1.73

The manufacturing tolerances of this prototype concentrator caused a variation of about ± 3 percent around the average increase in SCC of 1.73.

The average SCC ratios for four prototype concentrators are tabulated below.

	Prototype Number			
	#2	#4	#5	#6
Short-Circuit Current Ratio	1.69	1.73	1.65	1.71

Prototype No. 4 gave the best performance. It had the most specular reflector finish of any of the prototypes and had well formed, flat reflector surfaces. Although No. 2 had a good specular finish it had surface roughness. Both No. 5 and 6 had good manufacturing tolerances and flat reflecting surfaces, but had an inferior specular finish.

EOM Concentrator Solar Tests

The EOM-1A, EOM-2A, and EOM-2B concentrators were tested in sunshine at Paradise Park on Mt. Rainier. This test site is at an elevation of 5500 feet above sea level, and clear sunshine was available on the days the tests were conducted. The EOM-1B concentrator was delivered to JPL for evaluation without being tested.

For solar tests the concentrator was placed on the equatorial mount previously described and oriented toward the sun. A shade tube was placed over the concentrator to eliminate diffuse sky radiation. A volt-ampere curve was plotted with a Mosley X-Y recorder, and the short-circuit current and open-circuit voltage were calibrated with 1/2-percent accurate instruments. The volt-ampere curve was plotted for each concentrator with the reflectors covered and uncovered. Shading of the reflectors was accomplished by laying a flat aluminum mask across the top of the V-ridges. This sheet had rectangular slots slightly longer than and only as wide as the shingles mounted in the troughs, and allowed only direct sunlight to strike the cells. An attempt was made to record the data for the covered and uncovered condition of each concentrator at the same solar-cell temperature. The resulting curves are shown in Figures 35, 36, and 37.

From these volt-ampere plots, the following maximum-power values were obtained. Solar-cell temperature, where available, is shown in parentheses.

Concentrator	Maximum power, watts		Short-Circuit Current Milliamperes	
	Reflectors Exposed	Reflectors Covered	Reflectors Exposed	Reflectors Covered
EOM-1A (nine 5-cell shingles)	1.211	0.666	220.0	126.7
EOM-2A (three 15-cell shingles)	1.215	0.655	214.5	122.5
EOM-2B (three 15-cell shingles)	1.347 (39.3°C)	0.710 (35.7°C)	241.7	136.5

The contract requirement pertaining to specific power is:

> "The specific power (watts/sq. ft. of projected Concentrator-Structure area) of the concentrator structure shall be at least ninety percent (90%) of that obtained from a nonconcentrator structure with eighty-five percent (85%) active coverage of equivalent photovoltaic cells at the same temperature, spectral distribution and solar intensity. The specific power shall be determined in sunlight. The nonconcentrator structure specific power shall be calculated from measurements with the reflecting surfaces shadowed."

This requirement can be reduced to an equation,

$$SPR = \frac{P/A}{P_u/A} \qquad (46)$$

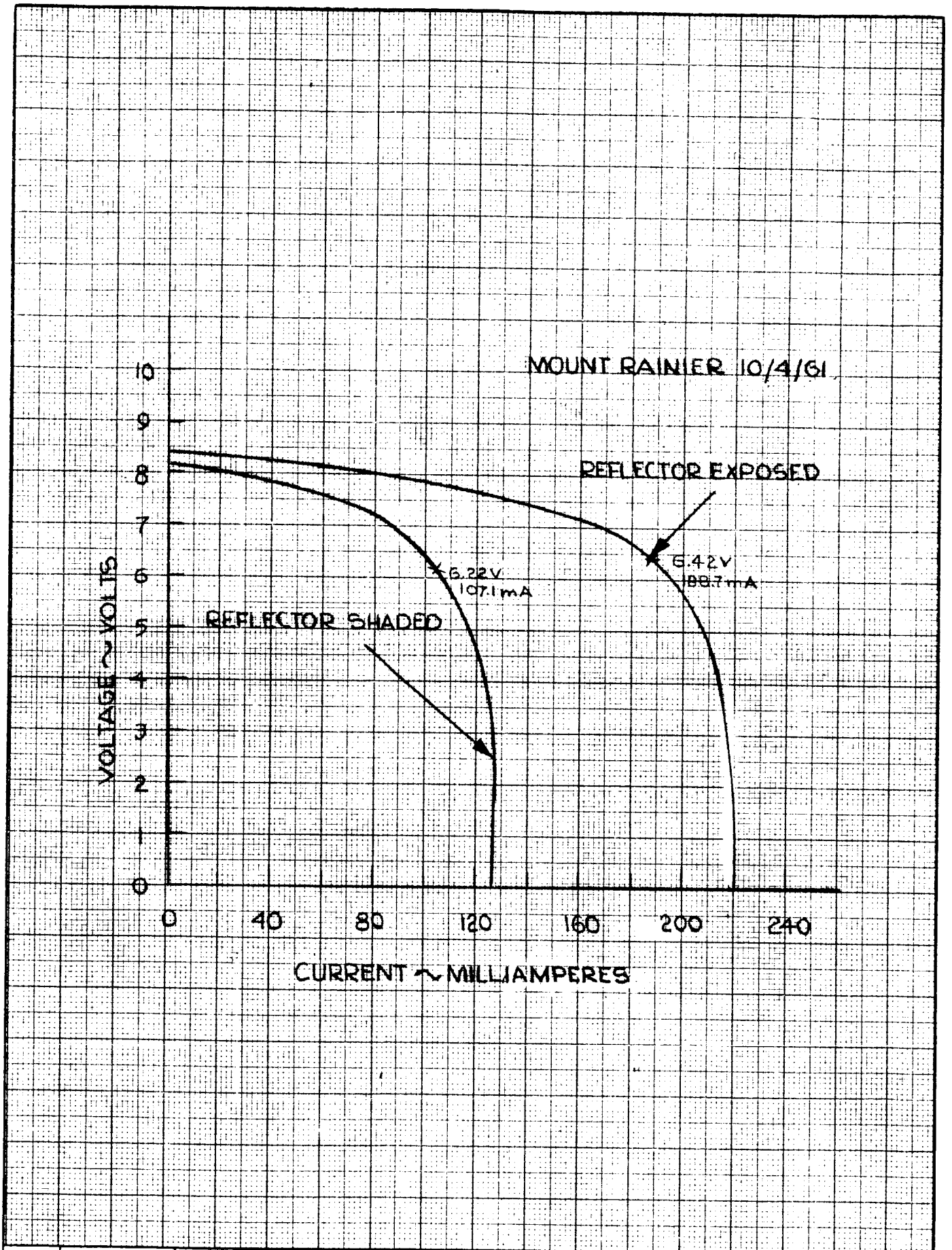

CALC			REVISED	DATE	VOLTAGE-CURRENT LOAD CURVES FOR EOM-1A CONCENTRATOR
CHECK					
APR					
APR					
					THE BOEING COMPANY

FIG 35

D2-90070A

PAGE 76

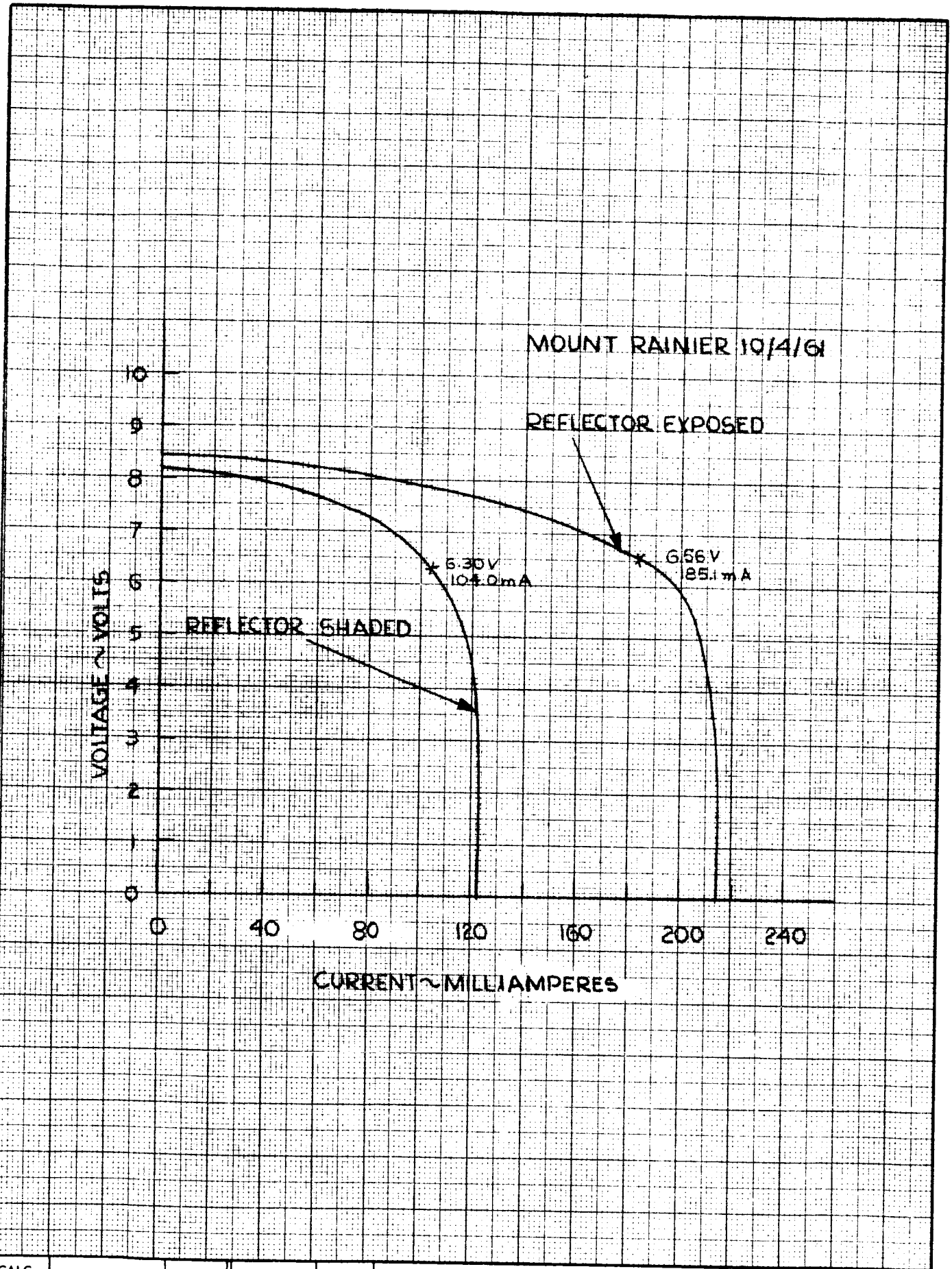

CALC			REVISED	DATE	VOLTAGE - CURRENT LOAD CURVES FOR EOM-2A CONCENTRATOR
CHECK					
APR					
APR					
					THE BOEING COMPANY

FIG 36

D2-20041A

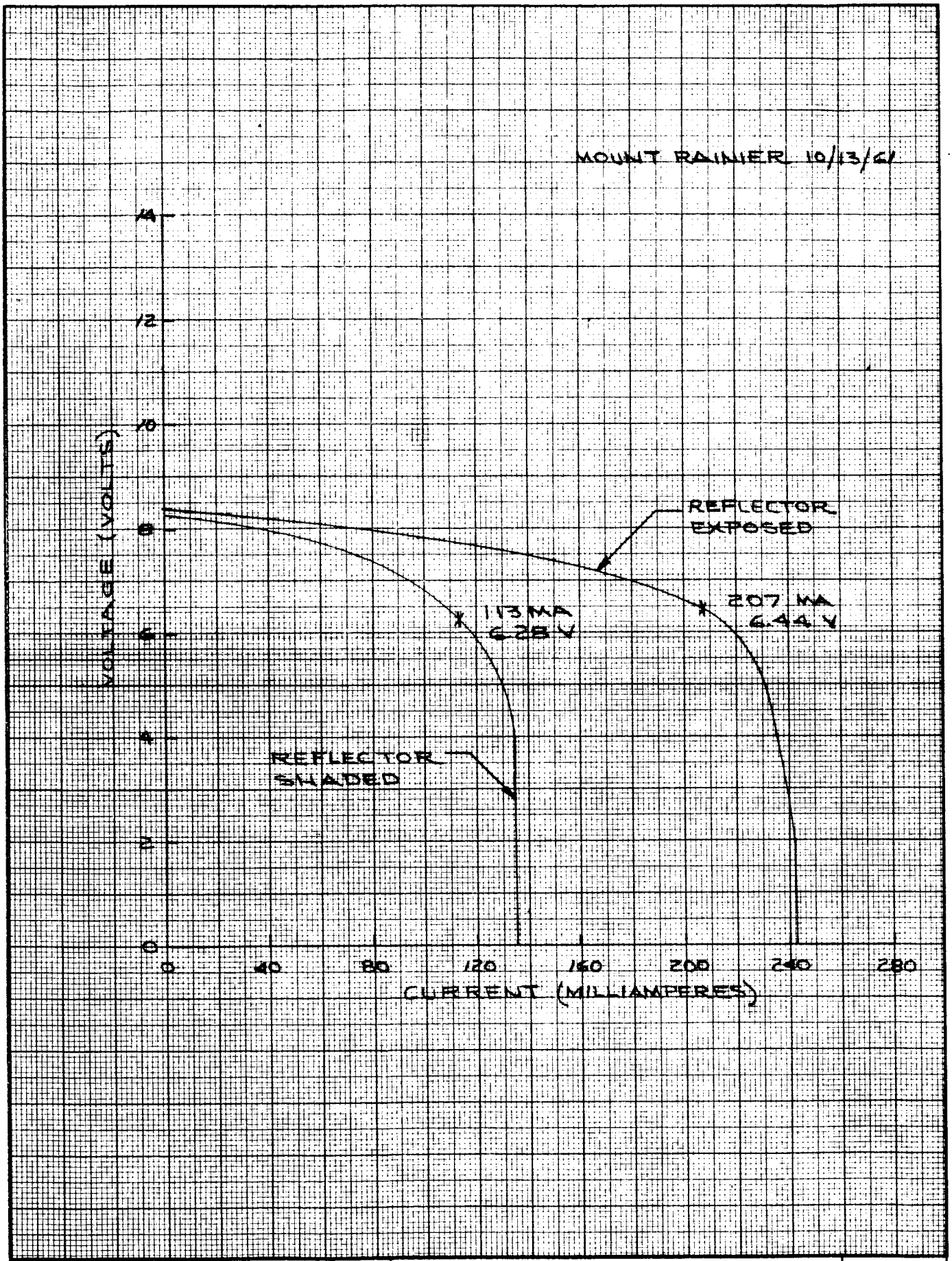

			REVISED	DATE
CALC				
CHECK				
APR				
APR				

VOLTAGE-CURRENT LOAD CURVES FOR EOM-2B CONCENTRATOR

FIG. 37

D2-90041A

BOEING AIRPLANE COMPANY

where SPR $\geq$ 90% = specific power ratio

P = Maximum power output of the solar cells with the reflectors exposed to sunlight

A = Area of the cells and the utilized area of the concentrator. This includes ridge bending radii, lost area between cell sides and reflectors, space between shingles, and the reflector area that illuminates the space between shingles.

P_u = Maximum power output of solar cells covering 85 percent of Area A.

P_u was computed as follows:

$$P_u = \frac{0.85A\ P_n}{A_c} \qquad (47)$$

P_n = Maximum power measured when concentrator was exposed to sunlight and the reflectors were covered.

A_c = Net area of solar cells in the concentrator that was solar tested.

Thus,

$$SPR = \frac{P\ A_c}{0.85\ A\ P_n} \qquad (48)$$

From EOM-1 solar test data and measurements

$P = 1.211$ watts

$A_c = 12.3$ sq. in.

$A = 27.0$ sq. in.

$P_n = 0.666$ watts

$$SPR = \frac{1.211 \times 12.3}{0.85 \times 27.0 \times 0.666} = 0.974$$

The above calculation of specific power ratio (SPR) was performed in accordance with the JPL Contract requirement for an area utilization factor (F_3) of 85 percent. As explained previously, JPL now suggests that a factor of 92 percent is more realistic in light of present solar panel design. Specific power ratio was calculated, following the above example, for all concentrators using both an 85 percent area utilization factor and a 92 percent area factor.

The calculated values of specific power ratio and also of power concentration ratio and short-circuit concentration ratio for each of the tested concentrators are presented in the following table:

Concentrator	Specific Power Ratio F_3 = 85%	F_3 = 92%	Power Conc. Ratio	Short-Circuit Conc. Ratio
EOM-1A	0.974	0.900	1.82	1.74
EOM-2A	1.028	0.948	1.85	1.75
EOM-2B	1.055	0.974	1.90	1.77

Pyrheliometer data were obtained in the solar tests of EOM-2B, and showed that solar intensity held constant at 98 milliwatts per sq. cm. during the entire test period. These data allow the conversion efficiency of the concentrator to be calculated.

From test data and measurements:

$S = 98 \text{ mw/cm}^2$

$P = 1347 \text{ mw}$

$P_n = 710 \text{ mw}$

$A_c = 12.4 \text{ sq. in.}$

$A = 26.2 \text{ sq. in.}$

Conversion efficiency with reflectors shaded:

$$\eta_n = \frac{P_n}{(2.54)^2 \times A_c S} \times 100 \qquad (49)$$

$$= \frac{710 \times 100}{(2.54)^2 \times 12.4 \times 98} = 9.1\%$$

Conversion efficiency with reflectors exposed:

$$\eta_e = \frac{P}{(2.54)^2 A S} \times 100 \qquad (50)$$

$$= \frac{1347 \times 100}{(2.54)^2 \times 26.2 \times 98} = 8.1\%$$

Prototype and EOM Concentrator Structural Tests

The contract requires the concentrator to be subjected to 1/4 and 1/2 of the vibration levels specified in JPL specification 30218-B, paragraph 4.3.2.

A prototype panel was used to develop the magnetic tapes required to apply the specified vibrations to the EOM panels. This panel was subjected to:

A. Sinusoidal vibration swept between 1 cps and 40 cps in eight minutes at a sweep rate proportional to the frequency.

This sinusoidal vibration was applied normal to the plane of the solar cells and was applied three times for a total time

of 24 minutes. The equipment used to apply this low frequency vibration consisted of a hydraulic vibrator controlled by an electronic function generator.

Displacement amplitudes of ± 1-1/2 inches were applied between 1 and 4 cps instead of between 1 and 3 cps as specified. The change to 4 cps was made because of equipment limitations and did not affect the subsequent performance of the panel.

1.5 "g" acceleration level was applied between 4 and 40 cps.

The high-frequency, complex-wave vibration test was accomplished on a 25,000 lb. electromagnetic vibrator driven by a 175 KVA LING amplifier and controlled by a magnetic tape through electronic mixers and amplifiers. The vibrations imposed on this preliminary panel were white gaussian vibration, band-limited between 15 and 1500 cps, with the following acceleration levels and in this chronological order.

B. 15 "g" rms acceleration for 6 seconds.

C. 5 "g" rms acceleration for 3 minutes.

D. 2-1/4 "g" sinusoidal vibration swept from 40 to 1500 cps in 2 minutes at a rate proportional to the frequency. This sinusoidal vibration was applied three times without the white gaussian vibration and was recorded on magnetic tape for subsequent mixing with the random vibration.

E. 2-1/4 "g" rms with a 2-1/4 "g" sinusoidal vibration swept from 40 to 1500 cps in two minutes at a rate proportional to the frequency. Three sweeps were applied for a total time in this condition of six minutes.

F. 7-1/2 "g" rms for 6 seconds.

There were no apparent failures in the structure of the prototype concentrator nor did subsequent tests indicate degradation of the solar cell installed in the center of the panel.

Concentrating panels similar to EOM panels were subjected to the above vibration specifications except for two items: (1) Item B - the acceleration was changed to the contract requirement of 7-1/2 "g" rms for six seconds, (2) Item D was eliminated because it is not a contract requirement and was used only for preparing the magnetic tape. In addition, a search was made for panel resonance between 50 cps and 5000 cps.

The high-frequency complex wave test was applied to the EOM-type panels first, followed by the low-frequency sinusoidal loading (Item A). This reversal of order was necessitated by availability of equipment, and had no significant effect upon the panel behavior.

Panel resonance was not observed at any time during any of the complex-wave tests. During the search for the panel resonant frequency it was necessary to dwell momentarily at near-resonant conditions. The panels varied in resonant frequency between 240 cps and 340 cps.

The resonant frequencies of the panels were found by applying a 1/2 "g" sinusoidal vibration and slowly sweeping the frequency to determine the frequencies at which the panels resonated. The 1100-H25 panel with doublers had a first mode resonant frequency of 240 cps, the 1100-H25 without doublers had a first mode resonant frequency of 300 cps, and the 6061-T4 panel with doublers had a first mode resonant frequency of 340 cps. The trough between the stiffeners indicated resonance at 170 cps.

It was assumed in the analysis that these panels would behave as flat plates fixed along two edges. This assumption seemed justified due to the stiffness of the edge attachment clips. If the panels were to behave as flat plates simply supported along two edges, their resonant frequencies should have been about 560 cps. Since the measured resonant frequencies were approximately 300 cps, the structural efficiency factor for the design must be approximately

$$\epsilon = \frac{300}{560} = 54\%$$

The ratio of effective EI to calculated EI is

$$\frac{EI_{Eff.}}{EI_{Calc.}} = \frac{(\omega \text{ measured})^2}{(\omega \text{ calculated})^2} = 0.54^2 = 0.291$$

This unusually low ratio may be due to the curved reflectors but is probably due to some other factors which have not been evaluated.

No EOM concentrator structures have failed under the structural vibration required by the Contract. An EOM-type concentrator structure was vibrated for 97 minutes at 15"g" in another test. The test was concluded because of failures at attachment points rather than failures in the panel.

B. CS-1 Concentrator Tests

Solar Tests

The CS-1 optical model and the CS-1 structural test model were tested in sunshine at the Boeing Solar Systems Laboratory in Seattle. Poor weather conditions at the test site on Mt. Rainier, where the EOM concentrators had been tested previously, prevented the use of that facility for the solar testing of CS concentrators.

The test procedure was the same as described for the EOM concentrators. The structural test concentrator, which contained five high-efficiency 5-cell shingles mounted in one channel for evaluation purposes, was solar tested both before and after it received vibration tests. The resulting volt-ampere curves for the CS-1 concentrator are shown in Fig. 38 and for the structural test model, before and after vibration tests, in Figs. 39 and 40 respectively.

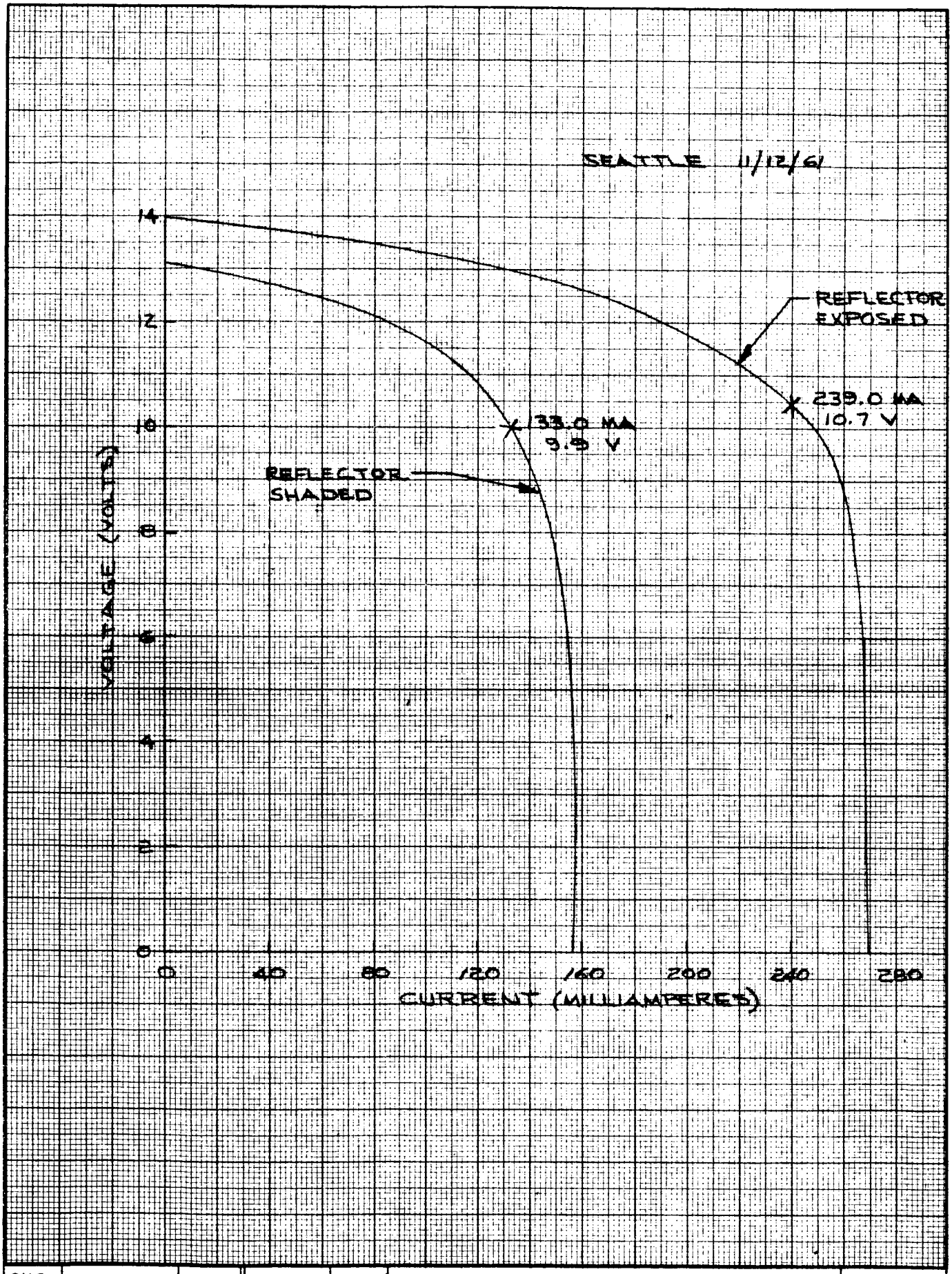

			REVISED	DATE
CALC				
CHECK				
APR				
APR				

VOLTAGE – CURRENT LOAD CURVES FOR CS-1 CONCENTRATOR

FIG. 38

D2-90041A

BOEING AIRPLANE COMPANY

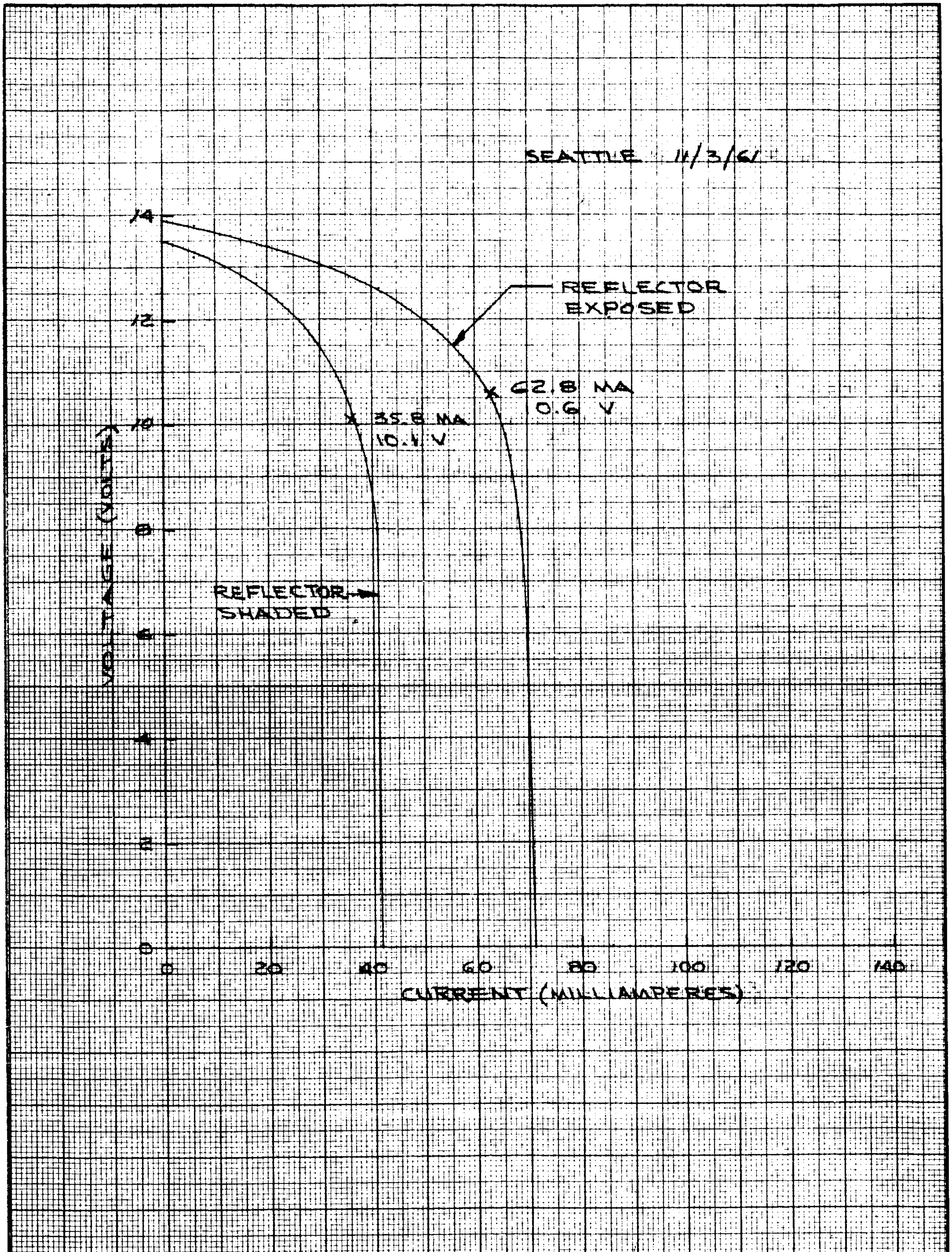

CALC			REVISED	DATE	VOLTAGE - CURRENT LOAD CURVES FOR CS MECHANICAL MODEL CONCENTRATOR (BEFORE VIBRATION TEST)	FIG. 39
CHECK						D2-90041A
APR						
APR					BOEING AIRPLANE COMPANY	PAGE 84

U3 4013 8000 WAS BA 461 R4

K•E ALBANENE 195L TRACING PAPER 60629

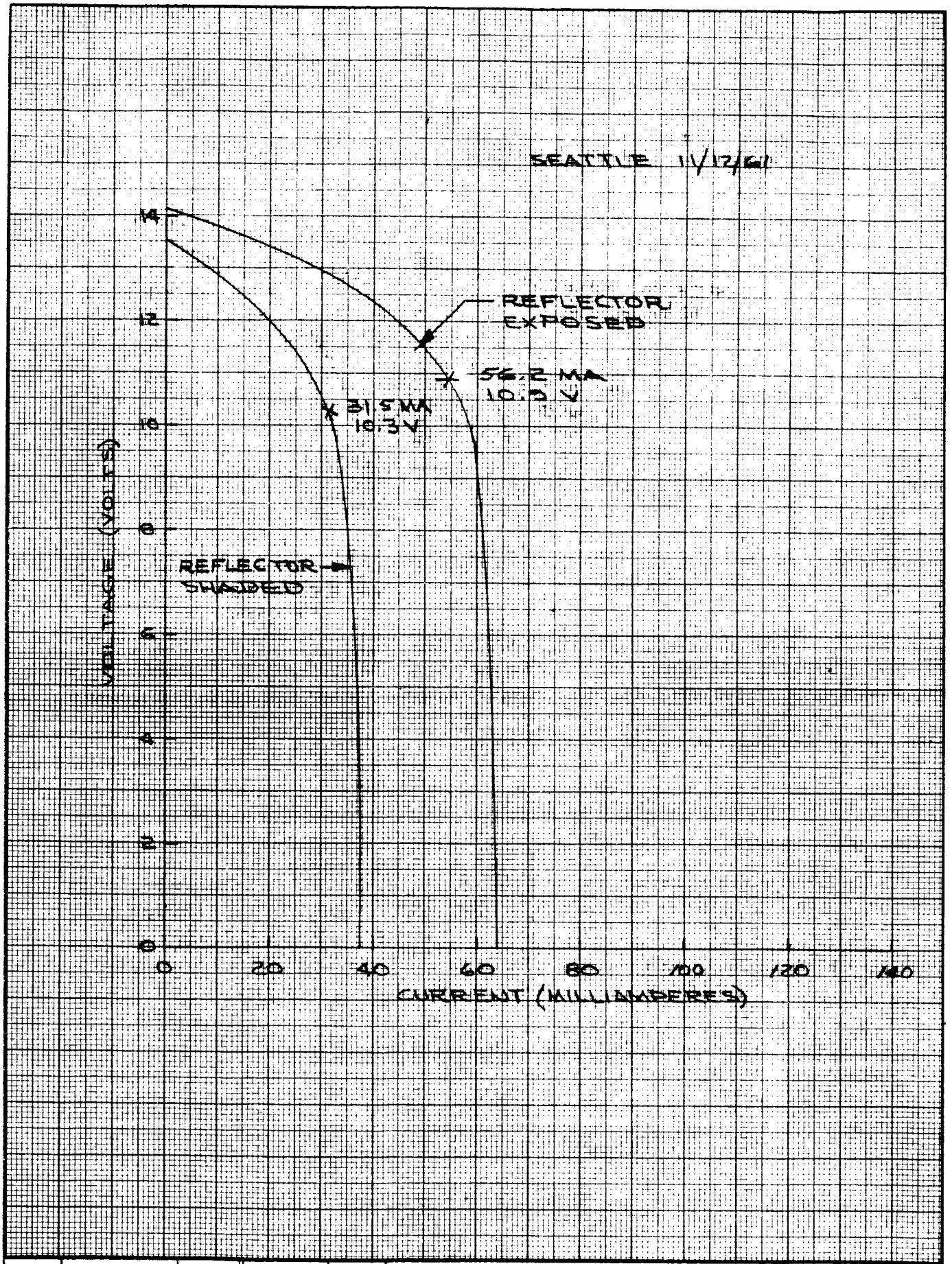

CALC			REVISED	DATE	VOLTAGE-CURRENT LOAD CURVES FOR CS MECHANICAL MODEL CONCENTRATOR (AFTER VIBRATION TEST)
CHECK					
APR					
APR					
					BOEING AIRPLANE COMPANY

FIG. 40

D2-90041A

PAGE 85

The following maximum-power values were obtained from the volt-ampere plots. Solar-cell temperature is shown in parentheses.

Concentrator	Solar Intensity MW/cm^2	Maximum Power, Watts: Reflectors Exposed	Maximum Power, Watts: Reflectors Covered	Short-Circuit Current, Milliamperes: Reflectors Exposed	Short-Circuit Current, Milliamperes: Reflectors Covered
CS-1 ((20) 5-cell shingles)	84.6	2.544 (26.0°C)	1.318 (25.0°C)	276.0	156.6
CS-Structural (five 5-cell shingles):					
Before Vibration	91.7	0.667 (29.8°C)	0.363 (26.3°C)	71.0	41.4
After Vibration	80.5	0.613 (21.6°C)	0.324 (19.0°C)	64.6	37.3

The specific power ratio was calculated using both an 85 percent area utilization factor (F_3) and a 92-percent area utilization factor. The specific power ratios, together with power concentration ratios and short-circuit concentration ratios, are tabulated below:

Concentrator	Specific Power Ratio F_3 = 85%	Specific Power Ratio F_3 = 92%	Power Concentration Ratio	Short-Circuit Current Concentration Ratio
CS-1	1.062	0.981	1.93	1.76
CS-1 Structural:				
Before Vibration	1.029	0.950	1.84	1.71
After Vibration	1.058	0.976	1.89	1.73

It should be noted that the difference in specific power ratio of the structural test concentrator before and after vibration test is almost entirely attributable to a difference in solar-cell temperature during the test. The short-circuit current ratio, which is relatively independent of temperature, indicates that no significant change in performance occurred as a result of vibration tests.

The conversion efficiency of the concentrators was calculated. The results are:

Concentrator	Conversion Efficiency, Percent: Reflectors Exposed	Conversion Efficiency, Percent: Reflectors Covered
CS-1	7.9	8.8
CS-1 Structural:		
Before Vibration	7.8	8.9
After Vibration	8.1	9.0

Structural Tests

The CS-1 concentrator was subjected to vibration and static bending tests. Solar tests were conducted before and after these structural tests, as previously explained.

The flexural rigidity of the concentrator was measured in a static bending test in which the panel was simply supported along the attachment edges and loaded with a line load along the centerline of the span. The EI was found to be 4010 $in.^2$ lbs. per corrugation. The calculated value for EI was 16,000 $in.^2$ lbs. per corrugation. No explanation for this difference between measured and calculated EI values has been found yet.

A resonant frequency calculation was made, using the experimental EI value and the actual shingle, bonding adhesive, and wiring weight of 0.0079 lbs. per shingle. The first mode resonant frequency for the EOM panels was found by calculation to be 300 cps, which agrees with the measured resonant frequency of 300 cps. In view of this agreement, the CS-1 resonant frequencies can be calculated with confidence from the experimental EI/m data. The first mode resonant frequency for the CS-1 panel was calculated to be 214 cps. The natural resonant frequencies for the CS-1 concentrator structure were not determined experimentally since it was considered undesirable to dwell at the resonance point long enough to make an accurate resonant-frequency measurement. The reason for this was that it would not have been possible in subsequent solar testing to distinguish between failures caused by the contract-specified vibration test and the resonance search.

The CS-1 concentrator structure was subjected to the vibration environment previously described under structural test items F, C, E, F, and A, in that chronological order. No structural failure occurred. One soldered connection to the paralleling strip in the back of the concentrator broke loose.

The flexural rigidity in a direction perpendicular to the reflector axis of the CS-1 concentrator structure was not measured since the calculated stiffness in this direction is so low compared with the stiffness in the reflector direction that it was not considered to be significant.

C. Analysis of Test Results

The contract requires that the losses which cause the performance of the concentrating photovoltaic structure to be less than theoretical shall be determined. These losses were established in independent tests which are described in Section IV. The effect of these losses on performance is discussed in Section III-D. In this section, the actual performance of a concentrator as measured in solar tests is compared with the performance that can be predicted from the losses as established in Section IV. It will be shown that the concentrator performance can be predicted thereby demonstrating that all factors affecting performance are understood and known. Concentrator structure EOM-2B is used as an illustration.

1. Short-Circuit Current Ratio

The short-circuit current ratio is defined as the ratio of the short-circuit current of the cells with concentration to

the short-circuit current without concentration, i.e.,

$$C_{IT} = \frac{I_c}{I_o} \tag{51}$$

It has been established that for the range of short-circuit currents under consideration and for a given spectrum, the short-circuit current is proportional to light intensity.* The short-circuit current ratio can be calculated from Eq. 41 in Section III-D by deleting the components of efficiency relating to power, η_c and η_t, and retaining only the term pertaining to short-circuit current, η_o - the relative quantum efficiency for non-normal light. Then:

$$C_{IT} = 1 + \frac{\eta_o F_2 KRA_r}{F_1 A_t} \tag{41A}$$

Concentrator structure EOM-2B was equipped with 15-cell shingles. The gross area of the trough containing the solar cells is:

$$A_t = \left[\text{(No. of cells)(length of active cell area) + (wiring allowance)}\right] \times \left[\text{width of trough}\right] \tag{52}$$

$$= \left[(15)(0.35) + 0.1\right] (0.8) = 4.27 \text{ sq. in.}$$

The gross projected area of the reflector surfaces is

$$A_r = \left[\text{(No. of cells)(length of active cell area) + (wiring allowance)}\right] \times \left[\text{projected width of two reflectors}\right] \tag{53}$$

$$= \left[(15)(0.35) + 0.1\right] (0.8) = 4.27 \text{ sq. in.}$$

The factor F_1 is:

$$F_1 = \frac{\text{active cell area}}{\text{gross trough area}} = \frac{(15)(0.35)(0.788)(100)}{4.27} = 97\% \tag{54}$$

The factor F_2 is:

$$F_2 = \left[\text{(Reflector projected width)-(bending and tolerance losses)}\right] \times \left[\text{active length of trough/total gross length of trough}\right] \tag{55}$$

If the concentrator had been formed exactly as specified in the drawing, then the net projected width would be the same as calculated in Section III-D, namely 0.88 in., and F_2 becomes:

$$F_2 = \frac{(0.88)(15)(0.35)(100)}{(15)(0.35) + 0.1} = 0.865$$

* See Boeing document D2-6935, "Measurement of Silicon Solar-Cell Spectral Response"

The reflectance of the aluminized lacquer surface was found to be 82 percent in measurements made with the Somor test fixture (Fig. 26). Since the reflectance values obtained with this fixture include the quantum efficiency of the cell for non-normal light, the factor is 1.0 when used with reflectance values obtained by this method. If the scatter factor K is assumed to be 97 percent, the same value assumed in Section III-D, the short-circuit current can be calculated by substituting the appropriate values in equation 41a as follows:

$$C_I = 1 + \frac{\eta_o F_2 KRA}{F_1 A_t} \qquad (41a)$$

$$= 1 + \frac{(1.0)(0.465)(0.97)(0.82)(4.27)}{(1.0)(0.97)(4.27)} = 1 + 0.708$$

$$= 1.71$$

The average observed short-circuit current ratio for EOM-2B was 1.77. Thus, the calculated ratio is 3.5 percent below that observed.

An effort was made to reconcile the difference between the observed and calculated short-circuit current ratio. For example, the dimensions of the concentrator structure were measured precisely with an optical comparator. Fig. 41 is a photograph of a typical reflector displayed on the comparator. It is apparent from this photograph that the reflecting surfaces are smooth and continuous and will not cause appreciable light scatter. The light scatter factor K should thus be unity. Fig. 42 lists the pertinent dimensions of the structure. The differences between the measured dimensions and those specified in the drawing (Fig. 28) were so insignificant that they could not have affected concentrator performance.

The light rays in a typical channel were traced to determine the active reflector areas (Fig. 43). The projected effective width of the reflector surfaces was found to be 0.335 inch for each reflector. With this dimension the short-circuit concentration ratio can be calculated from the following equation:

$$C_I = \frac{I_{sc} \text{ from direct light} + I_{sc} \text{ from reflected light}}{I_{sc} \text{ from direct light}} \qquad (55)$$

$$= 1 + \frac{I_{sc} \text{ from reflected light}}{I_{sc} \text{ from direct light}} \qquad (56)$$

$$= 1 + \frac{(\text{Intensity})(\text{Reflectance})(\text{Quantum Eff.})(\text{Project. width of active reflectors})}{(\text{Intensity})(\text{Width of active cell area})}$$

Using the measured value of reflector width, a reflectance of 82 percent, and a corresponding quantum efficiency of 1.0, the short-circuit current concentration ratio becomes

$$C_I = 1 + \frac{(0.82)(1.0)(0.335) \times (2)}{0.788}$$

$$= 1 + 0.698 = 1.70$$

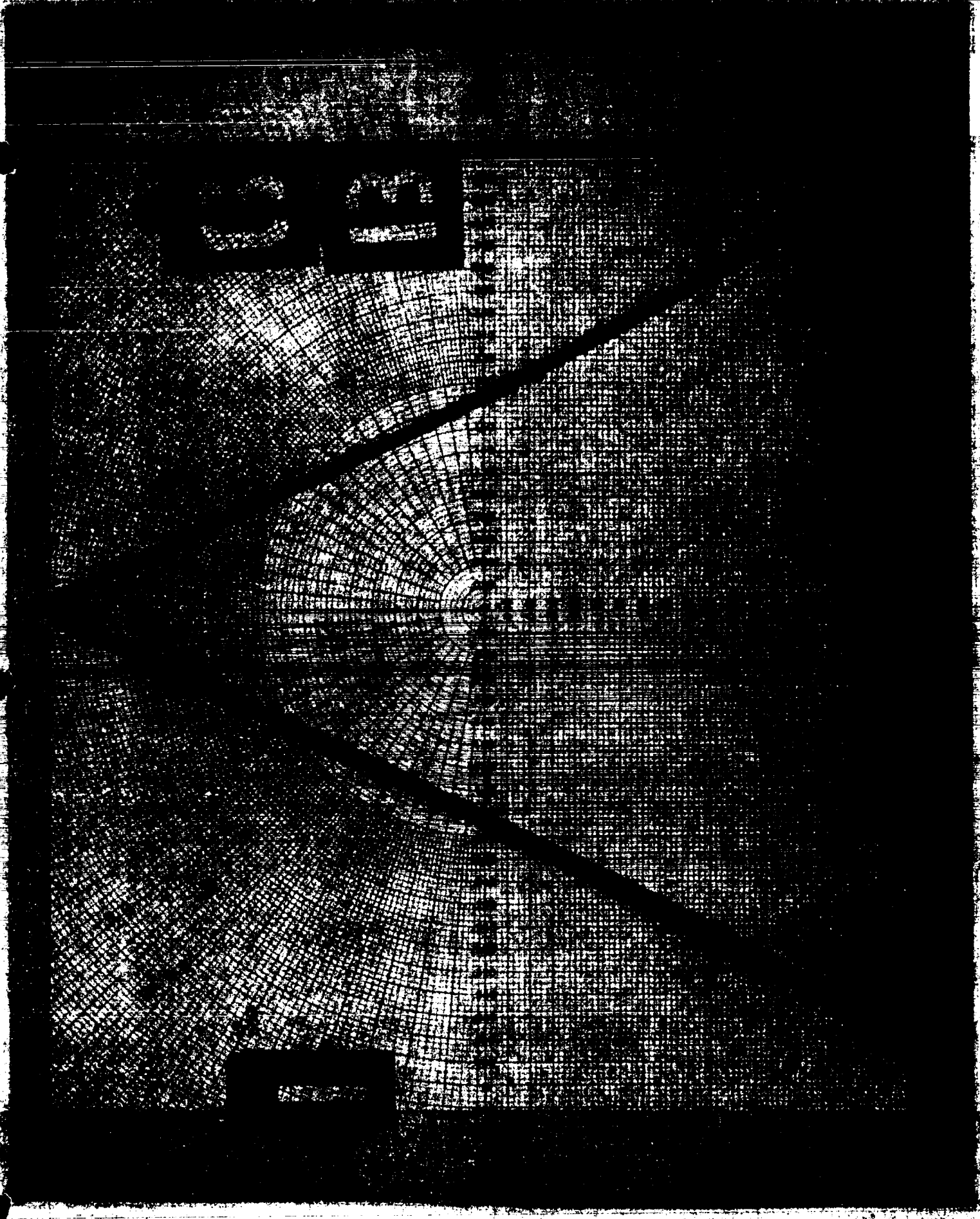

V-RIDGE DISPLAYED ON OPTICAL COMPARATOR
CONCENTRATOR STRUCTURE ECM-2B

Lineal Dimensions are measured in inches

Position	1_A	2_A	3_A	4_A	5_A	6_A	1_B	2_B	3_B	4_B	5_B	6_B
A_1	0.817	0.795	——	——	0.815	0.817	0.811	0.815	0.815	——	0.815	0.817
A_2	0.817	——	——	——	0.808	0.808	0.819	0.819	0.808	——	0.817	0.811
H	0.749	——	——	——	0.739	0.739	0.741	0.743	0.739	——	0.739	0.745
d	0.042	0.044	0.046	0.039	0.042	0.044	0.044	0.043	0.044	0.046	0.039	0.046
L	0.765	——	——	——	0.776	0.776	0.788	0.800	0.776	——	0.784	0.771
γ	49.8°	51.2°	50.6°	50.8°	50.7°	49.5°	49.6°	51.1°	50.4°	48.1°	49.2°	49.2°
ϵ_1	63.7°	——	——	——	61.5°	60.9°	60.7°	60.2°	59.1°	——	61.1°	60.1°
ϵ_2	62.6°	——	——	——	61.5°	60.5°	61.4°	60.6°	59.4°	——	60.4°	60.8°
M	0.808	——	——	——	0.813	X	0.802	0.806	0.804	——	0.804	
N	——	——	——	0.007	——	X	0.013	0.009	0.008	0.010	0.011	

AVERAGE DIMENSIONS

$A_1 = A_2 = 0.813$ inches

$H = 0.742$ inches

$d = 0.043$ inches

$L = 0.778$ inches

$\gamma = 49.95°$

$\epsilon_1 = \epsilon_2 = 60.94°$

$M = 0.806$ inches

$N = 0.010$ inches

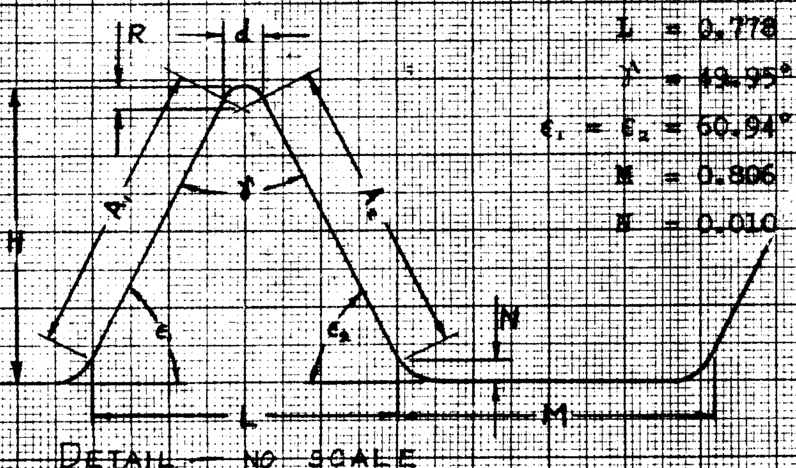

DETAIL — NO SCALE

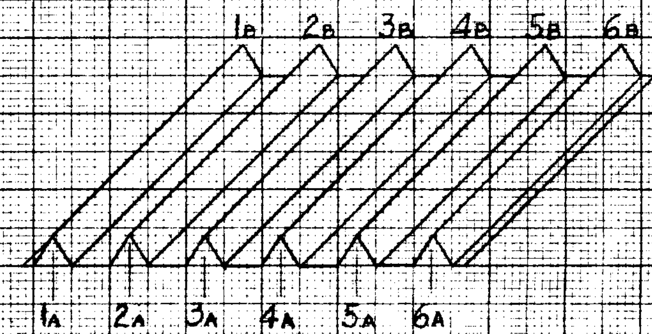

CALC			REVISED	DATE
CHECK				
APR				
APR				

SUMMARY OF DIMENSIONS
CONCENTRATOR STRUCTURE EOM-2B

FIG 42

D2-90041-A

BOEING AIRPLANE COMPANY

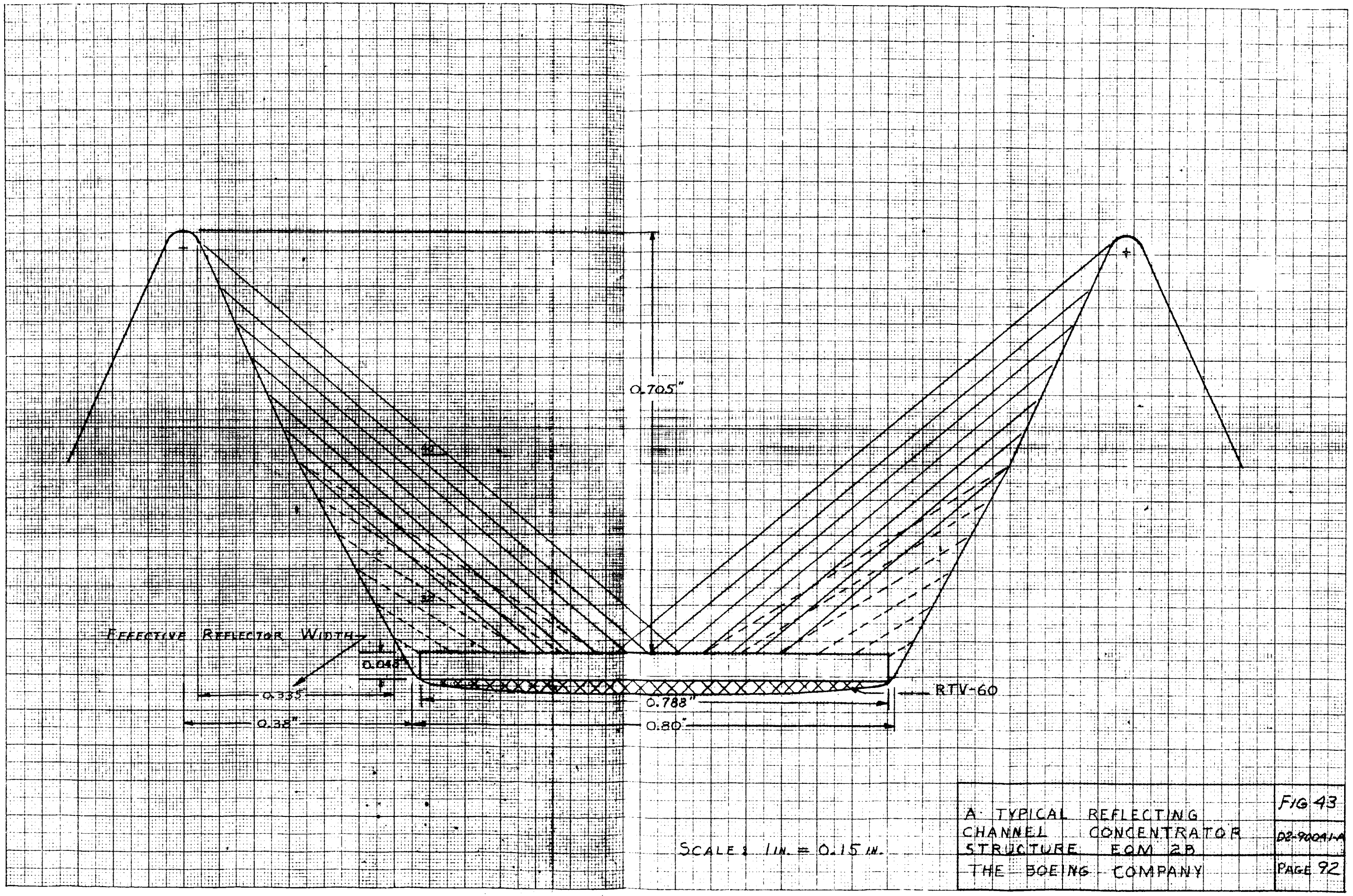

SCALE: 1 IN. = 0.15 IN.

A TYPICAL REFLECTING CHANNEL CONCENTRATOR STRUCTURE EOM 2B	FIG 43
THE BOEING COMPANY	D2-90041-A
	PAGE 92

The above calculated value does not agree with the observed value but instead agrees very closely with that calculated from Eq. 41a.

It is possible that this difference is a result of either an instrumentation error or a test procedure that is not rigorous. The short-circuit current was measured carefully to an accuracy of ± 1%, and thus is not a likely cause of the discrepancy. Two different procedures were used in testing the prototype panels. In one procedure the nonconcentrated short-circuit current was determined by shading the reflectors. This is the procedure that the contract specified for testing the EOM and CS models. In a second procedure the nonconcentrated short-circuit current was determined by removing the cells from the concentrator and testing the cells by themselves.

The first procedure gave a short-circuit concentration ratio which was about 5 percent greater than the second. The second test procedure appears more rigorous. If the observed short-circuit concentration ratio of the EOM-2B concentrator is reduced by 5 percent, the adjusted short-circuit concentration ratio C_I becomes 1.69, which is quite close to the calculated value.

The test procedure is the most plausible cause of the discrepancy between measured and calculated short-circuit current values. The discrepancy between the two test procedures could result from different amounts of sky being viewed by the solar cells under the two different test procedures. However, a rigorous analysis confirmed by test has not yet been made.

The EOM and CS-1 concentrators were evaluated by shading the reflectors as specified in the contract. Since the solar cells were bonded to the structure in both the EOM and CS models, it was not possible to test the models by both procedures. However, even if the test data were optimistic by 5 percent the contract performance requirements would be met.

2. Power Concentration Ratio

The EOM-2B concentrating structure produced a power concentration ratio of 1.88 which is significantly higher than the observed short-circuit concentration ratio of 1.77. This suggests that the conversion efficiency is greater at the higher light intensity levels than at lower levels that are present without concentration.

Originally it was assumed that the conversion efficiency remains constant over the light intensity ranges under consideration (100 to 200 milliwatts/sq. cm.). This assumption was based on the results of tests conducted with 13-percent-efficient conventional solar cells (Fig. 12). In subsequent tests of 10-percent-efficient blue-sensitive solar cells, it was shown that the conversion efficiency increases significantly with intensity. For example the efficiency is 10.0 percent at 100 mw/sq. cm. and 10.6 percent at 175 mw/sq. cm with the cell at a temperature of 45°C.

In one test with the EOM-2B concentrator, the following data were recorded:

P_n = 714 mw at 31°C (power without concentration)

I_o = 136.6 ma at 31°C (current without concentration)

P = 1342 mw at 40.5°C (power with concentration)

I_c = 243.0 ma at 40.5°C (current with concentration)

During this test, the solar intensity was constant at 98 mw/sq. cm. The measured concentration ratios are

$$C_I = \frac{243.0}{136.6} = 1.78$$

$$C_p = \frac{1342}{714} = 1.88$$

The effect of temperature on the efficiency of blue-sensitive solar cells can be extrapolated from Fig. 14. A temperature change of 33°C will cause a one percentage-point change in conversion efficiency.

Since the short-circuit current is a measure of the illumination intensity, the total illumination intensity as seen by the cells in the concentrator (S_c) is:

$$S_c = (S) \times \frac{\text{(short-circuit current with concentration)}}{\text{(short-circuit-current without concentration)}}$$

From pyrheliometer data, S = 98 mw per sq. cm. Then:

$$S_c = (98)\frac{(243.0)}{(136.6)} = 174 \text{ mw/sq. cm.}$$

The illumination contributed from the reflectors (S_r) is:

$$S_r = 174 - 98 = 76 \text{ mw/sq. cm.}$$

The conversion efficiency of the cells at an intensity of 174 mw/sq. cm. and a temperature of 40.5°C is:

$$\eta_c = 10.6 + \frac{45 - 40.5}{33} = 10.74\%$$

The efficiency increment corresponding to an intensity increment from 98 to 174 mw/sq. cm. and a temperature increment from 31°C to 40.5°C can be calculated by considering 1.0 sq. cm. of cell area.

$$\Delta\eta = \frac{\text{(Power @ 174 mw/sq.cm. and 40.5°C)- (Power @ 98 mw/sq.cm. and 31°C)}}{\text{Intensity Increment}}$$

$$= \frac{(174)(10.74) - (98)(10.42)}{174 - 98} = 11.18\%$$

Thus, the power output is expected to be:

$$P_n = \text{Power from direct light + Power from reflected light}$$

Since the reflected intensity is 77.6 percent of the direct intensity,

$$P_n = (714)\left[1 + (77.6)(11.18)\right] = (714)(1.87) = 1335 \text{ mw}$$

The computed value of power output with concentration compares very closely with the observed value of 1342 mw. Thus the power concentration ratio and the short-circuit current concentration ratio is clearly attributable to differences in conversion efficiency and temperature.

3. Specific Power Ratio

The measured specific power ratios are in excess of the 90 percent specified in the contract and are close to unity. This means that for a given power output the concentrating structure will require no more area than a non-concentrating panel having an area utilization factor of 85 percent. This is a surprising result, considering the absorption loss in the reflected component of light. However, there are two factors that offset the absorption loss:

(1) The conversion efficiency of a "blue" cell increases as light intensity increases. For example, the incremental efficiency corresponding to an increment in intensity from 100 mw/sq.cm. to 175 mw/sq.cm. is 11.5 percent, (Fig.14). The direct component of light is converted to electricity with an efficiency of 10.0 percent at a cell temperature of 45°C. The reflected light is thus 15 percent more effective. The absorption loss with aluminized lacquer reflecting surfaces having a reflectance of 82 percent is 18 percent. Thus the 15 percent gain in conversion efficiency nearly offsets the absorption loss.

(2) The solar cells can be mounted on the structure with no more, and possibly less, lost area than is required for mounting cells on a conventional panel. This is because the wiring can be located on the back of the panel. In the CS-1 concentrator, both the positive and negative leads of each shingle are brought out through a small opening at the base of the reflector.

The parallel and series connections are made on insulated copper paralleling strips bonded to the hat sections. With this wiring method, it was possible to reduce the separation between abutting shingles in the trough to about 0.03 inch.

The overall length of a solar cell shingle is 1.80 inches. Active cell area occupies 1.75 inches and the solder-strip of the positive terminal occupies 0.05 inch. The gross length of a shingle mounted in the structure is (1.80 + .03) inches or 1.83 inches. The minimum gross length that is possible with no separation between the mounted shingles is 1.80 inches. Thus, with a spacing between shingles of 0.03 inch the gross cell length of a 5-cell shingle plus wiring is within 1.5 percent of the ultimate minimum.

VIII. CONCLUSIONS

The basic optical design criteria for V-ridge type concentrators for solar-cell space-vehicle power supplies have been developed by means of analysis and test. Mechanical design criteria have been developed by vibration testing and analysis. Tools for bending reflectors have been built, and fabrication, wiring, and assembly techniques have been developed. An effective strippable coating for protecting reflecting surfaces from deterioration during manufacture has reduced the handling problems.

The EOM and CS-1 concentrators required by the contract have been designed, built, tested, and delivered. Vibration tests under the conditions specified in the contract have shown that the V-ridge concentrator design is basically stiff, the welds are strong, and the method of bonding solar cells to the concentrator trough is satisfactory. Solar tests have shown that the contract electrical-optical performance requirements, particularly specific power, have been exceeded by EOM and CS-1 concentrators.

The actual weight of the CS-1 concentrator, complete with solar cells, cover glasses, wiring, and adhesive, but without vibration-test supports, was 0.575 pounds per sq. ft. The measured conversion efficiency of the CS-1 concentrator with the reflecting surfaces covered was 8.8 percent, and with the reflecting surfaces exposed was 7.9 percent. The solar cells covered 46.8 percent of the concentrator area. Thus, for a given power output, the number of solar cells required in a V-ridge concentrating panel of the CS-1 type is only 52 percent of the number of cells required in a non-concentrating panel. If the non-concentrating panel is 90-percent covered with solar cells, its total area for a given power output will be the same as the area of an equivalent V-ridge concentrating panel. The V-ridge concentrating panel will weigh less than one-half as much as the non-concentrating panel.

IX. RECOMMENDATIONS

JPL Contract 950122 required that Boeing develop, build, test, and deliver EOM Electrical-Optical Model and CS-1 Type-Approval concentrators. The development of practical, stable, high-reflectance surfaces, although outside of the scope of this contract, was carried on in Boeing research on a modest basis. There are additional problems beyond the scope of this contract that must be solved before practical space-vehicle power supplies employing V-ridge concentrators can be designed. It is recommended that effort be immediately applied to the solution of these problems, which are described below.

A. Reflecting Surface Development

Optical performance, thermal emissivity, stability in adverse environments, and cost are factors that will affect the selection of the reflecting surface on the concentrator. This contract covers only optical performance studies. It is recommended that the remaining characteristics be carefully developed and evaluated by means of complete performance and environmental tests.

Several high-reflectance surfaces have been suggested. For example, ALCOA proposes cladding 99.99 percent pure aluminum to 1100 aluminum, resulting in a surface which when anodized will have a reflectance of 82 percent and a thermal emissivity of 70 percent. OCLI is prepared to develop a second-surface dielectric-film reflector on 0.003-inch thick micro-sheet glass. Such a design would have the desirable high emissivity and the protecting quality of the exposed glass surface. The extra weight of the glass could be compensated with lightening holes in the supporting aluminum.

B. Equilibrium Temperature

The power output of a concentrating solar-cell array depends strongly on the cell temperature. This temperature in turn depends on the effective emissivity of the cover glass, reflector, and concentrator back. Optimum designs of these surfaces need to be developed by analysis and test. A blackened liquid-nitrogen cooled vacuum chamber could be used for measuring the emissivity of surfaces and concentrators. There is a need for parametric curves from which the equilibrium solar-cell temperature can be predicted for any combination of reflecting surface, concentrator back surface, concentrator geometry, solar illumination, and back illumination.

C. Structural Design of Large-Area Panels

The 10-inch by 18-inch CS-1 panel delivered on this contract is a size convenient for optical evaluation. Panels for actual space vehicles will be much larger. Therefore, structural design of such large panels needs to be developed by analysis and test.

As an example, the trough length employed in the EOM and CS-1 concentrators was so short that the vibration-test results are not adequate to permit an optimum design of the sub-structure and panel assembly. It will be necessary to build and vibrate troughs several feet long to produce useful design criteria.

D. Curved-Surface Reflectors

The mathematical analysis showed that substantially higher concentration ratios can be obtained from ideal curved reflectors than

from flat reflectors. To evaluate curved surfaces fully it is necessary to examine possible manufacturing techniques, establish the effect of tolerances, and calculate the performance of real reflecting surfaces with real solar cells.

Manufacturing techniques for making curved surfaces, such as electroforming and explosive forming, need to be explored.

E. Altered Ultra-Violet Cutoff of Cover Glass

The OCLI cover glass does not have a sufficiently long cutoff wavelength for sunlight arriving at an oblique angle. As a result, the ultra-violet light in space may deteriorate the bonding adhesive between the cell and cover glass. It is recommended that a new interference film be developed for cover glasses used in V-ridge concentrators.

OCLI offers to develop a cover glass with such a film and sell samples for test at nominal cost. The use of ultra-violet resistant cover-glass cements needs to be explored also. Such a cement would be especially desirable for the new blue-sensitive solar cells which can utilize effectively radiation in the vicinity of 0.450 microns wavelength.

F. Manufacturing Techniques

The bending-brake used in making EOM and CS-1 concentrators is limited to a trough length of 12 inches. A larger tool must be built before larger concentrators can be built. Accessories, such as a bend-line locating jig and punching die are also required. No serious difficulties are anticipated in building these new tools.

X. NOMENCLATURE

The following expressions appear in several parts of this report.

A - Area of the solar cells and the utilized area of the concentrator. This includes the ridge bending radii, lost area between cell sides and reflector, space between shingles, and the reflector area that illuminates the space between shingles.

A_c - Active area of solar cells in a concentrator.

A_r - Projected area of reflector.

A_t - Gross area of cell trough.

a - Solar cell width.

b - Projected width of one reflector.

C - Theoretical concentration ratio with 100 percent reflectance surfaces.

C_I - Short-circuit current concentration ratio.

C_p - Power concentration ratio.

cps - Cycles per second.

F_1 - Factor to account for inactive area in cell trough due to wiring and cell-mounting allowance.

F_2 - Factor to account for loss in reflector area due to bending radii, cell height, and inactive space between cells in trough.

F_3 - Factor to account for wiring and cell mounting allowances in a a non-concentrating panel.

I_o - Short-circuit current with reflectors shaded - (No concentration).

I_c - Short-circuit current with reflectors exposed.

K - Factor to account for light scatter resulting from manufacturing variations.

m_1 - Weight of trough and solar cells, pounds per inch of length.

ℓ - Width of reflecting surface, i.e. the distance from the top of the ridge to the nearest edge of the trough.

n_1 - Weight of the reflector, pounds per inch of width for one inch of length.

OCLI - Optical Coating Laboratory, Inc.

P	Power output of solar cells mounted in concentrator and exposed to sunshine.
P_n	Maximum power measured when a concentrator is exposed to sunlight but the reflectors are covered.
P_o	Power output of a conventional panel having the same area as a specified concentrating structure.
R	Reflectance of reflectors.
S_o	Solar intensity in milliwatts per sq. cm.
S_c	Intensity of light on the solar cells with reflectors exposed in milliwatts per sq. cm.
S_r	Intensity of the light reflected onto the solar cells in milliwatts per sq. cm.
SCC	Short circuit current.
SPR	Specific power ratio.
η	Overall solar-cell conversion efficiency.
η_1	Conversion efficiency of solar cells applicable to direct-light power output.
η_2	Conversion efficiency applicable to reflected-light power output.
η_c	Factor to account for change in conversion efficiency resulting from an increase in the light intensity.
η_t	Factor to account for a change in conversion efficiency resulting from a higher equilibrium cell temperature.
η_o	Factor to account for a change in conversion efficiency resulting from the reflected light striking the solar cells at an angle.
θ	Angle between incoming solar rays and reflecting surface.
ϕ	Angle between solar-cell plane and light reflected from reflector.
α	Angle between reflector surface and solar-cell plane.
γ	Acute angle between reflector surfaces.

Conference Paper

SOLAR-CELL PERFORMANCE WITH CONCENTRATED SUNLIGHT

R. J. Tallent
Associate Member AIEE

Henry Oman
Member AIEE

Both of:
Boeing Airplane Co.
Seattle, Wash.

Submitted in abstract or outline form only to the AIEE Aero-Space Transportation Committee for presentation at the AIEE Aero-Space Transportation Conference, Philadelphia, Pa., June 26-30, 1961. Manuscript submitted April 11, 1961; made available for printing May 2, 1961.

Price: $ .50 To Members
$1.00 To Nonmembers

(5¢ per copy additional if first class mailing desired)

Paper No. CP
61-911

SOLAR-CELL PERFORMANCE WITH CONCENTRATED SUNLIGHT

R. J. Tallent Henry Oman

Silicon solar cells have been a good source of power for satellites and space probes. Their applicability for future vehicles with larger electric loads seems to be limited by cost and weight. For example, one by two cm silicon solar cells in the 10 to 13 percent efficiency range cost about $10 each, or about $350,000 per kw. Conventional panels containing silicon solar cells weigh in the order of 100 pounds per kw.

Concentrating sunlight on solar cells would seem to be a way of partially overcoming these limitations. If the power output per cell could be doubled, the cost per kw would be halved. If lightweight reflecting surfaces could be substituted for silicon photovoltaic material, the weight per kw might be reduced. The weight might be reduced even more significantly if the reflecting material could also serve as supporting structure.

Investigations were conducted in order to establish quantitatively the performance of power sources employing concentrated sunlight. The performance of solar cells in high-intensity sunlight was measured. A lightweight concentrating and support structure was designed and tested. The temperature in space of solar cells mounted in this structure was calculated. The performance of a simple concentrating photovoltaic power source was computed.

The results of these investigations are described in this paper.

SOLAR-CELL PERFORMANCE IN HIGH-INTENSITY SUNLIGHT

Several methods of obtaining high-intensity illumination for testing were considered. The use of an artificial light source was not seriously considered because the effect of a non-solar spectrum could not be readily interpreted. Concentrating sunlight with a lens did not appear satisfactory because the uniformity of illumination in the focal area could not be determined readily. A system employing an Archimedes array of six flat plate-glass mirrors shown in Fig. 1 was finally adopted. The mirrors were individually adjustable and the array was installed on a mount that permitted following the sun. The mirror array was mounted about 10 feet from the solar cells being tested so that the concentrated sunlight was nearly perpendicular to the cells.

With this array of mirrors the absolute intensity of the concentrated sunlight on the cells could be established only within the accuracy of pyrheliometric measurements. However, the relative illumination on the solar cells could be varied in discrete and very precise steps by uncovering different numbers of mirrors. Illumination intensities of three times that of sunlight in space outside of the Earth's atmosphere were obtained.

The high-intensity solar-cell performance measurements are useful only if cell temperature is known, because the efficiency of a solar cell is a function of temperature. 1. Constant cell temperature was achieved in the tests by soldering test cells on a water-cooled plate (Fig. 2). Constant water temperature was obtained from a water system having a pump, heater, and cold-water heat exchanger.

For each illumination level, the current and voltage were plotted for a varying load. A typical family of such volt-ampere curves is shown in Fig. 3. For reference, the illumination intensity in space outside of the Earth's atmosphere is about 140 milliwatts per sq cm. 2. However, the data in Fig. 3 can be used to predict solar-cell performance in space only if the difference between the Sun's spectrum on Earth and in space is taken into account.

The maximum power output of a solar cell can be readily determined from its volt-ampere curve. Fig. 4 shows the relation between this maximum power output and illumination intensity at a 40°C temperature. The maximum power output increases with intensity as expected, but the relation is not linear. The gain in power output for an incremental increase in intensity is not as large at high intensities as it is at low intensities. This suggests that with this particular cell, only marginal benefit is obtained from illumination intensities above 300 milliwatts per sq cm.

The maximum solar-cell power output divided by the power content of the radiation striking the cell gives the maximum cell efficiency. This maximum efficiency of a typical cell is plotted as a function of illumination intensity for several cell temperatures in Fig. 5. As expected, efficiency drops as temperature is increased. The manufacturer had rated this cell as 10-percent efficient, based on measurements made under a calibrated artificial light source.

CONCENTRATING STRUCTURE

The next problem examined was the design of a concentrating structure for solar cells. Many concentrator concepts were examined. Lenses are too heavy when the supporting structure is considered. Reflecting concentrators, such as Archimedes flat-mirror arrays and paraboloidal mirrors are at a disadvantage for low concentration ratios because a substantial part of the concentrator is shaded by the solar cells. High concentration ratios are not practical for solar cells because cell-cooling becomes a problem. By concentration ratio is meant the ratio of the intensity seen by the solar cells to the ambient solar radiation intensity.

The Somor concentrator (Fig. 6) appears to be the most practical for low concentration ratios. The geometrical limitation of the two-reflector Somor concentrator is such that with infinitely long reflecting surfaces having 100 percent reflectance a concentration ratio approaching three can be achieved. The relation between reflector angle, reflector length, and concentration ratio is shown in Fig. 7.

From a structural design standpoint the Somor concentrator is rigid in one direction, being not unlike a sheet of corrugated steel. Rigidity in the other direction must be obtained with auxiliary structure, such as a lightweight hat section. The solar cells can be fastened to the structure with a structural adhesive. The cells would be insulated from the metal of the structure.

One concept for a Somor concentrating structure is shown in Fig. 8. Structures of this type have been built of aluminum having thicknesses as small as 0.003 inches. A concentrator of the type shown in Fig. 8 was tested by comparing the solar-cell output with the reflecting surfaces covered and uncovered. The tests were conducted in sunshine on the Earth's surface. With anodized high-reflectivity aluminum the solar-cell short-circuit current was found to increase by 65 percent as a result of the reflected light. This corresponded to a 45 percent increase in solar-cell power output in space, when temperature effects and the spectrum in space are considered.

TEMPERATURE CONTROL

The Somor concentrator has an added advantage in that the reflecting surfaces are also available for radiating heat, and hence maintaining a low cell temperature in space. If the cell is to be cooled by conducting heat into the reflectors, the dimensions of the heat-transfer elements must be such that the temperature drop between the cell and reflectors is small. It was found that this low temperature drop could be attained with a reasonably thin metal by illuminating only one row of solar cells with a pair of reflectors.

Maximum heat radiation is obtained if both sides of the reflectors have high infra-

red emissivity. Back-surface emissivities higher than 0.9 can be obtained with black finishes or anodizing. The front surface, on the other hand, must have high reflectivity (low emissivity) to solar radiation and high emissivity at far infrared wavelengths. Only a few coatings have this property. The spectral reflectance of one anodized coating having this property is shown in Fig. 9. It has a total solar reflectance of 0.80 and an effective infrared emissivity of 0.75. The infrared emissivity can be increased to higher than 0.85 by employing an additional coating. 3.

Heat dissipation at the sun-facing sides of the solar cells is increased by the use of cover glasses which have an infrared emissivity much higher than could be obtained from the silicon surface of a solar cell. The cover glass also has interference coatings which reflect ultraviolet illumination that would otherwise be absorbed by the cell and create heat without generating output power. The optical performance of these cover glasses under normal-incidence illumination has been extensively investigated and reported. 4. The optical performance under oblique light such as would come from the Somor reflectors had not been reported previously, as far as is known. Therefore, the transmittance of cover glasses for light striking at various angles was measured. It was found that one cover glass had no shift in ultraviolet cutoff at angles of light up to 60 degrees from normal, but the transmission loss at 60 degrees increased by 10 percent. (Fig. 10) Another cover glass did not change appreciably in transmittance, but the ultraviolet cutoff shifted to a 500 Angstroms shorter wavelength when the incident light was 53 degrees from normal. (Fig. 11)

In a practical Somor concentrator the reflected light will strike the cells at an angle of about 60 degrees from the normal. About 10 percent of this reflected light can be lost because of decreased cover-glass transmittance. The higher ultra-violet transmittance of a cover glass would raise cell temperature as a consequence of higher radiation input. Both of these effects will tend to reduce slightly the power output achievable with concentration of sunlight on solar cells.

EFFECT OF MISORIENTATION

An advantage of arrays having solar cells with no concentration is that orientation is not critical. For example, an orientation error of 8 degrees will result in only a one-percent loss of output power. In contrast with a system employing a paraboloidal concentrator and a high-temperature thermionic converter a fraction of a degree of misorientation can cause a substantial loss of output. For example, with one solar thermionic converter system, calculations showed that a 13-minute misorientation resulted in a 15 percent drop in concentrator-absorber efficiency.

The combination of a Somor concentrator and solar cells is affected by misorientation, (Fig. 12), but not as much as is the high-concentration thermionic converter system. It will be noted that misorientation about the longitudinal axis is more serious than misorientation about the transverse axis. This sensitivity to misorientation in the longitudinal axis can be reduced by designing the bottom of the Somor trough to be slightly wider than the solar cell. Thus the first few degrees of misorientation will not result in cell area that does not receive full reflected light. The increase in structural weight for such a feature would not be significant compared to the advantage of a reduced orientation accuracy requirement.

EXAMPLE DESIGN

A preliminary design of a concentrating solar cell array for space use was made to develop system weight and performance estimates. The following design criteria were

Solar-cell efficiency, no concentration 9 percent

Concentration ratio, effective	1.65
Solar intensity	140 milliwatts/sq cm
Cover-glass emissivity, infrared	0.84
Back surface emissivity, infrarod	0.85
Absorptivity of cover glass and cell	0.78
Reflecting surface emissivity, infrared	0.75
Thermal conductivity of silicon	0.2 cal/sec-cm-°C
Thermal conductivity of aluminum	0.4 cal/sec-cm-°C
Thermal conductivity of bonding cement	0.002 cal/sec-cm-°C

The temperatures of different parts of the structure were calculated in a conventional manner. Once the temperature is known, the performance of the solar cells can be determined from the experimental data previously discussed. The following results were obtained from the calculations:

Reflector temperature	48°C
Solar-cell temperature	51°C
Solar-cell efficiency, with concentration	8.1 percent
Power output per cell	30 milliwatts
Power output per cell, no concentration	21 milliwatts
Weight-to-power ratio, of cells, reflectors, and structure	65 pounds per kw

Further development will undoubtedly reduce the weight-to-power ratio of the concentrating solar-cell power source.

CONCLUSIONS

Tests and calculations indicate that a solar-cell space-vehicle power source employing Somor concentrators will provide power at lower cost and less weight when compared with conventional non-concentrating solar-cell power sources. However, the concentrating system does require better orientation.

It should be recognized that the computations and experiments described in this paper were conducted to establish feasibility. Additional engineering and development must be accomplished before the Somor-concentrator solar-cell power source is ready for space use.

REFERENCES

1. Silicon Solar Energy Converters, M. B. Prince. Journal of Applied Physics, vol. 26, number 5, May 1955, pp. 534-540.

2. Solar Constant and Spectral Distribution Factors for Solar Energy Converters Intended for Space Applications, Daniel Friedman, NRL Memorandum Report 1005, U. S. Naval Research Laboratory, Washington, D. C.

3. Vanguard Emittance Studies at NRL, Louis F. Drummeter, Jr. and E. Goldstein. Surface Effects on Spacecraft Materials (book), pp. 152-163, John Wiley & Sons, Inc., New York, N.Y.

4. Optical Characteristics of Silicon Solar Cells and of Coatings for Temperature Control, C. A. Escoffery and Werner Luft. Solar Energy, vol. IV, number 4, October, 1960, pp. 1-9.

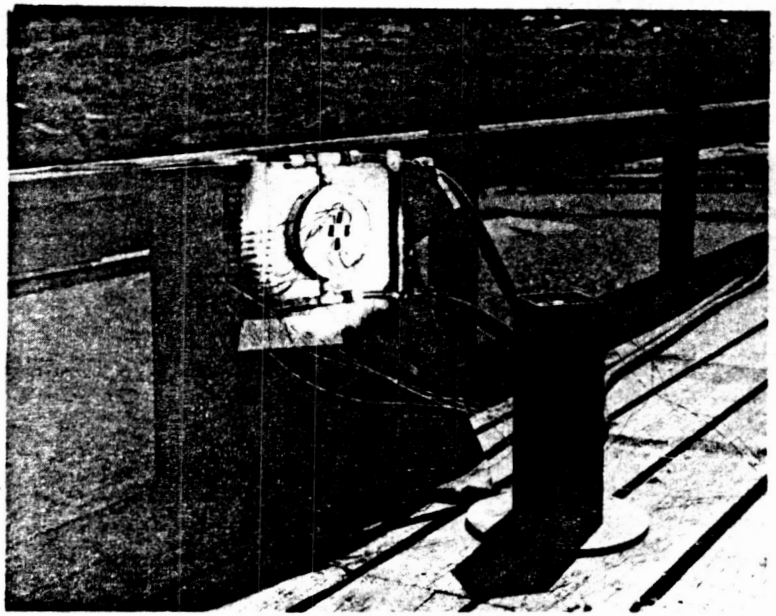

Fig. 1. Archimedes array of mirrors which was used to concentrate sunlight on solar cells.

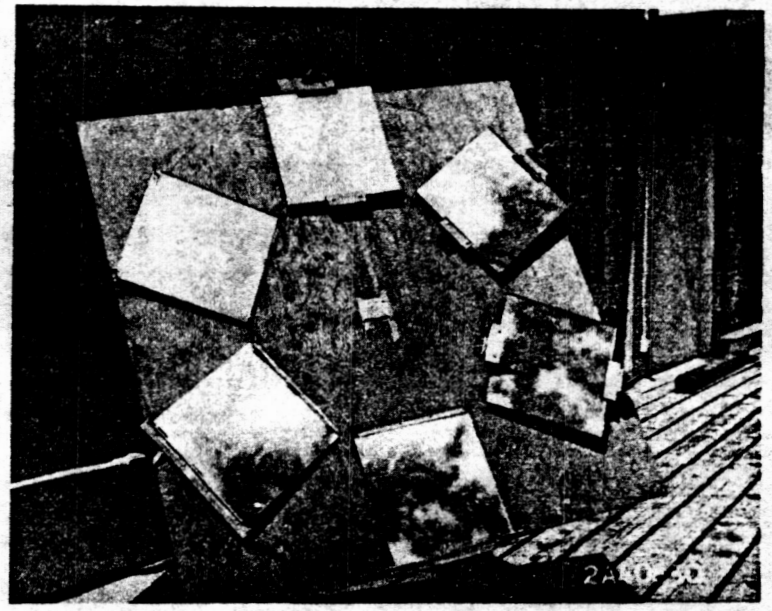

Fig. 2. Four silicon solar cells mounted on a water-cooled plate.

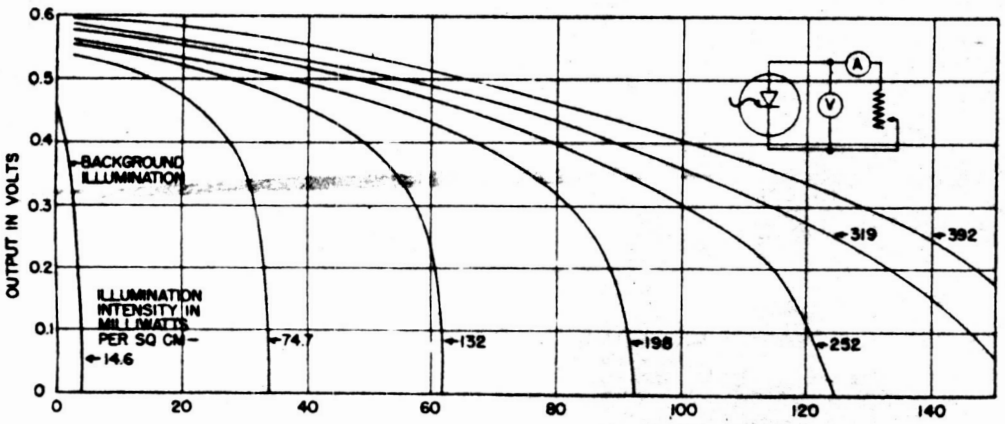

Fig. 3. Volt-ampere characteristic of a typical solar cell under various intensities of illumination. Cell temperature was 40°C.

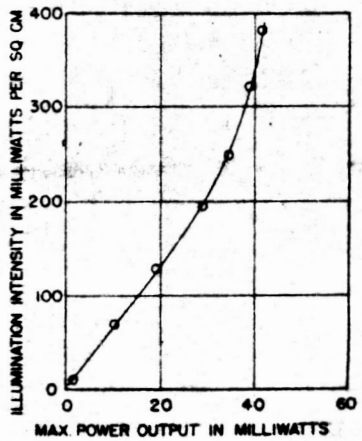

Fig. 4. Maximum power output of a typical solar cell under various intensities of illumination.

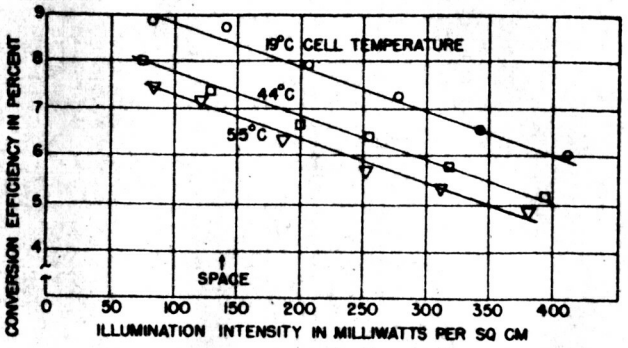

Fig. 5. Efficiency of a typical solar cell at various intensities of illumination.

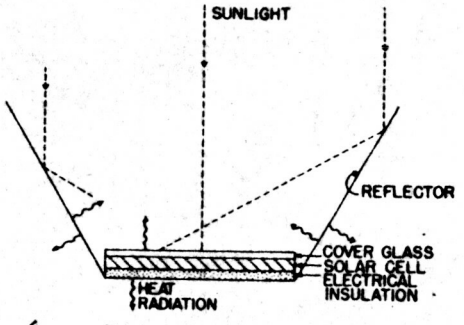

Fig. 6. Principle of a Somor concentrator.

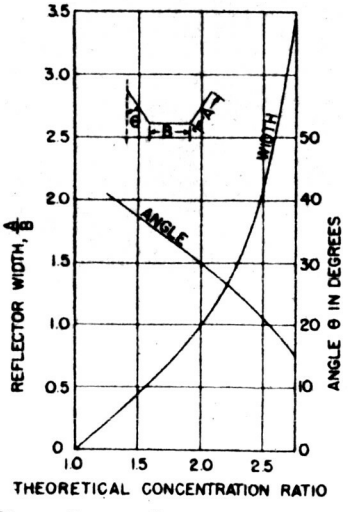

Fig. 7. Concentration ratios obtainable with Somor concentrators.

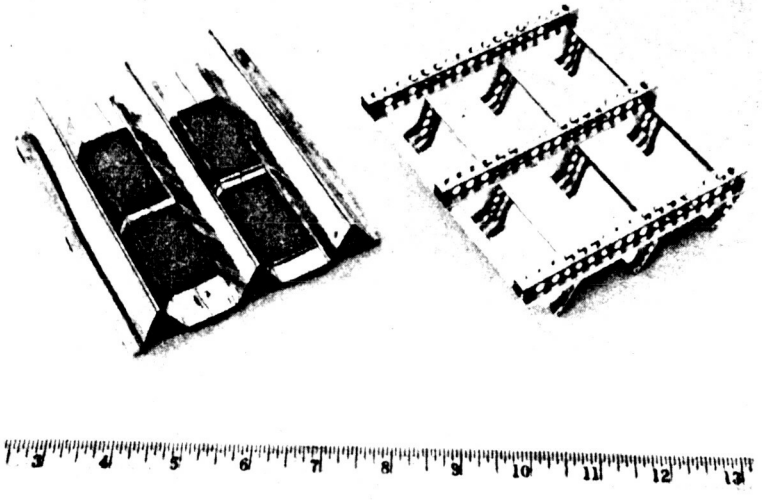

Fig. 8. Somor concentrator for use with solar cells.

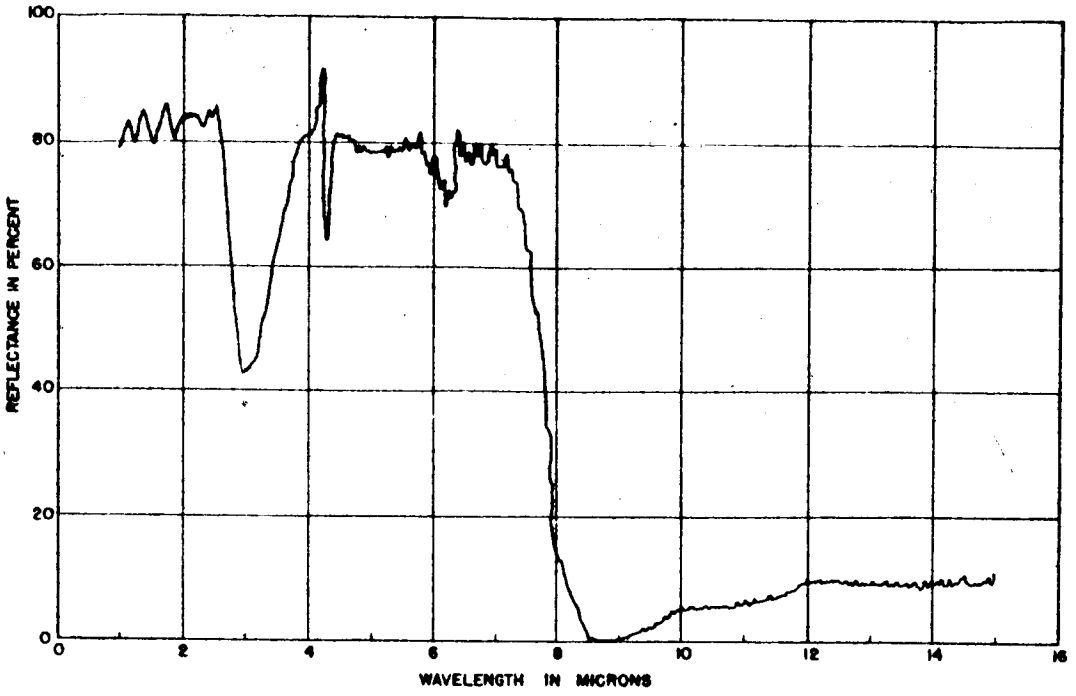

Fig. 9. Spectral reflectance of an anodized aluminum.

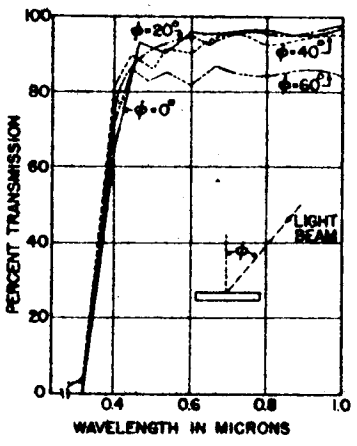

Fig. 10. Spectral transmission of a Bausch and Lomb cover glass.

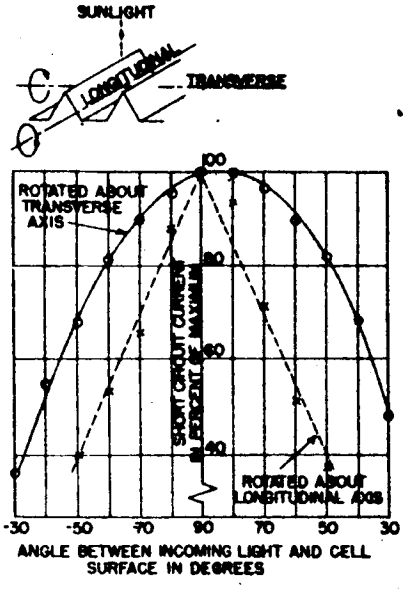

Fig. 12. Effect of misorientation on solar cells illuminated by a Somor concentrator.

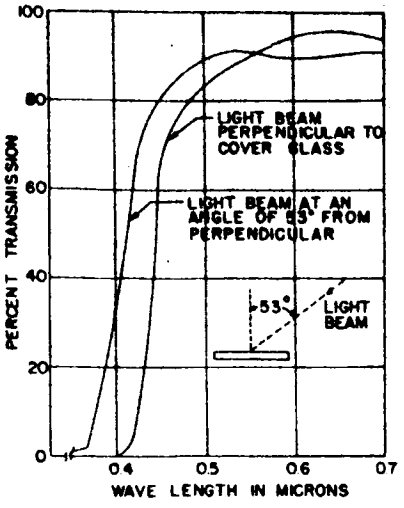

Fig. 11. Spectral transmission of an Optical Coatings Laboratory cover glass.